A THERMODYNAMIC EVALUATION OF 1,4,7,10-TETRAAZACYCLODODECANE-1,4,7,10-TETRA (METHANE-PHOSPHONIC ACID) (DOTP) AS A COMPONENT OF THE BONE-SEEKING RADIOPHARMACEUTICAL [^{177} LU]LU(III)-DOTP, TOWARDS ESTABLISHING BLOOD PLASMA MODEL FOR LU(III)

L.C. SEPINI

A thermodynamic evaluation of 1,4,7,10-tetraazacyclododecane-1,4,7,10-tetra(methane-phosphonic acid) (DOTP) as a component of the bone-seeking radiopharmaceutical [^{177}Lu]Lu(III)-DOTP, towards establishing blood plasma model for Lu(III)

L.C. Sepini

Dissertation submitted in fulfillment of the requirements for the degree of *Master of Science* in the Faculty of Agriculture, Science and Technology at Mafikeng Campus of North West University

Supervisors: **Prof Dr J.R Zeevaart**
Dr N.V Jarvis
Dr D.R Jansen

Declaration

I hereby declare that the work presented in this dissertation has never been submitted to any institution for a degree and that this is my original work except where due reference is made.

L.C. Sepini

Signature: .....

Date: .....

Acknowledgements

I would like to acknowledge and express my sincere thanks to the following people:

- My supervisors Prof Dr J.R Zeevaart, Dr N.V Jarvis and Dr D.R Jansen for their mentorship and guidance. Your input to this work is much appreciated.

- To my family, more especially my mom Kefilwe Sepini and my Uncle Shimane Sepini, for believing in me and for their continued support over the years. I would not be where I am if it weren't for their encouragement and inspirations.

- Many thanks to North West University (CARST) for introducing me to the nuclear science world.

- To NECSA (Radiochemistry Department), for financial assistance and for offering me a suitable environment for doing my research.

- To the Lord God Almighty, the one who sustains me. I thank Him for giving me the wisdom to carry out this research, and opening doors for me. In Him I live and move.

Oral Presentation

ASSAf-DST-NRF Second Annual South African Young Scientists' Conference. Diep in Die Berg Conference and Function Centre, Pretoria. September 2011, Establishing a blood plasma model for Lu(III). Sepini L, Jarvis N.V, Jansen D.R, Zeevaart J.R.

Publication

Sepini L.C, Jarvis N.V, Jansen D.R, Zeevaart J.R. Thermodynamic evaluation of the stability of the bone-seeking radiopharmaceutical [177Lu]Lu(III)-DOTP under simulated blood plasma conditions. Analytica Chimica Acta. 2012, 730: 66-70

Abstract

The stability and *in vivo* robustness of [^{177}Lu]Lu-DOTP as a potential bone-targeting radiopharmaceutical was determined with the aid of thermodynamic blood plasma modeling simulations. The use of radionuclides for treatment of bone metastasis and pain palliation proved effective and preferable. ^{153}Sm-EDTMP and ^{186}Re-HEDP are examples of radiopharmaceuticals that are successful in this regard. The radioisotope ^{177}Lu possesses favourable radiation characteristics (in comparison with the two mentioned radionuclides) for consideration in radiotherapy and, more specifically, in bone metastasis. It emits lower energy betas with a reasonably low range in bone tissue, which makes it possible to increase the administered dose with low radiotoxicity to the sensitive bone marrow. There is currently a great interest in ^{177}Lu to be used in many radiopharmaceuticals. It can be made from the nuclear reaction ^{176}Lu(n,γ)^{177}Lu in almost any reactor as it has a high cross section and for bone treatment one does not need high specific activity of the radionuclide.

Glass electrode potentiometry was employed to measure the stability constants of the complexes of Lu^{3+} with DOTP. Similarly, the complexes of DOTP with a selection of the important physiological metal ions: Ca^{2+}, Mg^{2+}, and Cu^{2+} were determined, representing the typical interactions that the ligand would encounter upon administration. This made possible the construction of a blood plasma model of DOTP, aiding in establishing the potential susceptibility of the radiopharmaceutical. The ligand binds predominantly to calcium *in vivo*, accounting for 59.6% of that initially introduced as a component of the Lu-DOTP complex. Furthermore, due to the preference of the DOTP to bind to Cu^{2+} it causes mobilization of the ions in blood plasma, and would therefore indicate a deficiency if the ligand is administered at a concentration of 8.5×10^{-5} mol.dm^{-3}. The lutetium-ions are preferentially bound to DOTP, with as much as 98.1% of the Lu^{3+} occupying the ligand under physiological conditions.

Table of Contents

Declaration		i
Acknowledgements		ii
Oral Presentation		iii
Publication		iii
Abstract		iv
Table of Contents		v
List of Figures		vii
List of Tables		x
List of Abbreviations and Symbols		xi
Chapter 1 Introduction		**1**
1.1	Introduction	2
1.2	Radiopharmaceuticals	3
	1.2.1 Diagnostic radiopharmaceuticals	3
	1.2.2 Therapeutic radiopharmaceuticals	5
1.3	Lanthanides in radiopharmaceuticals	6
1.4	Macrocyclic chelators complexed with lanthanides	10
1.5	Research objectives	11
1.6	Thesis outline	14
Chapter 2 Theoretical Background		**15**
2.1	Determination of formation constants with Potentiometry	16
	2.1.1 Glass Electrode Potentiometry	18
2.2	Programs for analyzing Potentiometric data	20
	2.2.1 ESTA	20
	2.2.1.1 ESTA1	22
	2.2.1.2 ESTA2	24
2.3	ECCLES	24

2.4 Linear Free Energy Relationships 26

Chapter 3 Experimental **29**

3.1 Reagents 30

3.2 Methods 30

3.2.1 Preparation of solutions 31

3.2.2 Experimental set-up 32

3.3 Glass Electrode Potentiometry 32

3.3.1 Electrode and instrumentation 32

3.3.2 Glass electrode calibration 33

3.3.3 Experimental Procedure 33

Chapter 4 Results and Discussion **36**

4.1 Introduction 37

4.2 Protonation studies of the ligand DOTP 40

4.3 Complexation of DOTP with Lu^{III} 42

4.4 Speciation of DOTP with major metal-ions in blood plasma- Ca^{II}, Mg^{II}, Cu^{II} 45

4.3.1.1 Ca-DOTP model 45

4.3.1.2 Cu-DOTP model 47

4.3.1.3 Mg-DOTP model 48

4.5 Discussion 52

4.6 Speciation of Lu^{II} with EDTMP and selected blood plasma ligands – Citrate, Lactate, Glutamine, Threoninate, Glycinate 55

Chapter 5 Conclusion **59**

5.1 Conclusion 60

5.2 Future Work 61

5.3 References 62

5.4 Appendices 68

List of Figures

Figure 1.1 ^{99m}Tc-MDP bone scan, anterior and posterior views and the ^{153}Sm post-therapy scan, anterior and posterior views of male cancer patients with multiple skeletal metastases [16].

Figure 2.1 Diagram of a glass combination electrode.

Figure3.1 The experimental set-up in the titration vessel.

Figure 3.2 TitraLab (TIM 865 titration manager) with Metrohm 665 Dosimat.

Figure 4.1 The structure of DOTP

Figure 4.2.1 Experimental (points) and modelled (lines) protonation formation curves for DOTP. The titrations are represented by (Δ) 0.001249 M DOTP, 0.012612 M HCl, (□) 0.002499 M DOTP, 0.012618 M HCl and (O) 0.003749 M DOTP, 0.012619 M HCl. All solutions were at 25°C and 0.15 M ionic strength.

Figure 4.2.2 Speciation diagram for acid dissociation of DOTP at 25 °C and 0.15 mol.dm^{-3} total ionic strength

Figure 4.3.1 $\bar{Z}$ curves for the complexation of DOTP with Lu^{3+}. Experimental points are represented by the points and modeled protonation formation curves represented by the solid lines. The three titrations are depicted as follows: (○) 1 mmol.dm^{-3} Lu^{3+} and 1 mmol.dm^{-3} DOTP, (Δ) 1 mmol.dm^{-3} Lu^{3+} and 2 mmol.dm^{-3} DOTP, and (□) 1 mmol.dm^{-3} Lu^{3+} and 3 mmol.dm^{-3} DOTP. All titrated against 0.05 mmol.dm^{-3} NaOH in 0.10 mol.dm^{-3} NaCl, at 25.0 °C and 0.15 mol.dm^{-3} total ionic strength. Along the x-axis pA is the negative log of the free ligand concentration

Figure 4.3.2 $\bar{Q}$ curves for the complexation of DOTP with Lu^{3+}. Experimental points are represented by the points and modeled protonation formation curves represented by the solid lines. The three titrations are depicted as follows: (○) 1 mmol.dm^{-3} Lu^{3+} and 1 mmol.cm^{-3} DOTP, (Δ) 1 mmol.dm^{-3} Lu^{3+} and 2 mmol.dm^{-3} DOTP, and (□) 1 mmol.dm^{-3} Lu^{3+} and 3 mmol.dm^{-3} DOTP. All titrated against 0.05 mmol.dm^{-3} NaOH in 0.10 mol.dm^{-3} NaCl, at 25.0 °C and 0.15 mol.dm^{-3} total ionic strength. The dashed line represents the $\bar{n}$ curve, which is the protonation state of the ligand in the absence of the metal ion

Figure 4.3.3 Speciation diagram for the distribution of Lu-DOTP complexes over the pH range 2 to 11, at 25.0 °C and 0.15 mol.dm^{-3} total ionic strength

Figure 4.4.1 Experimental (points) and modeled (lines) formation for Ca^{2+} complexation by DOTP. pA is the negative log of the free ligand concentration. The 3 titrations are represented by (○) 1 mmol.dm^{-3} Ca^{2+} and 1 mmol.cm^{-3} DOTP, (Δ) 1 mmol.dm^{-3} Ca^{2+} and 2 mmol.dm^{-3} DOTP, and (□) 1 mmol.dm^{-3} Ca^{2+} and 3 mmol.dm^{-3} DOTP. All titrated against 0.05 mmol.dm^{-3} NaOH in 0.10 mol.dm^{-3} NaCl, at 25.0 °C and 0.15 mol.dm^{-3} total ionic strength

Figure 4.4.2 Experimental (points) and modeled (lines) formation for Ca^{2+} complexation by DOTP. pA is the negative log of the free ligand concentration. The 3 titrations are represented by (○) 1 mmol.dm^{-3} Lu^{2+} and 1 mmol.cm^{-3} DOTP, (Δ) 1 mmol.dm^{-3} Ca^{2+} and 2 mmol.dm^{-3} DOTP, and (□) 1 mmol.dm^{-3} Ca^{2+} and 3 mmol.dm^{-3} DOTP. All titrated against 0.05 mmol.dm^{-3} NaOH in 0.10 mol.dm^{-3} NaCl, at 25.0 °C and 0.15 mol.dm^{-3} total ionic strength

Figure 4.4.3 Species distribution for the complexation of Ca^{2+} with DOTP.

Figure 4.5.1 Experimental (points) and modeled (lines) formation for Cu^{2+} complexation by DOTP. pA is the negative log of the free ligand concentration. The 3 titrations are represented by (○) 1 mmol.dm^{-3} Lu^{2+} and 1 mmol.dm^{-3} DOTP, (Δ) 1 mmol.dm^{-3} Cu^{2+} and 2 mmol.dm^{-3} DOTP, and (□) 1 mmol.dm^{-3} Cu^{2+} and 3 mmol.dm^{-3} DOTP. All titrated against 0.05 mmol.dm^{-3} NaOH in 0.10 mol.dm^{-3} NaCl, at 25.0 °C and 0.15 mol.dm^{-3} total ionic strength

Figure 4.5.2 Experimental (points) and modeled (lines) formation for Cu^{2+} complexation by DOTP. pA is the negative log of the free ligand concentration. The 3 titrations are represented by (○) 1 mmol.dm^{-3} Cu^{2+} and 1 mmol.dm^{-3} DOTP, (Δ) 1 mmol.dm^{-3} Cu^{2+} and 2 mmol.dm^{-3} DOTP, and (□) 1 mmol.dm^{-3} Cu^{2+} and 3 mmol.dm^{-3} DOTP. All titrated against 0.05 mmol.dm^{-3} NaOH in 0.10 mol.dm^{-3} NaCl, at 25.0 °C and 0.15 mol.dm^{-3} total ionic strength

Figure 4.5.3 Species distribution for the complexation of Cu^{2+} with DOTP

Figure 4.6.1 Experimental (points) and modeled (lines) formation for Mg^{2+} complexation by DOTP. pA is the negative log of the free ligand concentration. The 3 titrations are represented by (○) 1 mmol.dm^{-3} Mg^{2+} and 1 mmol.cm^{-3} DOTP, (Δ) 1 mmol.dm^{-3} Mg^{2+} and 2 mmol.dm^{-3} DOTP, and (□) 1 mmol.dm^{-3} Mg^{2+} and 3 mmol.dm^{-3}

DOTP. All titrated against 0.05 mmol.dm^{-3} NaOH in 0.10 mol.dm^{-3} NaCl, at 25.0 °C and 0.15 mol.dm^{-3} total ionic strength

Figure 4.6.2 Experimental (points) and modeled (lines) formation for Mg^{2+} complexation by DOTP. pA is the negative log of the free ligand concentration. The 3 titrations are represented by (○) 1 mmol.dm^{-3} Mg^{2+} and 1 mmol.cm^{-3} DOTP, (Δ) 1 mmol.dm^{-3} Mg^{2+} and 2 mmol.dm^{-3} DOTP, and (□) 1 mmol.dm^{-3} Mg^{2+} and 3 mmol.dm^{-3} DOTP. All titrated against 0.05 mmol.dm^{-3} NaOH in 0.10 mol.dm^{-3} NaCl, at 25.0 °C and 0.15 mol.dm^{-3} total ionic strength

Figure 4.6.3 Species distribution for the complexation of Mg^{2+} with DOTP

Figure 4.7.1 Blood plasma model for DOTP showing the complexation preferences of the ligand under physiological conditions for Lu: DOTP of 1:10

Figure 4.7.2 Blood plasma model for Lu when administered as Lu-DOTP

Figure 4.8 Blood plasma mobilization indexes (PMI) of DOTP for Ca^{2+}, Mg^{2+} and Cu^{2+}

Figure 4.9 Linear free energy relationship of formation constants for blood plasma ligands (◆) represents literature constants:Lu^{+3} vs Gd^{+3} and (Δ) represents the calculated constants for Lu^{3+}

List of Tables

Table 1.1 Radiation properties of reactor-produced radiolanthanides used in radiotherapy.

Table 3.1 Composition of protonation titrations for all ligands studied

Table 3.2 Composition of metal-ligand titrations

Table 4.1 Acid dissociation equilibria and constants for (DOTP) and the complex formation constants with selected metal ions of physiological significance (where L represents the deprotonated ligand). Determined by glass electrode potentiometry and ESTA modeling, at 25 °C and ionic strength (μ) of 0.15 mol.dm^{-3} NaCl.

Table 4.3 ECCLES results of potential ligands that will complex with Lu^{3+}

Table 4.4 Protonation constants of citrate, Lactate, Glycinate, Glutaminate, and Threoninate determined at 25 °C and 0.15 M NaCl.

Table 4.5 The dominant species of each system at the physiological pH 7.4 and their percentage mole fraction.

List of Abbreviations and Symbols

APD	1-Hydroxy-3-amino-propylidene diphosphonate
APDDMP	N, N-dimethylenephosphonate-1-hydroxy-4-aminopropylidene-diphosphonate
β	decay by emission of beta-particle
Bq	Becquerel a unit of radioactivity which is equal to one decay/s
°C	degrees Celsius
Ci	Curie a unit of radioactivity, $1Ci = 3.7 \times 10^{10} Bq$
CT	Computed Tomography
DTPA	Diethylenetriaminepentaacetate
DOTMP	1, 4, 7, 10-tetraazacyclododecane-1, 4, 7, 10-tetramethylene-phosphonic acid
E°	Electrode constant
ECCLES	Evaluation of Constituent Concentration in Large Equilibrium Systems
EDTMP	Ethylenediamine tetramethylenephosphonate
ESTA	Equilibrium Simulation for Titration Analysis
GEP	Glass Electrode Potentiometry
HEDP	1, 1-hydroxyethyline diphosphonate
keV	kilo electron volt
L	ligand
LFER	Linear Free Energy Relationship

log β	logarithm of the overall formation constant
log K	logarithm of the stepwise formation constant
M	metal ion / $mol.dm^3$
MeV	mega electron volt
MDP	Methyl diphosphonate
MRI	Magnetic Resonance Imaging
Necsa	South African Nuclear Energy Corporation
pA	negative logarithm of the free deprotonated ligand concentration
pH	negative logarithm of the free acid concentration
PET	Positron Emission Tomography
R	Gas constant
SCE	Saturated calomel electrode
CARST	Centre for Applied Radiation, Science and Technology
DOTA	1, 4, 7, 10-tetraazacyclododecane-1, 4, 7, 10-tetraacetic acid
CTMP	1, 4, 8, 11-tetraazacyclotetradecane-1, 4, 8, 11-tetramethylene-phosphonic acid
JESS	Joint Equilibrium Speciation System
GLY	Glycine
THR	Threonine
CTA	Citrate
LTA	Lactate

GLN	Glutamine
LU+3	Lu^{3+}

Chapter 1

INTRODUCTION

1.1 Introduction

Cancer cells which are abnormal keep dividing even when new cells are not needed. The skeleton is frequently affected by painful metastases from advanced breast, prostate, lung, kidney, thyroid, and renal cancers [1, 2, 3]. Bone metastasis occurs when cancer cells from the primary tumor relocate to the bone. Cancer metastasizes (spreads) when cells from cancerous tumor (a primary tumor) break away and travel to other parts of the body through the bloodstream or lymph vessels. Moving through the bloodstream or lymphatic system, cancer cells can lodge in an organ at a distant location and establish a new (secondary) tumor. A tumor that has metastasized to bone consists of abnormal cancer cells from the original tumor site and not of bone cells. Paget [2] proposed that the affinity of certain cancers to metastasize to bone is due to the fact that the bone provides a 'fertile soil' or environment for the cells to germinate.

Bone pain due to metastasis is often considered a unique type of pain. It is initially a dull or aching pain, worse at night [3]. If pain increases with physical activity, the risk of imminent fracture is increased. There are two types of bone lesions: lytic lesions, which destroy bone material, and blastic lesions, which fill up bone with extra cells. Normal bone is in a constant state of remodeling - being broken down and rebuilt. Cancer cells that have spread to the bone disrupt this balance between the activity of cells that break down bone (osteoclasts) and cells that make bone (osteoblasts). Bone metastasis may be found anywhere in the skeleton, but generally occur in the central parts of the skeleton. More than 90% of all metastases are found in the back, pelvis, upper leg, ribs, upper arm, and skull. Although bone metastases are often clinically silent, they can lead to serious sequelae, such as pain, hypercalcemia, increased risk of fracture, raised calcium levels in the blood, nerve compression, and a decreased blood cell count. These complications often reduce performance status and decrease the quality of life [4]. Bone metastases are found more commonly in middle-aged to elderly people and uncommon in children.

Cancer cells that spread to bone can cause damage in two ways:

- The tumor may wear away bits of bone, creating small holes called osteolytic lesions. This process can make bones fragile and weak so that they can break or fracture easily.
- The tumor may stimulate bone to form and build up abnormally. These areas of new bone are called osteoblastic or osteosclerotic lesions. They are weak and unstable and may break or collapse [1].

1.2 Radiopharmaceuticals

Radiopharmaceuticals are generally classified as either being diagnostic or therapeutic in their application. These radiopharmaceuticals are helpful in diagnosing the disease and also render an antitumor effect at low chemical levels. A therapeutic radiopharmaceutical emits particulate radiation that typically travels short distances in body tissue, where it destroys or inflicts damages on the surrounding cells bringing pain relief in the area to which it has distributed [5]. An ideal radiopharmaceutical to be used for bone pain palliation should therefore selectively localize in bone and concentrate in skeletal lesions, thereby delivering adequate dose at the osteoblastic lesion sites at skeletal surface while rendering minimum dose to the red bone marrow [6]. Also, detection of bone of tumor in bone metastases is essential for optimal therapy. This leads to development of diagnostic radiopharmaceuticals which could be used to detect bone metastases as early as possible.

1.2.1 Diagnostic Radiopharmaceuticals

Skeletal involvement occurs in 30 to 70% of all cancer patients, with breast cancer being the leading cause for bone metastases in women and prostate cancer in men followed by lung cancer [7]. Therefore skeletal imaging is very vital. The purpose of imaging is to identify bone metastases as early as possible, thereby determining the full extent of the disease, evaluating the presence of complications that may accompany malignant bone involvement, monitoring response to therapy and guiding biopsy if histological confirmation is needed [8]. Because of radiation's damaging effect on tissues, it is important to target the biodistribution of radiopharmaceuticals as accurately as possible.

Ideal diagnostic radiopharmaceuticals possess a radioactive isotope with the characteristics of a gamma ray emitter. The ideal energy range for the radioisotope is 100-250 keV and must decay by electron capture or isomeric transition. Therefore bone scintigraphy (BS) is a commonly used method for detection of bone metastases because it is widely available and provides an entire skeletal visualization within a reasonable amount of time and cost [9]. Examples of these radioisotopes are ^{99m}Tc, ^{201}Tl, ^{133}Xe, and ^{18}F.

The most frequently used imaging isotope is technetium. In technetium-based imaging, many different molecules can be labeled by means of this isotope. These molecules are administered to the patient, enabling visualization of the radiopharmaceuticals by means of specific imaging equipment. This application is used for diagnostic purposes in various medical areas, including oncology and cardiology, as well as in bone scanning and the functional imaging of organs such as kidneys, liver, brain and lungs. The most widely used nuclide in diagnostic nuclear medicine is the metastable isotope of technetium (^{99m}Tc). ^{99m}Tc is an ideal radionuclide for organ imaging studies because of its optimum energy (140 keV), short half-life (6 h), low cost and wide availability [10]. ^{99m}Tc can be labeled with a variety of compounds which stabilize the nuclide and direct it to the part of the body that needs to be imaged. For example, ^{99m}Tc-Methylene diphosphonate (^{99m}Tc-MDP) is the most commonly used diagnostic radiopharmaceutical and Figure1.1 illustrate images produced using this radiopharmaceutical. Another new potential technetium radiopharmaceutical is ^{99m}Tc-5-etoxycarbonyl-4-phenyl-6-methyl-3,4-dihydro-(1H)-pyrimidine-2-one (DHPM) [11] which is suitable for lung perfusion imaging.

Another approach that may offer advantages for detecting, characterizing, and quantifying changes in bone metastases is the use of ^{18}F-fluoride PET. ^{18}F is taken up by mineralizing bone in proportion to osteoblastic activity [12]. The uptake mechanism of ^{18}F-Fluoride is similar to that of ^{99m}Tc-MDP. After diffusion through capillaries into bone extracellular fluid, fluoride ions exchange with hydroxyl groups in hydroxylapapite crystal bone to form fluroapatite, which is deposited mainly at the surface, where bone remodeling and turnover are greatest. There are various morphologic and functional

imaging modalities for the assessment of bone involvement , including plain radiography (XR), CT, MRI, bone scintigraphy (BS), PET with ^{18}F-FDG or ^{18}F-Fluoride, and recently, integrated SPECT/CT and PET/CT. [9,13,14]

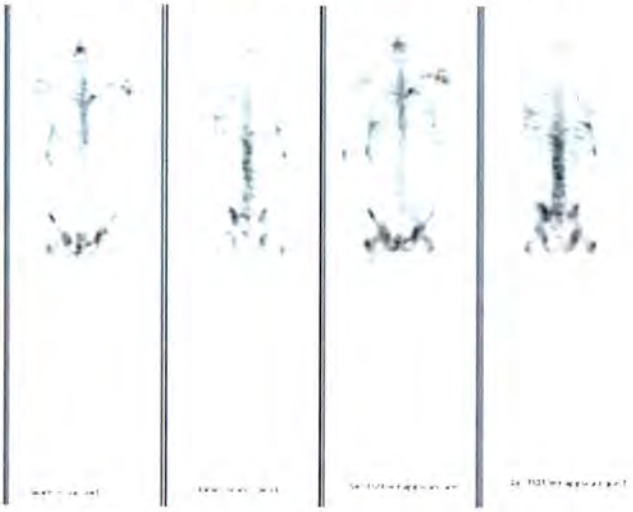

Figure 1.1 ^{99m}Tc-MDP bone scan, anterior and posterior views and the ^{153}Sm post-therapy scan, anterior and posterior views of male cancer patients with multiple skeletal metastases [15].

1.2.1 Therapeutic Radiopharmaceuticals

Palliative relief of bone pain is a very important factor for cancer patients, and quality of life can be maintained by effective pain palliation treatment. Bone metastases can be treated using various methods, for example: external beam radiation therapy, gene therapy, chemotherapy, stimulation of bone formation, hormone manipulation agents, analgesic therapy, bisphosphonates, and radiation therapy using radiopharmaceuticals [6]. Although many of these treatments are used to the present day, they are limited in their efficacy or duration and have significant side effects that seriously limits the life of the cancer patient. Radionuclide therapy employing bisphosphonates labeled with bone-seeking radionuclides, and which emit β^- or conversion electrons is an effective option for bone pain palliation and could provide a significant improvement in the quality of life of the patients [16]. A therapeutic radiopharmaceutical emits particulate radiation that typically travels short distances in body tissue, where it destroys or inflicts damages on the surrounding cells bringing pain relief in the area to which it has been distributed [7]. An ideal radiopharmaceutical to be used for bone pain palliation should therefore

selectively localize in bone and concentrate in skeletal lesions, thereby delivering an adequate dose at the osteoblastic lesion sites at the skeletal surface while rendering minimum dose to the red bone marrow [8]. It has been demonstrated that the penetrating ability of the particulates emitted from the radionuclides can have profound implications on the potential success of the bone pain palliatives, and consequently, moderate energy β^- emitting radionuclides are considered to be efficacious. β-emitting radiopharmaceuticals for bone targeting, such as ^{32}Phosphate and ^{89}Sr- chloride, have been used clinically for treatment of bone pain [17]. Although these β-emitters relieve bone pain associated with metastatic lesions in the skeleton, bone marrow toxicity is a disadvantage as it limits the use of high dose radiations to prevent tumor progression due to the long radiation range of β-particles. To overcome this problem, clinical use of several low-energy β-emitters, including ^{153}Sm, ^{177}Lu, and ^{186}Re and the conversion electron emitter ^{117m}Sn [18], have been examined.

Among these radionuclides, ^{153}Sm complexed with ethylenediamine-tetramethylenephosphonic acid (EDTMP) has been approved for use in palliation of bone pain. In this study ^{177}Lu is complexed to EDTMP and 1,4,7,10-tetraazacyclododecane-1,4,7,10-tetra(methane-phosphonic acid) (DOTP). The mechanisms by which pain relief is thought to occur remain ambiguous. The theory on how radiopharmaceuticals work in pain palliation treatment is that the radionuclide is carried by the bone-seeking ability of its carrier (ligand) to areas of increased osteoblastic activity, where it then chemisorbs to the osseous tissue [19]. Radiation of the attached radionuclide will then cause percentage cell apoptosis within the range of the β (2mm soft tissue penetration for ^{177}Lu and 3mm for ^{153}Sm) or of the electron (<1mm for ^{117m}Sn). The resulting reduction for intra-osseous mass and pressure brings pain relief to the patient.

1.3 Lanthanides in Radiopharmaceuticals

The use of lanthanides complexed with bone-seeking bisphosphonates for palliation of bone pain due to metastatic skeletal lesions from several types of primary and secondary cancers has been a topic of considerable interest for the last decades [20-24]. The

chemistry of the lanthanides differs from the main group elements and transition metals because of the nature of the 4f orbitals. These 4f electrons are buried into the core of the atom and unable to participate in bonding. The effect results in the poor shielding of nuclear charge by 4f electrons which produces a steady increase in the effective nuclear charge (Z_{eff}). Thus, each unit increase in nuclear charge produces a net increase in attraction for the whole extranuclear electron charge cloud and each ion shrinks slightly in comparison with its predecessor. This leads to smaller atomic radii than would normally be expected. This trend is called the Lanthanide Contraction. Lanthanides adapt the +3 oxidation state in compounds, except for cerium (Ce) and europium (Eu) which can exist as tetravalent species (Ce^{4+}) and bivalent species (Eu^{2+}). Lanthanides are highly electropositive and reactive metals. Their coordination number is variable across the series ranging from 6 to 12, but with a preferred coordination number of 8 or 9. The lanthanide ions are very close to Ca^{2+} in their properties and their pharmacological effects originate from their deviation in charge, radii and 4f orbital involvement. The toxicity of lanthanides decreases with increasing atomic number, due to a greater solubility, and ionic stability, and smaller radius [25].

Most lanthanides have properties that are useful for diagnosis and therapy. Gadolinium(III) (Gd^{3+}) complexes dominate the research work into macrocyclic contrast agents and their clinical application in magnetic resonance imaging (MRI) [26, 27, 28]. Gd^{3+} has two key properties that make it an ideal choice, it is highly paramagnetic due to its seven unpaired electrons and also has relatively slow electronic relaxation due to its symmetric S-state. Gd^{3+} has a high magnetic moment ($\mu^2 = 63\ \mu_B^2$) which is an important property that is useful for enhancing MRI scanning of tumors. Of the six MRI contrast agents now available clinically, four are Gd^{3+}-based, and all are in clinical use [29]. For example, Gd^{3+}-DTPA and Gd^{3+}-DOTA are clinically used as bone-seeking contrast imaging agents. Recently, a new application for lanthanum carbonate (Fosrenol) as a phosphate binder for the treatment of hyperphosphatemia in renal dialysis patients has been approved [30]. Rapid and complete excretion of the lanthanum is generally desirable and lanthanum carbonate is a good counter-example because it is thermodynamically stable.

The lanthanides have also been investigated for the treatment of liver toxicity, atherosclerosis, rheumatoid arthritis, as luminescence probes in cell studies, and for palliative treatment of skeletal metastases. Regarding the latter, an important class of radiotherapy agents has been evaluated and developed for effective pain palliative therapy and treatment of skeletal metastases. Most of the radiolanthanides emit both β^- electrons that are used for therapy and γ-rays that are appropriate for imaging. These therapeutic agents must possess an affinity for bone tissue, as well as low levels of toxicity to the healthy bone marrow which is very sensitive. The radiolanthanides are particularly attractive and advantageous in the development of radiotherapeutic agents in that they have relevant properties (e.g. high specific activity and radionuclide purity, radiation characteristics, and half life) specifically needed for them to be considered for use in radiotherapy [20]. In addition, the production of many radiolanthanides via (n,γ) reaction in high yields is possible due to the relatively high neutron cross sections of the lanthanide target materials. It has been demonstrated that the penetrating ability of the particulates emitted from the radionuclides have profound implications on the potential success of the radiopharmaceuticals used in bone pain palliation, and consequently moderate energy β^- or conversion electron emitting radionuclides are considered to be the most efficacious candidates [31].

^{153}Sm, ^{166}Ho, ^{175}Yb, and ^{177}Lu are radiolanthanides that exhibit these properties for use in treatment of bone pain palliation. These radioisotopes which emit β^- particles suitable for radiotherapy have been largely evaluated with bone-seeking multidentate aminomethylenephosphonic acids (EDTMP, DOTP, CTMP, etc.) forming well-characterized thermodynamic and kinetic stable complexes. Enriched ^{152}Sm is normally used as the target for the preparation of ^{153}Sm-EDTMP. However, due to logistic reasons, ^{153}Sm ($T_{½}$ = 46.3 h) needs to be produced in adequately high specific activity for the administration of required doses to patients, which in turn necessitates handling of high amounts of activity during processing. In this study, ^{177}Lu is regarded as an attractive and most promising alternative radiolanthanide to the well established ^{153}Sm-EDTMP for bone pain palliation. The important attributes of ^{177}Lu as an attractive radionuclide for bone pain palliation emerge from its suitable nuclear decay characteristics [$T_{½}$ = 6.73 d,

$E_{\beta(max)}$ = 497 keV, E_γ = 113 keV (6.4%) and 208 keV (11%)] which are ideally suited for imaging the *in vivo* localization [28]. The long half-life of ^{177}Lu provides a logistic advantage for facilitating supply to places far away from the reactors [32] as compared to other lanthanides previously evaluated for bone pain palliation (Table 1.1). Taking into consideration the use of 6 x $T_{½}$ for complete decay when applied for tumour cell inactivation, ^{177}Lu is advantageous compared to other bone-seeking radioisotopes such as ^{89}Sr (50.5 d), ^{32}P (14.3 d), and ^{117m}Sn (13.6 d) which requires radiation safety precautions for the collection of urine and for the mortuary and crematorium personnel should the patient die shortly after treatment.

Table1.1 Radiation properties of reactor-produced radiolanthanides used in radiotherapy

Radionuclide	Maximum β Energy (MeV)	Half-life	Cross-section (barns)	
			Thermal	Epithermal
^{140}La	1.34	0.3 h	9.2	11.6
^{142}Pr	2.16	19.1 h	11	17
^{153}Sm	0.81	46.3 h	210	3168
^{159}Gd	0.95	18.6 h	3.1	96
^{165}Dy	1.29	2.33 h	2720	510
^{166}Ho	1.86	26.8 h	58	636
^{170}Tm	0.968	128.6d	105	1700
^{177}Lu	0.43	6.71 d	2100	1160

The energies of ^{177}Lu being adequately low, and with an average penetration range of 2 mm in soft tissue [32], it is expected to have minimum bone marrow suppression on accumulation in skeletal lesions. Considering that 50-70 mCi is the patient dose for ^{153}Sm, 35- 40 mCi for ^{186}Re and about 4-5 mCi for ^{89}Sr for the same application, the dose requirement for ^{177}Lu is expected to be lower, say ~ 15-20 mCi, than that of ^{153}Sm and ^{186}Re to give the same cumulative dose. Taking into consideration the comparatively lesser decay loss as well as the lower per patient dose, it will be possible to treat at least 10 times more patients with the same amount of activity with ^{177}Lu as compared to ^{153}Sm.

The logistic advantages obtained from the use of ^{177}Lu having a comparatively longer half-life as well as the possibility of its production with adequately high specific activity in moderate flux reactors due to the high thermal neutron capture cross-section (σ = 2100 b) of the reaction [$^{176}Lu(n,\gamma)^{177}Lu$] are additional and definitive advantages towards regarding this isotope for bone pain palliation [33].

1.4 Macrocyclic chelators complexed with lanthanides

In designing suitable radiolabeled agents for palliative care of bone pain due to metastatic skeletal lesions, multidentate macrocyclic polyaminophosphonic acids are also found to be the most promising candidates as carrier ligands owing to their high bone affinity, selective localization in skeletal lesions and ability to form metal chelates with high *in vivo* stability, especially with lanthanides [34, 35]. These lanthanides are caged by the organic chelates which consist of arms with negatively charged groups, for example PO_3^-. The electrostatic attraction between these arms and the positively charged lanthanide ion results in folding of the arms to form a cage separating the toxic lanthanide from the biological environment [36]. Based on this appendix A provides a possible structure of Lu-DOTP. At the same time, the overall charge of the chelate, being negative, increases the uptake of the agent by the skeletal system, for example due to the electrostatic attraction of the positive ions of Ca2+, which are present in bone tissue [36]. These macrocyclic ligands are designed as the tissue selective cage encapsulating the lanthanide ion, forming monomeric and water-soluble complexes, in order to address it to a particular place in the organism to detect and eventually cure the tissue from cancer. The symmetry, geometry and structural properties of organic chelators such as DOTA, DOTP, EDTMP and CDTMP are well described in literature [36]. Because of the cyclic and organized nature of ligands, the complexes are thermodynamically stable and kinetically inert [37]. Thermodynamic stability of the metalloradiopharmaceutical is a very important aspect as the dissociation of the radiometal from the chelate in blood circulation may result in accumulation of radioactivity in non-target organs [33]. Therefore stability is a key issue for any complex in a biological system, as to retain its

desired functionality, the metal ion must remain bound, and in some cases the complex must be excreted intact.

Kinetic inertness which involves structural factors such as the rigidity, the cavity size, and the nature and number of donor atoms of the macrocyclic bifunctional chelators [38] also plays an important role for the *in vivo* stability of a metal chelate as accumulated body of literature [39, 40, 41] has shown that corresponding complexes containing macrocyclic chelators are much more kinetically inert than acyclic chelators [42]. Macrocyclic chelators are widely used as bifunctional chelators to bind copper radionuclides to antibodies and peptides owing to their relatively high stability under biological conditions. Three tetraaza macrocyclic ligands with two, three, and four pendant methanephosphonate functional groups namely 1,4,7,10-tetraazacyclododecane-1,7-di(methane-phosphonic acid) (DO2P), 1,4,7,10-tetraazacyclododecane-1,4,7-tri(methane-phosphonic acid) (DO3P), and 1,4,7,10-tetraazacyclododecane-1,4,7,10-tetra(methane-phosphonic acid) (DOTP) were all radiolabeled with ^{64}Cu and the thermodynamic stability constants of the Cu(II) complexes with these three ligands were determined [43].

1.5 Research Objectives

This research focuses on developing the effective therapeutic radiopharmaceuticals that will treat cancer arising from distant organs (prostate, breast, etc) and metastasizing to bone. These radiopharmaceuticals are intended for bone pain palliation ensuring low levels of toxicity to the more sensitive bone marrow and also avoiding accumulation of radioactivity in non-target organs resulting from the dissociation of the radiometal chelating in blood circulation. The aim was to study the behaviour of ^{177}Lu with selected blood plasma ligands thereby determining the stability of their complexes. In so doing their susceptibility to competition by the free metal-ions and ligands that are typically present within human blood plasma can be evaluated and therefore be accounted for with the aid of a computer program ECCLES (Evaluation of Constituent Concentrations in Large Equilibrium Systems) and hence establishing a blood plasma model for ^{177}Lu. This

objective involved studying the protonation of the physiological ligands (citrate, lactate, glycinate, glutaminate and threoninate) which exhibit affinity for Lu^{3+} and their complexation behaviour with Lu^{3+} by glass electrode potentiometry (GEP). These blood plasma ligands where selected by running both ECCLES and JESS program, and from ECCLES taking all the lutetium complexes, and from JESS extracting all the ligands complexing with Gd^{3+} and Sm^{3+}. All the values were added into ECCLES and then the program was run to give forth the ligands. These ligands were then taken to be evaluated with Lu^{3+} as they showed competition for EDTMP in blood plasma. Glutamine was included because its formation constants with Gd^{3+} and Sm^{3+} could not be found in both ECCLES and JESS databases.

The data obtained from potentiometric experiments will be processed by a computer package of programs known as ESTA (Equilibrium Simulation by Titration Analysis) for the optimization of data and refinement of formation constants. These formation constants are used to simulate the binding interactions of *in vivo* free metal ions and ligands using ECCLES and thereinafter to extrapolate the unknown constants for the remaining blood plasma ligands by means of linear free energy correlations (LFER), and hence develop a blood plasma model for ^{177}Lu. Once the blood plasma model has been determined then it will be clearly seen whether the potential ligands, ethylenediaminetetramethylene phosphonic acid (EDTMP) and 1,4,7,10-tetraazacyclododecane-1,4,7,10-methylene phosphonic acid (DOTP) which exhibit affinity for bone will be able to survive the free metal ions (Ca^{2+}, Mg^{2+}, Cu^{2+}, and Zn^{2+}) in the body and be successfully delivered to the target organ still intact with ^{177}Lu. EDTMP was chosen as an alternative ligand because it forms complexes of high stability with lanthanide ions (Ln^{3+}). ^{153}Sm-EDTMP is used routinely as a radiopharmaceutical for bone pain palliation treatment. All the experimental work in this thesis was performed with stable Lu which served as a simulant for ^{177}Lu as they have similar chemical properties.

The following are the structures of the ligands studied with Lu^{3+}.

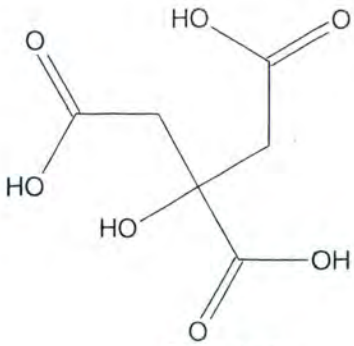

Citric Acid

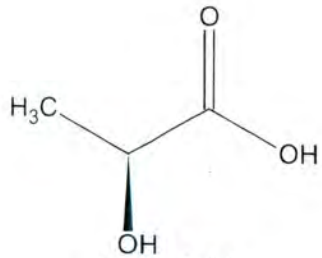

Lactic Acid

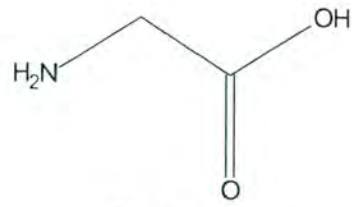

Glycine

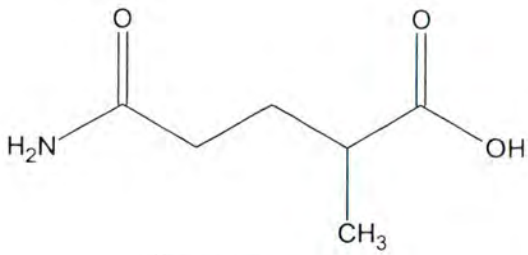

Glutamine

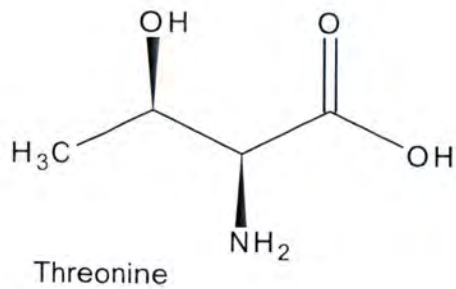

Threonine

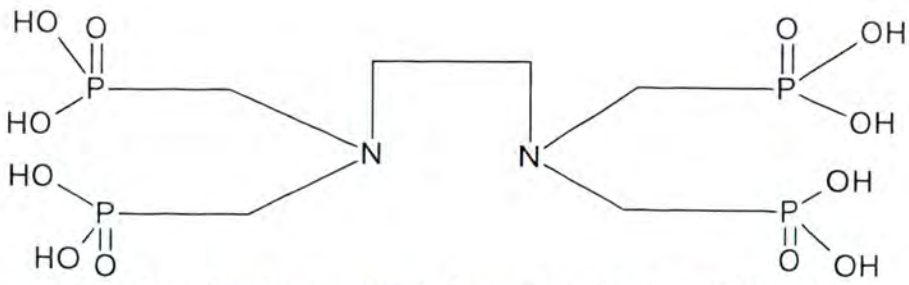

Ethylenediaminetetramethylene phosphonic acid (EDTMP)

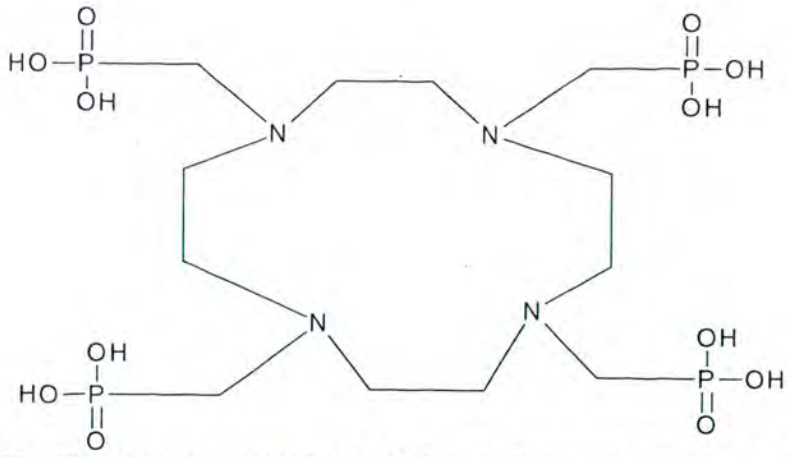

1,4,7,10 –tetraazacyclododecane-1,4,7,10-tetramethylenephosphonic acid (DOTP)

1.6 Thesis outline

Chapter 1 gives an insight into basic background about how cancer can spread from other parts of the body to bone and the therapy options available for bone pain metastases. A discussion on how bisphosphonates and macrocyclic chelators are potential ligands that can be used as a form of bone seeking radiotherapeutic agents is included in this chapter. An explanation of how ^{177}Lu is regarded as a potential radionuclide. The objectives of this study are also described in detail. Background information about the methodology used to determine formation constants is described in more determined in Chapter2. Chapter 3 explains in detail how all the experiments were performed. The results of all the experiments performed are discussed in this chapter. This entails the measurement of the stability constants of Ca^{2+}, Cu^{2+} and Mg^{2+} with DOTP. Blood plasma models and PMI curves are constructed in this chapter. Chapter 5 focuses on concluding on the findings and recommendations of future work. It focuses on the achievements of the objectives and recommends a way forward on improving the radiopharmaceutical. The failure to conclude the EDTMP work which led to unsuccessful establishment of a blood plasma model for Lu(III). References are included in this chapter.

Chapter 2

THEORY

2.1 Determining formation constants with potentiometry

Potentiometry is the main technique used to determine the formation constants of metal ions and ligands that constitute the essential input needed to construct blood plasma modeling. Basically the method is based on the interpretation of electrode potentials generated by the electrochemical interaction between Lewis acids (metal ions) and bases (ligands). The electrode potentials arise due to the movement of electrons between the two entities consisting of what is called half reactions. During the reaction, the rates of the two half-reactions become equal and equilibrium is reached [44]. The redox potential difference is measured with respect to a standard electrode. Several sorts of electrodes are commonly used. The standard electrode is a hydrogen half-cell, with the following reaction:

$$H_2\,(gas) \rightleftharpoons 2H^+ + 2e^- \qquad (2.1.1)$$

and schematically represented as

$$Pt,\ H_2(p = 1.00\ atm)\ |\ ([H^+]) = 1M)\| \qquad (2.1.2)$$

where all components are in their standard states (1 atm pressure for the gas, 1 M activity for the proton, or pH 0). Standard Hydrogen Electrode (SHE) consists of a catalytic Pt surface in contact with an acidic solution in which $A_{Ag^+} = 1$. The platinum metal serves as a site for electron transfer and does not take part in the reaction. The function of the SHE is to bubble hydrogen gas over the platinum metal. The standard hydrogen electrode is an ideal reference electrode with a potential of 0.000 V. The net reaction is composed of a reduction reaction and oxidation reaction. The redox potential for a couple is usually assumed to be the value with respects to the standard electrode potential [45]. The equilibrium reduction potential of a half-cell in an electrochemical cell can be determined by the Nernst equation which relates the cell potential to the standard potential and to the

activities of the electroactive species. The electrode potential of a half-reaction can be calculated from the concentrations of the individual species comprising the process, as well as the conditions such as temperature and, in some instances, pressure. For the reaction

$$aA + bB + \ldots ne^- \rightleftharpoons cC + dD \qquad (2.1.3)$$

where A, B, C, D represent molecular species, e^- denote the electron, and the lower case a, b, c, d indicate the number of moles of each species (including electrons) participating in the given half-cell reaction. The electrode potential E for this reaction can be written as

$$E = E^{0} - \frac{RT}{nF} ln \frac{[C]^c[D]^d}{[A]^a[B]^b} \qquad (2.1.4)$$

where E° is the standard electrode potential. The Nernst equation is more commonly written in base 10 log form, ln = 2.303log, and substituting the constants R = 8.314 JK^{-1}, T = 298K (25 °C), F = 96485 C/mol, the equation becomes:

$$E = E^{0} - \frac{0.0592}{n} \log \frac{[C]^c[D]^d}{[A]^a[B]^b} \qquad (2.1.5)$$

Potentiometric titration is a useful analytical tool because small changes in parameters such as analyte concentration can be observed during titrimetric experiments, therefore it provides accurate determination of end-points or inflections. The stepwise dissociation of a ligand can be elucidated by gradually increasing the pH. The titration data can be analysed by software programs such as ESTA (Equilibrium Simulation for Titration Analysis).

2.1.1 Glass electrode potentiomentry

Glass electrode potentiometry (GEP) is essential to determine which species are present in solution and to determine the stability constants of these species. In GEP, the glass electrode develops potential corresponding to the activities of the species in solution, thus the use of a large excess of a neutral background electrolyte is required to keep the ionic strength of a solution and activity coefficient of all species present in a solution constant.

Figure 2.1 shows a diagram of a typical combination electrode, incorporating both the glass and reference electrodes in one body. An electrochemical cell for pH measurement always consists of an indicating electrode whose potential is directly proportional to pH, a reference electrode whose potential is independent of pH, and the aqueous sample to be measured. The pH-sensitive part is the thin glass in the shape of a bulb at the bottom of the electrodes.

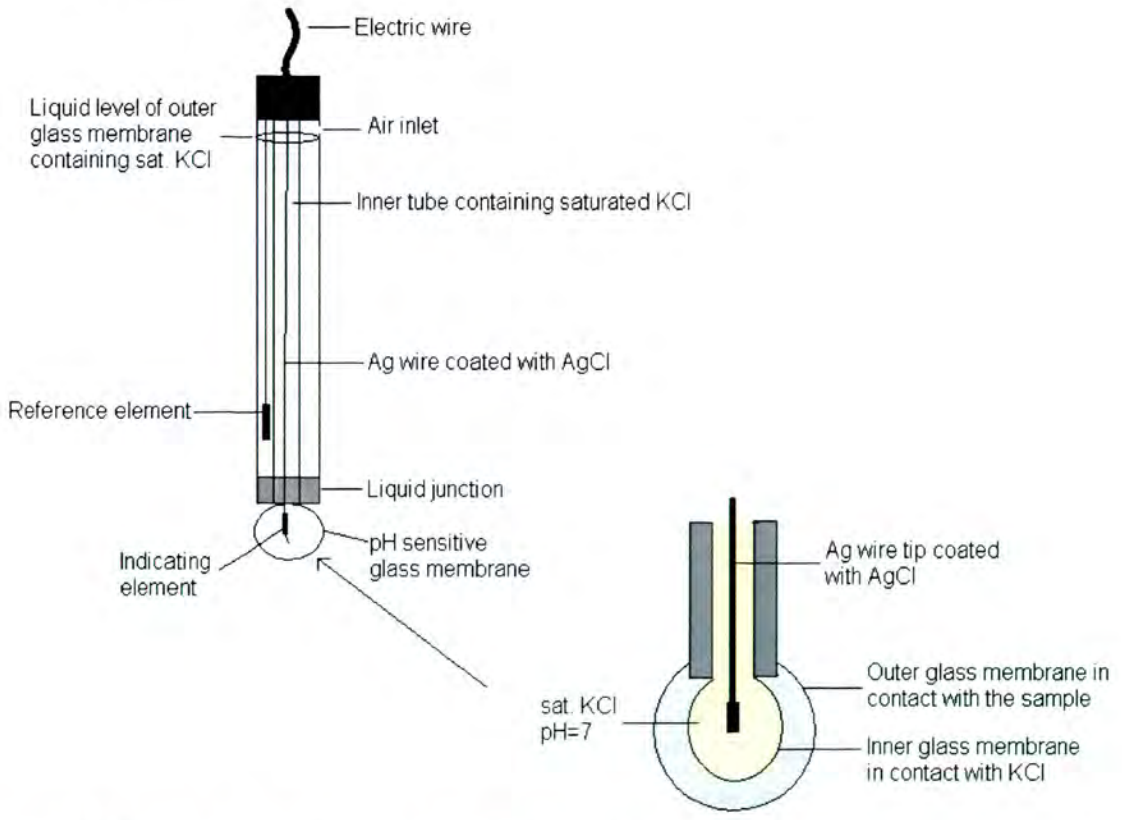

Figure 2.1 Diagram of a glass combination electrode.

When the pH probe is in contact with a solution a potential forms between the pH probe and the reference probe. The reference electrode is a silver wire coated with silver chloride in contact with a defined electrolyte solution. The liquid junction provides the electrical connection between the reference electrode and the sample being measured. Saturated KCl allows the reference system to work in a wide temperature range. At higher temperatures the additional crystals can dissolve and still maintain a saturated solution. At low temperatures more crystals form, but since the solution is already saturated, the KCl concentration is still saturated. After a soaking a glass electrode in an aqueous solution to hydrate the outer surface and convert the outer ion-exchange layer largely to the hydrogen form, it is ready for use. A potential quickly builds up on the outer surface, this potential is a function of the hydrogen-ion concentration of the test solution. This is because the hydrogen ions from the test solution enter the hydrated layer, where the activity is less then in the aqueous solution. It can be used in determination of stability constants for systems such as the following:

$$pM + qL + rH \rightleftharpoons M_pL_qH_r \qquad (2.1.6)$$

where M represents the metal, L the ligand and H the proton or hydroxide within the complex and p, q, r are the number of moles of the respective participating species. The same equation can be used to describe the proton dissociation constant of the ligand when the metal is omitted, i.e. p = 0. The equilibrium constant β, for the reaction (Equation 2.1.6) is given by:

$$\beta_{pqr} = \frac{[M_pL_qH_r]}{[M]^p[L]^r[H]^r} \qquad (2.1.7)$$

The abovementioned equation is used to calculate formation constants or protonation constant. The formation constants can only be evaluated by refining a set of initial estimates on the assumption that all the predominant complexes in the experimental solutions are already known [46]. Searches are then made with the aim of finding the correct set of species, defined as those which give the "best agreement" (using mass balance equations and minimization routines described in section 2.2) between the calculated and the experimental data.

2.2 Programs for analyzing potentiometric data

2.2.1 ESTA

The potentiometric data in this study was analyzed using the Equilibrium Simulation by Titration Analysis (ESTA) library of programs as described by May et al [47, 48]. These programs are used to calculate equilibrium distributions of chemical species, to analyse potentiometric titration data and to manipulate titration data for a variety of other purposes. ESTA imposes conditions on mass-balance equations in a standard fashion as shown by the following equation:

$$T_i^r = T_i^c, \quad i = 1 \ldots NC \tag{2.2.1}$$

Where T_i^r is the real/experimental total concentration, T_i^c is the calculated total concentration of the *i*th component, NC is the general index for the components. T_i^r and T_i^c are given by the following equations:

$$T_i^c = [X_i] + \sum_{J=1}^{NJ} r_{ji} \Gamma_j \beta_j \prod_{n=1}^{NC} [X_n]^{rjn} \tag{2.2.2}$$

$$T_i^r = \frac{C_i^v V^\circ + \sum_{m=1}^{NB} C_{im}^B \nu_m}{V^\circ + \sum_{m=1}^{NB} \nu_m} \tag{2.2.3}$$

$$\Gamma = \left(\prod_{n=1}^{NC} \gamma_n^{rjn} \right) \Big/ \gamma_j \tag{2.2.4}$$

where:

$[X_i]$ = free concentration of the *i*th component

r_{jn} = stoichiometric coefficient of component *i* in complex j

NJ = number of complexes

C_i^V = initial concentration of the ith component in the vessel

C_{im}^B = concentration of the ith component in the mth burette

V_m = total titre volume added from mth burette

V° = initial vessel volume

NB = number of burettes

γ_n = activity coefficient of species n

γ_j = activity coefficient of species j

The free concentration of hydrogen ions is known at any given time in glass electrode potentiometry and is usually calculated from the observed emf. The electrode equation is evaluated by calculating concentrations for "NC-free" concentrations to obtain the free electrode-ion concentrations. This emf is linked to the concentration of the electrode ion (hydrogen) by ESTA at each kth titration step shown by the following equation:

$$E_k = E_k^\circ + E_k^{IS} + E_k^{LJ}, k = 1, 2, 3, \ldots, n \qquad (2.2.5)$$

where E_k° is the electrode response intercept, E_k^{IS} is the electrode sensitivity, and E_k^{LJ} is the liquid junction potential. ESTA accommodates the effects of other interfering ions in solution using the Eisenman equation. The liquid junction potential term can be derived using the Henderson equation defined as follows:

$$E_k^{LJ} = -\left(\frac{RT}{F}\right)\ln\left(1 + \frac{d[XH]}{I}\right) \qquad (2.2.6)$$

where I is the concentration of the background univalent electrolyte. The Henderson [49] equation is used to correct the changes in the liquid junction potential when the glass electrode is calibrated. The equation is applicable at pH smaller than 2 where the liquid junction potential becomes significant. The more robust Secant method [50] can also be used to solve the equations for free concentrations only, in the event where the Newton-Raphson calculation is unsuccessful.

The program simulates the experimental titration data in an attempt to derive a favourable representation of the formation of complexes in the system. Electrode potentials are available and initial estimates of the corresponding free electrode-ion concentration can therefore be calculated. Initial estimates of all parameters at the third and each point of titration are best obtained by linear extrapolation of the solution from the previous two points, based on the change in the electrode potential. The Gauss-Newton algorithms are used to optimize a calculated model representation of the experimental data. The estimates of the parameters are refined repeatedly, until they are sufficiently close to the fitted model, judging by low Hamilton R-factor, and its limit. The extent to which the calculated parameters fit the experimental data is determined by observing the standard deviation of the parameters, the Hamilton R-factor, and the Hamilton R-limit. The Hamilton R-factor is the measure of the difference between the objective function (parameters being refined) and experimental data points. The closer the R-factor is to the R-limit the better the calculated parameters fit the measured data. The ESTA computer series of programs contains modules, namely ESTA1 and ESTA2, which perform one or more kinds of calculations.

2.2.2.1 ESTA1

The ESTA1 program can determine mass balance equations (m.b.e) on a point-by-point basis, single values for almost any titration parameter. The calculations fall into two categories, namely: potentiometric titration calculations, and species distribution calculations. This sequential analysis of data allows for the calculation and refinement of parameters such as the initial vessel concentrations, initial burette concentrations, and total analytic concentrations, and even the determination of emf values and electrode slope. Following are several functions used to generate results, namely:

I. $\bar{Z}_H$, the protonation function, which is defined as the average number of protons bound by the ligand (in absence of complexation) at respective pH values and is given by the equation:

$$\bar{Z}_H = \frac{[boundH]}{L_T} \qquad (2.2.2.1)$$

where

$$[\text{bound H}] = H_T - H + [OH^-] = H_T - H + K_w H^- \qquad (2.2.2.2)$$

where OH^- is the hydroxide ion and K_w is the dissociation constant of water attainable from literature, and therefore:

$$\bar{Z}_H = \frac{(H_T - H + K_W H^-)}{L_T} \qquad (2.2.2.3)$$

where H_T is the total hydrogen concentration, and L_T is the total ligand concentration. The calculated and the observed protonation constants are compared and optimized until they have comparable values. The graph $\bar{Z}_H$ vs. pH which provides information about the state of the ligand at a particular pH can therefore be plotted.

II. $\bar{Z}_M$, the complex-formation function, defined as the number of ligands bound per metal-ion(s) at respective pH values.

$$\bar{Z}_M = \frac{L_T - [H_T - H + K_W H^-]}{\bar{Z}_H} \Big/ M_T \qquad (2.2.2.4)$$

where $\bar{Z}_H$ is defined in Equation 2.2.2.3 above and M_T is the total concentration of the metal-ion. $\bar{Z}_M$ is plotted against pH, the negative logarithm of the free ligand concentrations.

III. $\bar{Q}$, the deprotonation function, defined as the average number of protons released per metal-ion due to complexation by the ligand at respective pH, and is given by:

$$\overline{Q} = \frac{\left(T_H^* - T_H\right)}{T_M} \qquad (2.2.2.5)$$

where T_H^* is the calculated total concentration of protons of the system at a certain pH. These functions can be converted into graphs by plotting the calculated potentials, E_k^{calc}, *i.e.* pH *vs* $\overline{Z_H}$ or $\overline{Q}$ (with $\overline{n}$), and $\overline{Z}$ *vs* pA, whereby the observed (experimental) functions can be compared. Species distribution of the corresponding complexes can be determined as soon as the acceptable model of formation constants, representing the interactions between the ligand and a metal-ion of interest has been derived.

2.2.1.2 ESTA2

The ESTA2 module contains two optimization programs, viz ESTA2A and ESTA2B which differ only in the way data are weighed [51]. These programs are used to determine the best values for one or more parameters based on least-square procedure applied to the whole titration. The programs allow the refinement of the following parameters:

a) Formation constants
b) Vessel and burette concentrations
c) Electrode slope and initial vessel volume

Refinement can be done by grouping any parameters together as a single entity. The approach is to model the formation constants with ESTA2A until the best values for the standard deviations and Hamilton factors are reached. Thereafter, the proposed model of formation constants can be evaluated by $\overline{Q}$ and $\overline{Z}$ comparisons. In ESTA2B, the weights are calculated once from the initial estimates of the parameters being optimized.

2.3 ECCLES

In the body, metal-ions can be found as components of proteins, complexed to low-molecular weight ligands (LWLs) that occur naturally in blood plasma, or as water-solvated aqua-ions. Calculating the speciation for a particular ligand and radionuclide

combination in blood plasma will indicate whether a complex will survive the competition of metal-ions and LWL occurring naturally in blood plasma. The blood plasma modeling provides insight into the *in vivo* behavior of the proposed bone-seeking radiopharmaceuticals. Evaluation of Constituent Concentrations in Large Equilibrium Systems (ECCLES) [18] is used to predict the speciation of metal-ions or ligands in biological fluids such as blood plasma. The program takes into account the reactions between free metal ions and LWLs. The total concentration of proteins present in blood plasma greatly exceeds the total metal-ion concentration and the free metal-ion concentration is much less than that of the protein bound metal-ions, therefore the protein binding (irreversibly or reversibly) on metal ion-LWL equilibria is important, to buffer the free metal-ion concentration so that it remains constant. In developing a speciation model, a series of chemical equilibria denoting all the chemical species being investigated are generated and the equilibrium constants for the reaction have to be specified.

$$S_j = \beta_j \prod_i X_i^{k(i,j)} \qquad (2.3.1)$$

where S_j is the species concentration, β_j is the equilibrium constant, X_i is the free component concentration and k(i,j) is the component stoichiometric coefficient. The series of equilibria, together with the total or free concentration, establish the computer model of the system. From these, mass-balance equations can be solved iteratively for the free component concentrations using the ECCLES computer program.

$$T_i = X_i + \sum_j S_j k(i,j) \qquad (2.3.2)$$

During blood plasma calculations, the free metal-ion concentration is fixed, whilst the total metal-ion concentration is allowed to vary, but within blood plasma levels. The distribution of essential transition metal-ions (Ca^{II}, Mg^{II}, Zn^{II}, Fe^{II}, Mn^{II}, Pb^{II}, Cu^{I}, Ni^{II}, Cu^{II}, and Fe^{III}) is calculated as they are bound among a variety of ligands, forming different complexes. The calculations allow for the complexation of more than one ligand per metal-ion, that is binary and ternary complexes. Part of the output of the ECCLES program is the plasma-mobilization index (p.m.i.). This is defined as the ratio of the total

concentration of low-molecular-mass (l.m.m.) species of the metal ion after addition of the species to blood plasma to the total concentration of l.m.m. complexes before addition.

$$\text{pmi} = \frac{\text{total concentration ion of low-molecular-mass metal complexes in normal plasma}}{\text{total concentration ion of low-molecular-weight metal complex species in the presence of the drug}}$$

The p.m.i. values give an indication of which blood plasma metal ions are mobilized by the added ligand (which will act as a drug). This may be used as a screening method to predict the loss of biologically important metal-ions from blood plasma. The metal-ions which are mobilized by the ligand can then be accounted for by giving patients mineral supplements. In this study, p.m.i values were computed by ECCLES for the blood plasma metal-ions Ca^{II}, Mg^{II} and Cu^{II}.

2.4 Linear Free Energy Correlations

The use of linear free energy relationships (LFER) to determine stability constants is well known [48, 52]. These relationships can be useful in helping to elucidate reaction mechanisms and in predicting unknown formation or rate constants. Hammett was the first to illustrate this relationship [53]. He noted that a particular substituent on a benzoic acid ring would affect its degree of ionization (pK_a) in a similar manner as it would effect other reactions. By way of an illustration: a *meta*-chloro group would affect the pK_a of benzoic acid in a manner similar to that of phenylacetic acid. The plot is shown in Figure 2.4.1. The LFER approach was extensively used to estimate the formation constants of Sn^{II} [50] and Sn^{IV} [54] by blood plasma ligands. In the former, the formation constants of Sn^{IV} by some of the blood plasma ligands that are available in the literature were correlated with the constants for these ligands with Cu^{II}, Pb^{II} and Zn^{II}. An example of this correlation is shown in Figure 2.4.2 [50]

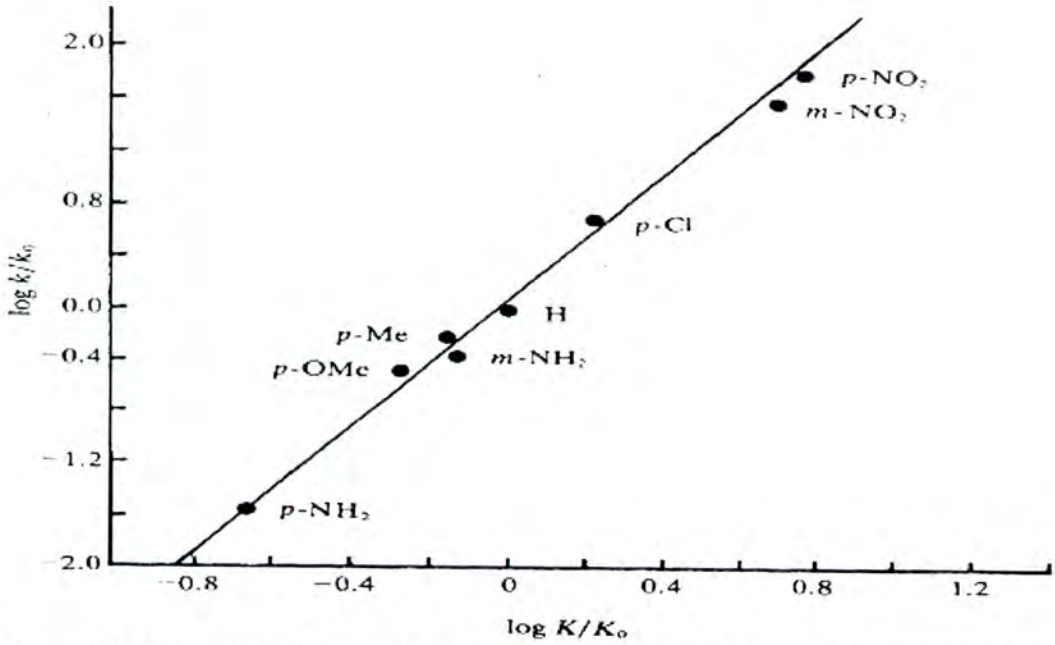

Figure 2.4.1 *Correlation of acid dissociation constants of benzoic acids with rates of alkaline hydrolysis of ethylbenzoates. [53]*

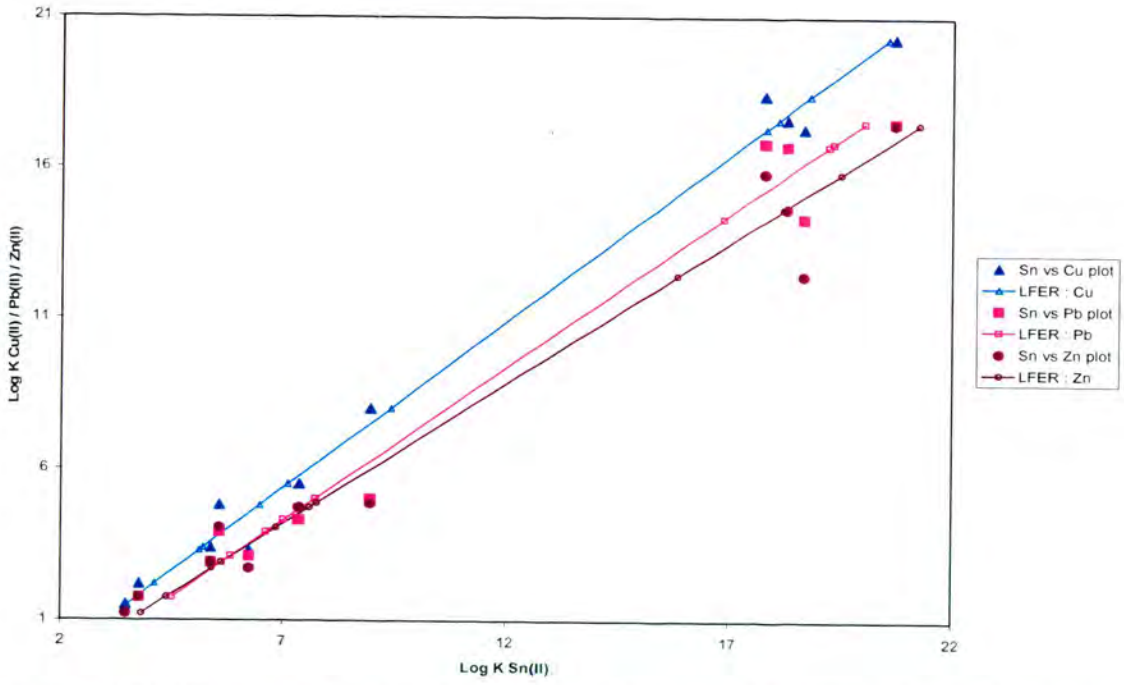

Figure 2.4.2. *Linear free energy plots fot the relation between the first formation constants of the complexation of Sn^{II} by a selected number of blood plasma ligands and the first formaiton constant of Cu^{II} (▲), Pb^{II} (■), and Zn^{II} (●) with each of these ligands. Shadow points on the regression lines indicate to what metal-ion the regression refers. Only values that were used in the regression are shown and not formation constants deduced from the regression.[50]*

Regarding the latter, the LFER's (Figure 2.4.3 shown as an example) were generated from measured stability constants of Sn^{IV} by correlating them to those of Cu^{II}, Pb^{II} and Zn^{II}, so as to estimate values for other amino acids that were considered to be of significance in the distribution of the [^{117m}Sn]Sn(IV)-PEI-MP in blood plasma. Since their formation constants with blood plasma ligands are available from literature, constants for Sn^{II} could be estimated from this relationship. [50]

The LFER correlations was also employed to predict the first formation constants (log K_{a1}) for the ligand, methylene disphosphonic acid, MDP with ^{153}Sm and ^{166}Ho using the logK values from literature and logK values for Cd^{II}, Zn^{II}, and Pb^{II} reported by Cukrowski et al [55].

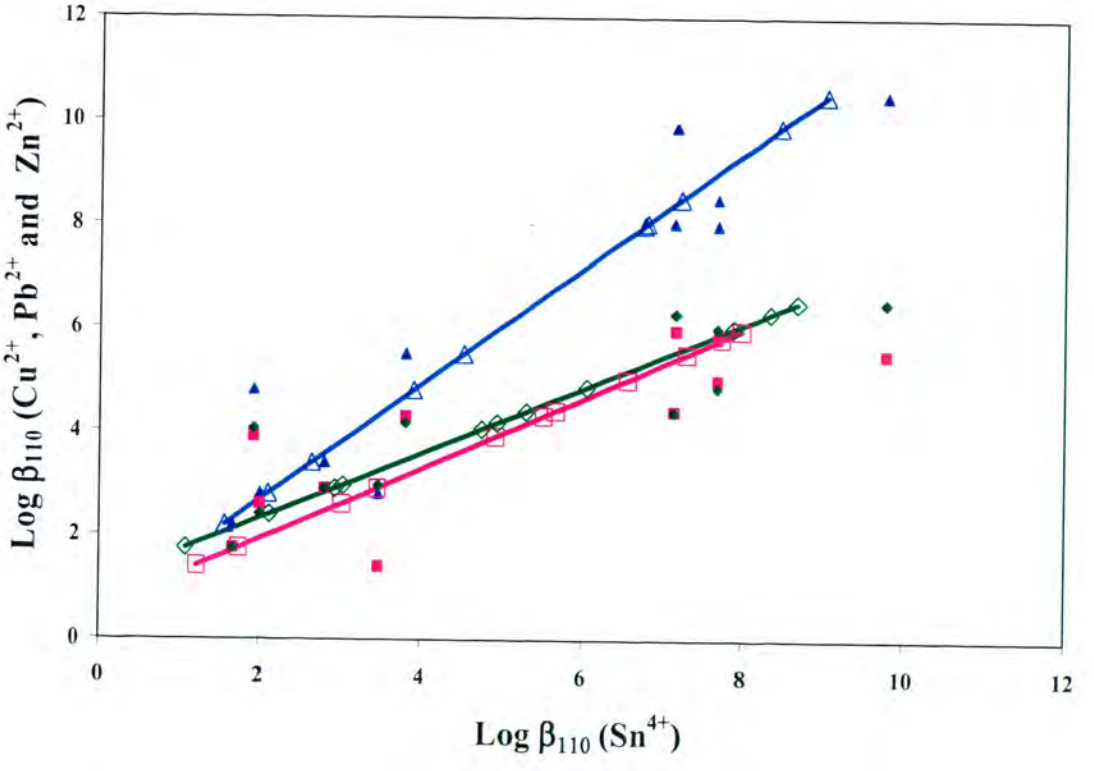

Figure 2.4.3. *Linear free energy relationship (LFER) curves correlating the log β_{110} values of Sn^{4+} with those of Cu^{2+}, Pb^{2+} and Zn^{2+} for their respective complexes with the selected blood plasma ligands: aspartate, serinate, glycinate, citrate, lactate, malate, oxalate, salicylate, succinate, histidinate and tartrate. Where: (▲) Sn^{4+} vs Cu^{2+} (R^2: 0.88); (■) Sn^{4+} vs Pb^{2+} (R^2: 0.66); (♦) Sn^{4+} vs Zn^{2+} (R^2: 0.78), and their respective LFER curves: (-△-) Cu^{2+}; (-□-) Pb^{2+} and (-◇-) Zn^{2+}.[54]*

Chapter3

EXPERIMENTAL

Experimental

3.1 Reagents

The reagents were of analytical grade: hydrochloric acid (HCl, F.W. 36.46, 32 % pure, density = 1.16 kg/l), sodium chloride (NaCl, F.W. 58.44 $g.mol^{-1}$, 99.5 %), sodium hydroxide titrisol (NaOH, 0.1M in 500ml solution), calcium chloride ($CaCl_3$, F.W. 110.99), zinc chloride ($ZnCl_3$, F.W. 136.28, 98%) are the products obtained from MERCK. Citric acid (F.W. 192.1), glycine (F.W. 75.07, 99 %), threonine (F.W. 119.12), glutamine (F.W. 146.1, 99 %), lutetium chloride ($LuCl_3$, F.W. 389.42, 99.99 %), magnesium chloride anhydrous (F.W. 95.22) were obtained from SIGMA-ALDRICH. Lactic acid (F.W. 90.08, 75 % pure, density = 1.21$g.ml^{-1}$) and copper chloride ($CuCl_3.2H_2O$, F.W. 170.48, 98 %) were obtained from BDH Laboratory Chemicals. DOTP (F.W. 548.30) was purchased from Macrocyclics. Demineralised water used in the preparations of solutions was prepared by passing de-ionised water through a Milli-Q-water purification system (Millipore, Bedford, MA, USA). Lu metal ion was standardised by ICP. EDTMP was synthesized according to the method of Moedritzer and Irani [56] and found to be pure by microanalysis. The results for microanalysis for EDTMP: found %C = 15.655, %H = 4.872, and %N = 6.136; calculated %C = 16.524, %H = 4.622 and %N = 6.423. The analysis was performed at Pelindaba Analytical Laboratories (PAL) which is a SANAS accredited laboratory. It was then used without further purification. Potentiometric titrations to determine protonation to determine protonation were used to double-check the purity of the ligand.

3.2 Methods

3.2.1 Preparations of Solutions

Background electrolyte solution of 0.15 M NaCl was prepared in a 2 dm^3 volumetric flask by weighing 17.532 g of salt, dissolving and filling it to the mark in de-ionised water. The appropriate amount (11.688 g) of 0.1 M NaCl was weighed and added into a 2

dm^3 volumetric flask, and a solution of 0.05 M NaOH in 0.1 M NaCl (Titrisol) was added and filled to the mark. The 0.05 M HCl in 0.1 M NaCl solution was also prepared by weighing out the required amount (5.844 g) of NaCl into a 1 dm^3 volumetric flask and adding the measured amount (4.91 ml) of HCl and diluting to the mark with de-ionised water. The concentration of all the ligands used in all titrations was about 1 x 10^{-2} M. These solutions were prepared by weighing out the required amount of ligand and NaCl salts and dissolving into the 100ml flask filling to the mark. The metal ions used in the titrations were weighed and added directly into the reaction vessel. A solution of 3 M KCl was prepared by weighing the correct amount (22.368 g) of KCl salt, adding it into 100 m^3 volumetric flask and filling to the mark with de-ionised water.

3.2.1 Experimental Set-up

All potentiometric titrations were performed using a Metrohm Titroprocessor TIM 865 jacketed glass vessel with a Metrohm 665 dosimat, a model 6.0259.100 (Metrohm) combination electrode (Ag/AgCl reference) and equipped with a magnetic stirrer. The dosimat is not connected to the system. It was used to add 0.15 M NaCl directly into the vessel. The electrode was calibrated regularly using strong acid-base titration data.

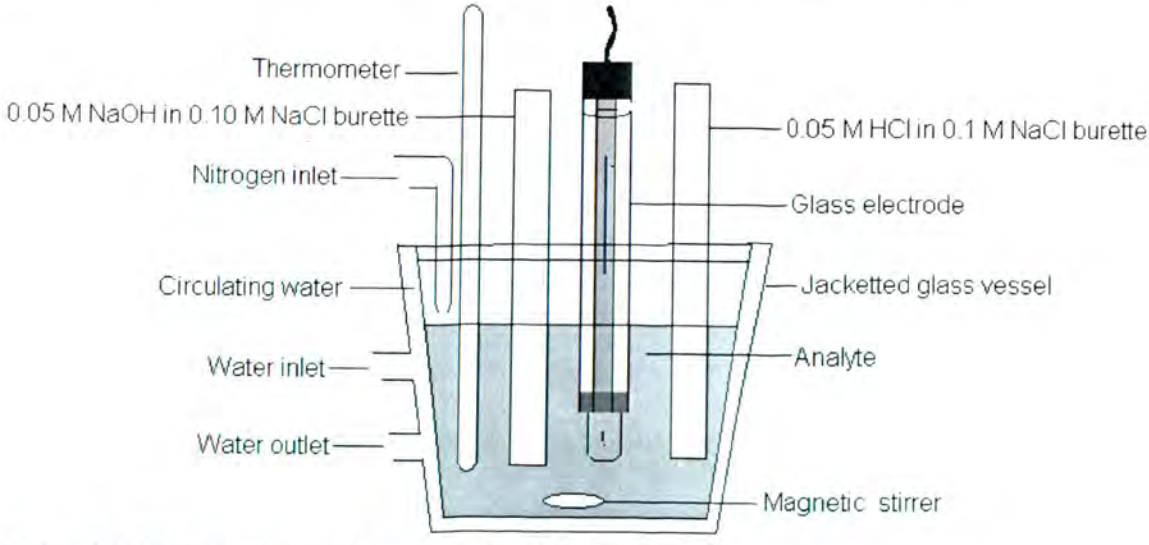

Figure3.1 The experimental set-up in the titration vessel.

All titrations were performed under inert atmosphere by bubbling Nitrogen gas through and solutions were held at a constant ionic strength of 0.15 M NaCl which simulated that of blood plasma and a temperature of 25°C which was attained by circulating water through a jacketed vessel. Titrations were performed starting at low pH and ending at high pH, by adding 0.10 ml aliquots of 0.050 ml NaOH (carbonate-free) in 0.10 ml NaCl. To determine protonation constants of the ligand, protonation titrations were performed, followed by metal-ligand titrations in which the data was used to determine formation constants. The concentration of the ligand was increased in relation to the various hydrochloric acid concentrations to accumulate data for 3 titrations. For metal-ligand titrations, formation constants were determined from five titrations of different ligand-to-metal ratio which are 1:1, 1:2, 1:3, 2:1, and 3:1. A 5-digit scale was used to weigh out all the salts including the metal-ion salts.

3.3 Glass electrode potentiometry

3.3.1 Electrode and instrumentation

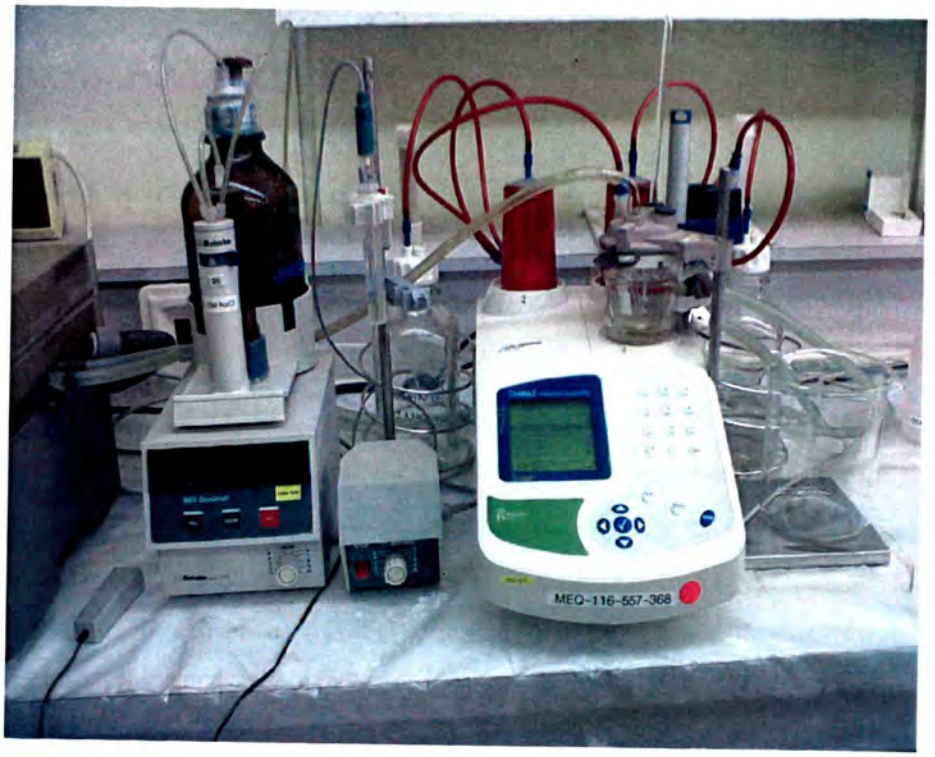

***Figure 3.2**. TitraLab (TIM 865 titration manager) with Metrohm 665 Dosimat*

3.3.2 Glass electrode calibration

The calibration of the electrode is crucial to the determination of stability constants by potentiometric titrations, as an error in the calibration becomes a systematic error in the interpretation of titration data [57]. The electrode was calibrated after seven days. The electrode was calibrated with three standard buffers (pH 4.00, pH 7.00 and pH 10.00). The electrode probe must be cleaned first before calibration by rinsing it with de-ionised water and gently drying with an absorbent material to avoid producing static charge on the glass. The electrode is then immersed into the first standard buffer solution (pH 4.00), stirred with a magnetic stirrer and allowed to reach equilibrium for at least 5 minutes. After each single measurement, the probe is rinsed with de-ionised water to remove any tracers of the solution being measured, blotted to absorb any remaining water which could dilute the sample. It is the quickly immersed into the second standard solution (pH 7.00). The same was done with the third standard solution of pH 10.00 until electrode stabilizes. The glass probe tip must be kept wet at all the times when not in use to avoid the pH sensing membrane dehydration and the subsequent dysfunction of the electrode. A 3M KCl solution was used for this purpose to prevent the diffusion of the electrolyte (KCl) out of the liquid junction.

3.3.3 Experimental Procedure

I. Standardization of 0.05 M NaOH in 0.1 M NaCl with potassium hydrogen phthalate (KHP).

The accurate amount of KHP (0.1021 g) was weighed such that in 10 ml the concentration is 0.05 M. KHP was added directly to the vessel for the titration. After adding the KHP crystals to the vessel, 20 ml of 0.15 M NaCl was added and the solution was stirred to dissolve the KHP. The solution was then titrated with 0.05 M NaOH in 0.1 M NaCl at 25°C until the end point was reached. The end point volume was then used to calculate the actual concentration of NaOH.

II. Determination of E_0 and Gradient (Standard electrode potential)

This was determined daily before titrations. 5.0 ml solution of 0.05 M HCl in 0.1 M NaCl and 20 ml solution of 0.15 M NaCl was added into a reaction vessel and then titrated with 0.05 M NaOH in 0.1 M NaCl at 25 °C. The data was refined using a computer program ESTA and the results used when determining the protonation constants of the ligand. See appendix B for an example of the experimental data and the subsequent fit of the data in the plot provided.

III. Determination of ligand protonation constants

To study the metal complexes of a specific ligand, it is important to know the form of the ligand throughout the entire pH of interest. Therefore determining the protonation constants is vital. The protonation constants of the ligand were determined from the following titrations:

Table 3.1 *Composition of protonation titrations for all ligands studied*

Titration number	0.05M Ligand in 0.15M NaCl (ml)	0.01M HCl in 0.15M NaCl (ml)	0.15M NaCl (ml)
1	5	10	25
2	10	10	20
3	15	10	15

IV. Determination of metal- ligand equilibrium constants

After determining protonation constants, metal-ligand complexation titrations were determined and the titration data was analyzed with ESTA computer program. All the titration data is found in appendix C. The data was refined with optimization mode ESTA2A. The hydrolysis constant of lutetium and pK_w were taken from literature and held constant [58, 59]. The metal-ligand complexation titrations are given in Table 3.2.

After successfully determining the formation constants, which was shown by low Hamilton R factors and low standard deviations of log β values, the constants were fed into ECCLES computer program for the simulation of blood plasma and to calculate the Plasma Mobilization indices.

Table 3.2 *Composition of metal-ligand titrations*

L:M	0.01 M Ligand in 0.15M NaCl (ml)	0.05M HCl in 0.01 M NaCl (ml)	0.15 M NaCl (ml)	$LuCl_3$ (mg)
1:1	4	10	26	15.576
1:2	8	10	22	15.576
1:3	12	10	18	15.576
1:4	16	10	14	15.576
2:1	2	10	28	31.153
3:1	1.33	10	28.7	40.889

Chapter 4

RESULTS AND DISCUSSION

4. Results and Discussion

4.1 Introduction

Multidentate aminomethylenephosphonic acids such as 1,4,7,10-tetraazacyclododecane-1,4,7,10-tetra(methane-phosphonic acid) (DOTP) - Figure 4.1, form stable complexes with different radionuclides and have already proven to be effective for bone pain palliation [36, 39, 40, 41]. The steric rigidity of macrocyclic ligands facilitates the formation of thermodynamically and kinetically stable complexes [60]. The chelate cavity accommodates a variety of metal ions. The ring can be modified to a desired size, as well as functionalized with additional pendent arms such as carboxylic acids and methylenephosphonates to preferentially insert metal ions of a specific size and nature. Trivalent lanthanides and transition metal ions are particularly favourable for the formation of stable water-soluble mononuclear (ML - type) complexes [60]. The ideal radiopharmaceutical, especially those of the radiolabeled metal-chelate type, should be stable to withstand dissociation during systemic circulation. For internal radiotherapy it is essential that the drug retains its integrity for effective targeting and localization at the intended site, and furthermore avoid undesired distribution and accumulation of the radionuclide in non-target organs. The radioactive dose should be localized to the tumour to afford effective antitumour activity, whilst sparing healthy and more sensitive tissue.

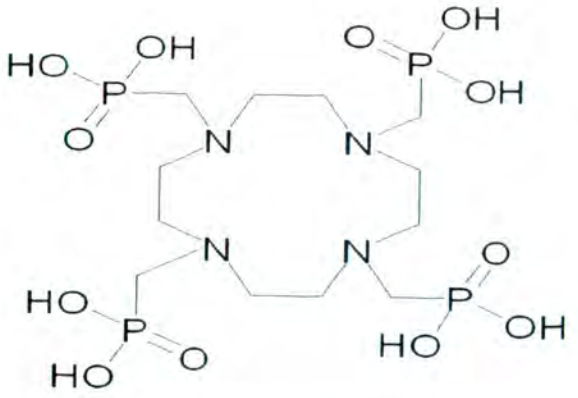

Figure 4.1 The structure of DOTP

Structural factors such as the rigidity, the cavity size, and the nature and number of donor atoms of the macrocyclic bifunctional chelators play a significant role in the chemical and biological behavior of their complexes [35, 61]. The choice of using a cyclic chelator is based on the more pronounced thermodynamic stability and kinetic inertness of their lanthanide complexes when compared to that of their acyclic analog [40, 41]. This study evaluates [^{177}Lu]Lu-DOTP as a promising radiopharmaceutical for bone pain palliation. To gain some knowledge into the behaviour of the ligand (DOTP) and the metal ion (^{177}Lu) in blood plasma complex-formation constants for important blood plasma metal ions, Ca^{+2}, Cu^{+2}, and Mg^{+2} and trivalent lanthanide ^{177}Lu were measured by glass electrode potentiometry at 25 C and I = 0.15 M. Computer program ECCLES was used to construct blood plasma models. ^{177}Lu is extensively hydrolysed in solution. This hydrolysis can be represented by Equation 4.1.1, in which for convenience, waters of coordination have been omitted.

$$[Lu]^{3+} + H_2O = [Lu(OH)]^{2+} + H^+ \qquad (4.1.1)$$

where the hydrolysis constant of Lu^{3+} above is given by:

$$K = \frac{[Lu(OH)_n][H^+]}{[Lu(OH)_{n-1}} \qquad (4.1.2)$$

The hydrolysis constant of Lu(III), together with the total concentration of the metal ion, was used in refining the metal-complexes of ^{177}Lu with the ligands, (EDTMP, DOTP and amino acids) and in calculating the speciation of the complexes formed in the solution. One would simply measure the constants of the ligand with the main blood plasma metal ions, and see whether there is a significant binding of blood plasma metal ions to the ligand. If this is not the case, one can assume that the Lu-ligand complex stays intact when introduced in the blood plasma. The complexation of the ligand with blood plasma metal ions at physiological pH 7.4 was therefore investigated.

Table 4.1 *Acid dissociation equilibria and constants for DOTP and the complex formation constants with selected metal ions of physiological significance (where L represents the deprotonated ligand). Determined by glass electrode potentiometry and ESTA modeling, at 25 °C and ionic strength (μ) of 0.15 mol.dm^{-3} NaCl.*

Equilibrium/Species#	***Log K***		***Hamilton R-Factor***	***References***
	This work	***Literature***		
	(25 °C, μ 0.15)	***(25 °C, μ 0.1)***		
$L + H \rightleftharpoons [HL]$	(13.19 ± 0.01)	(12.8)	0.01213	[68]
$[HL] + H \rightleftharpoons [H_2L]$	(10.92 ± 0.01)	(11.44)		[68]
$[H_2L] + H \rightleftharpoons [H_3L]$	8.58 ± 0.01	8.90		[68]
$[H_3L] + H \rightleftharpoons [H_4L]$	7.50 ± 0.01	7.71		[68]
$[H_4L] + H \rightleftharpoons [H_5L]$	5.86 ± 0.01	5.99		[68]
$[H_5L] + H \rightleftharpoons [H_6L]$	5.02 ± 0.01	5.13		[68]
Lutetium				
$Lu + OH \rightleftharpoons Lu(OH)$	-7.99*			
$Lu + L \rightleftharpoons [LuL]$	24.78 ± 0.04		0.02073	
$[LuL] + H \rightleftharpoons [LuHL]$	8.228 ± 0.04			
$[LuLH] + H \rightleftharpoons [LuH_2L]$	6.63 ± 0.06			
$[LuL] + OH \rightleftharpoons [LuL(OH)]$	2.95 ± 0.08			
$[LuLH_2] + 3H \rightleftharpoons [LuH_5L]$	16.73 ± 0.03			
$2Lu + L + 2H \rightleftharpoons [Lu_2H_2 L]$	53.02 ± 0.04			
Calcium				
$Ca + L \rightleftharpoons [CaL]$	(10.42 ± 0.02)		0.01197	
$2Ca + L \rightleftharpoons [Ca_2L]$	(14.87 ± 0.14)			
$[Ca_2L] + H \rightleftharpoons [Ca_2HL]$	9.74 ± 0.15	9.65		[69]
$[Ca_2HL] + H \rightleftharpoons [Ca_2H_2L]$	7.66 ± 0.06	7.71		[69]
Magnesium				
$Mg + L \rightleftharpoons [MgL]$	8.72 ± 0.05		0.01883	
$2Mg + L \rightleftharpoons [Mg_2L]$	13.99 ± 0.03			
$[Mg_2L] + 2H \rightleftharpoons [Mg_2H_2L]$	18.36 ± 0.05			
Copper				
$Cu + L \rightleftharpoons [CuL]$	24.20 ± 0.04	26.2 ±0.2	0.02073	[68]

$Cu + L + H \rightleftharpoons [CuHL]$	8.43 ± 0.04
$Cu + L + OH \rightleftharpoons [CuL(OH)]$	3.32 ± 0.10
$2Cu + L + H \rightleftharpoons [Cu_2HL]$	46.03 ± 0.05
$[Cu_2LH] + H \rightleftharpoons [Cu_2H_2L]$	6.40 ± 0.07

[#] *The charges on the ligands and complexes have been omitted for simplicity.*
[*] *Hydrolysis constant for Lu was obtained from literature [70] and included in the model.*

All these constants were incorporated into the model and the speciation of the proposed metal-ligand systems (at certain concentration) was computed. From the results one can deduce several things, for instance whether the complex remains intact in the blood plasma or the species forming at a blood pH of 7.4 are neutral and could therefore be filtered by the liver.

4.2 Protonation studies of the ligand DOTP

The stepwise protonation constants of DOTP with standard deviations, Hamilton R-factors and the complexes that it forms with Lu^{3+}, Ca^{2+}, Mg^{2+}, and Cu^{2+} are presented in Table 4.1. Three titrations determined by glass electrode potentiometry where performed. (The titration data is found in appendix C). Plausible models between the experimental and calculated protonation function were obtained for each system. The calculated function follows the experimental data very closely (Figure 4.2.1) in the protonation curve for DOTP. The value for the dissociation of water under the condition of the titrations done in this study and employed in the computations was as given in Equation 4.2.1.

$$K = [H^+]\,[OH^-] = 10^{-13.79} \qquad (4.2.1)$$

The protonation represented graphically by the $\overline{Z_H}$ curve (Figure 4.2.1), showing the extent of protonation of the ligand at a given pH. It is worth noting that the ionic strength used during these experiments (μ 0.15) differs from literature (μ 0.10), which could account for the deviation in the log K values from the cited values. It can be seen that the calculated data (represented by solid line) agree well with the experimental data (points).

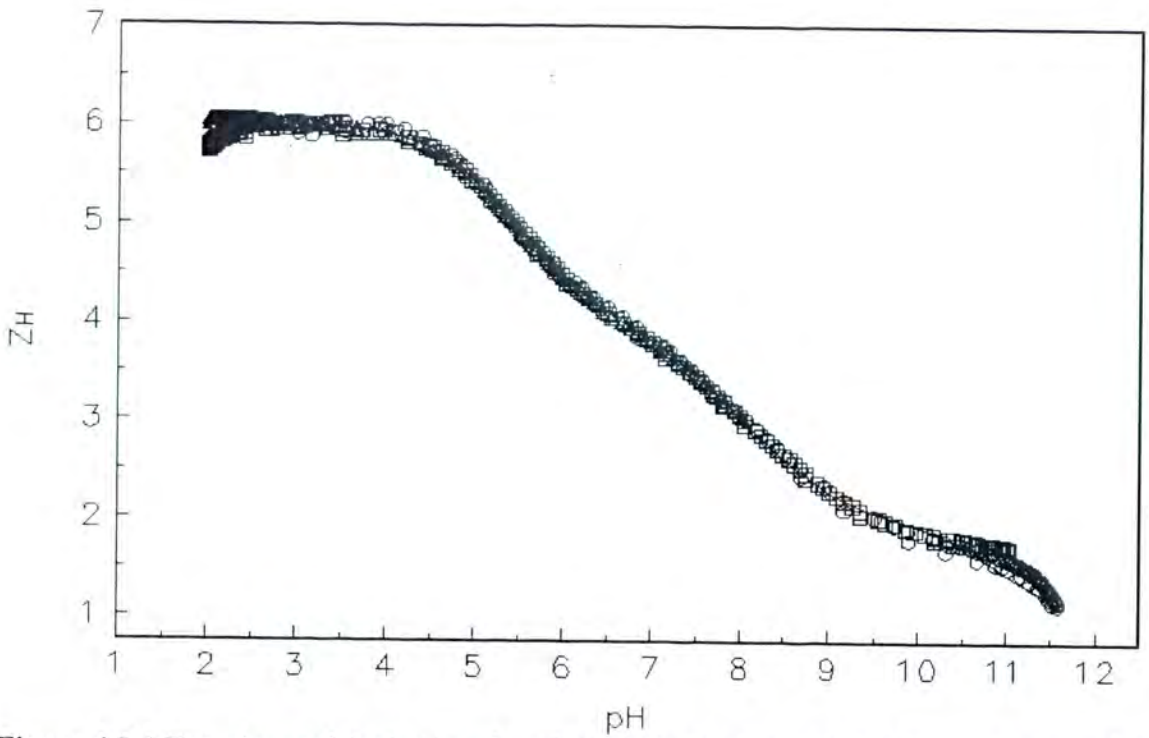

Figure 4.2.1 *Experimental (points) and modelled (lines) protonation formation curves for DOTP.* $\bar{Z}_H$ *is the protonation formation function (the average number of protons bound per ligand) and pH is the negative logarithm of the free hydrogen ion concentration. The titrations are represented by (Δ) 0.001249 M DOTP, 0.012612 M HCl, (□) 0.002499 M DOTP, 0.012618 M HCl and (O) 0.003749 M DOTP, 0.012619 M HCl. All solutions were at 25°C and 0.15 M ionic strength.*

There are 8 sites of protonation (proton dissociation) whereby the first dissociation is at the higher pKa_1 of 13.92 this is due to the dissociation at an amine centre. It can be deduced that no further protons are lost beyond pH 12. Below pH 4, the curves level off at 6 indicating that 6 protons have been added to DOTP and these are the 6 protons that have been determined in this study. Figure 4.2.2 shows the respective acid species of the ligand relative to pH. The most predominant species exist between pH 4-9 in the form of H_4DOTP with 80% mole fraction. At pH 3, the H_6DOTP constitute 100% of the total ligand concentration. H_4DOTP and H_3DOTP constitute almost 50% each at the physiological pH 7.4 which is of great interest when taking the in vivo conditions into consideration.

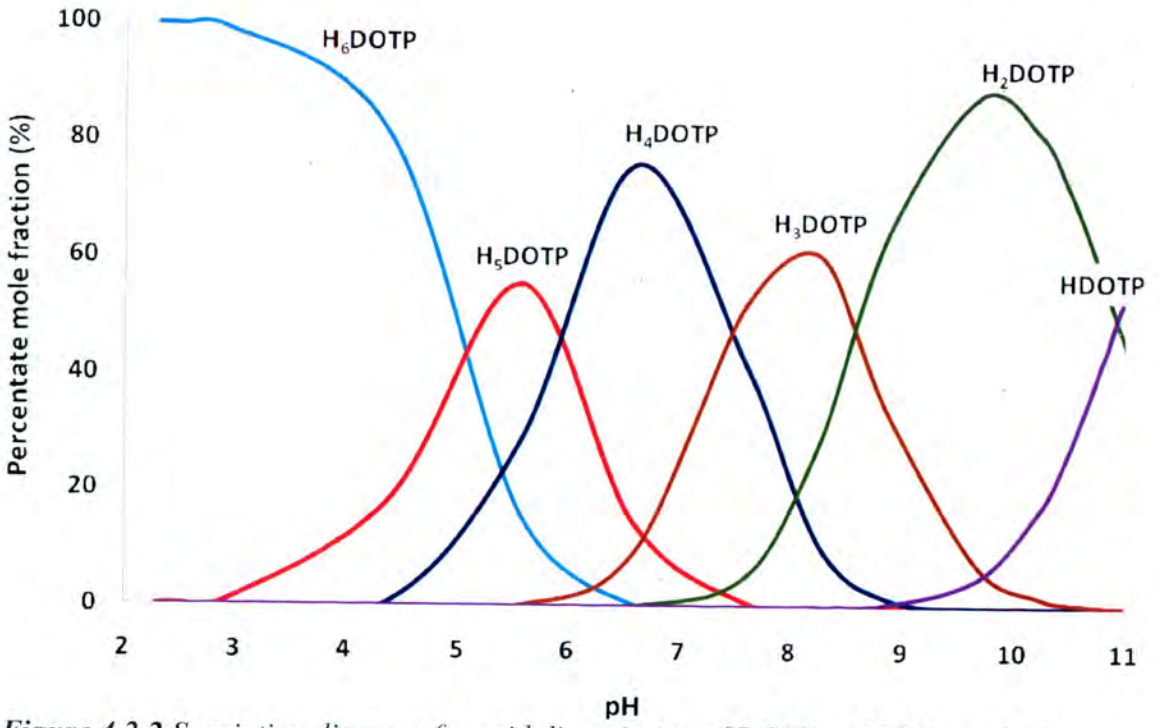

Figure 4.2.2 *Speciation diagram for acid dissociation of DOTP at 25 °C and 0.15 mol.dm^{-3} total ionic strength.*

4.3 Complexation of DOTP with Lu^{III}

ESTA 1 and 2 programs which are basic mass balances that optimizes through simple error minimization routines as stated in Chapter 2, where successfully applied in generating the $\overline{Z}_H$, $\overline{Z}$, $\overline{Q}$ plots and speciation curves (The ESTA output results of all titrations is found in appendix D). The $\overline{Z}$ curve (Figure 4.3.1) represents the complexation function, illustrating the number of ligands bound per metal ion. There is backfanning at low pA (negative logarithm of the free ligand concentration) which reveals the presence of hydrolysis species (MLH_{-1} or ML(OH)). Good agreement can be found between the calculated and experimental points. This is also true for the $\overline{Q}$ curve (Figure 4.3.2) as well. The $\overline{Q}$ curve is the deprotonation function, denoting the average number of protons released on complexation per metal-ion and the dashed curve is $\overline{n}$ which is the protonation states of the repeating unit in the absence of the metal-ion. At pH 7.4 the $\overline{Q}$ curve tends to 2.5, indicating the presence of binuclear complexes (e.g. M_2L) after which it goes down to 2 at pH 9. The $\overline{Q}$ goes above the $\overline{n}$ curve at pH 10

confirming the presence of hydrolysis or (OH) containing species which could be interpreted as $M(OH)_2$ being present because the $\overline{Q}$ tends to 2. At pH 6, $\overline{Q}$ curve is at 1.5 which implies that 3 protons are lost per complexation with two metal-ions and the $\overline{n}$ curve is at 4 or LH_4 verifying the presence of binuclear species M_2LH.

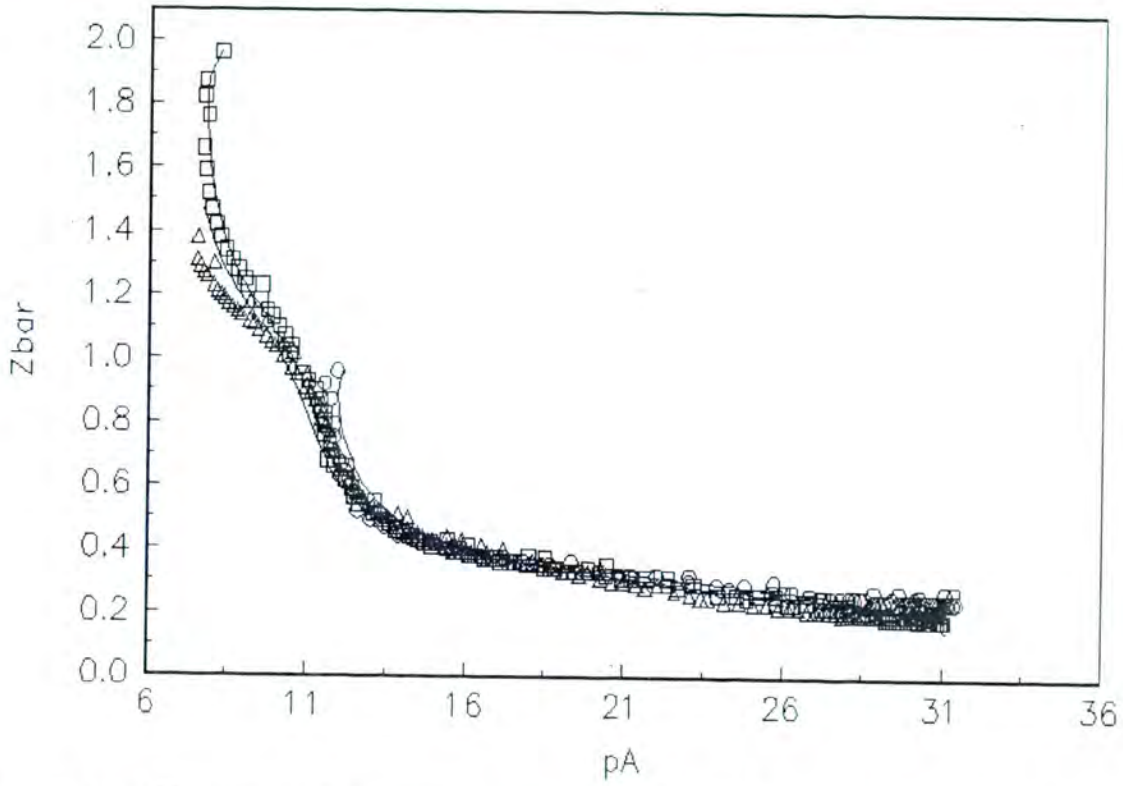

Figure 4.3.1 *$\overline{Z}$ curves for the complexation of DOTP with Lu^{3+}. Experimental points are represented by the points and modeled protonation formation curves represented by the solid lines. The three titrations are depicted as follows: (○) 1 mmol.dm^{-3} Lu^{3+} and 1 mmol.dm^{-3} DOTP, (Δ) 1 mmol.dm^{-3} Lu^{3+} and 2 mmol.dm^{-3} DOTP, and (□) 1 mmol.dm^{-3} Lu^{3+} and 3 mmol.dm^{-3} DOTP. All titrated against 0.05 mmol.dm^{-3} NaOH in 0.10 mol.dm^{-3} NaCl, at 25.0 °C and 0.15 mol.dm^{-3} total ionic strength.*

These titrations were performed in high ligand content (1:1, 1:2, and 1:3). As shown in the speciation diagram (Figure 4.3.3), the most predominant species of the Lu-DOTP complexes at physiological pH 7.4 are: Lu(HDOTP), $Lu_2(H_2DOTP)$, $Lu(H_2DOTP)$ and Lu(DOTP), with the distribution of the ligand being 59.6, 19.8, 14.3, and 6.3%, respectively. Hydroxide complex, Lu(DOTP)(OH), exist in the high pH region with a mole fraction of 35%. The deprotonated ML form reaches its maximum quantity in the solution at the pH 9.5.

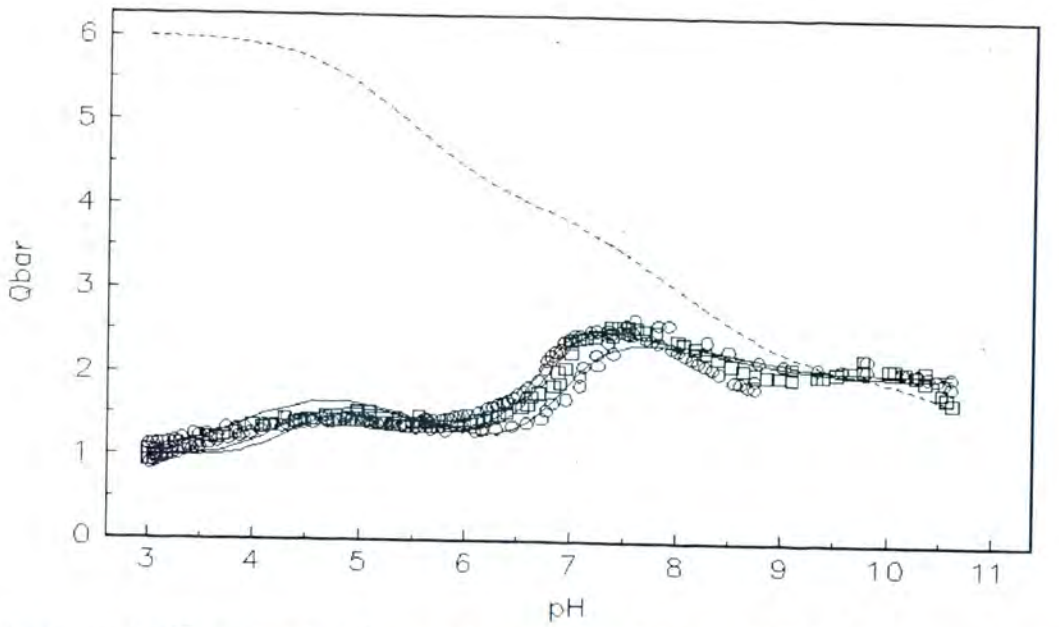

Figure 4.3.2 *$\bar{Q}$ curves for the complexation of DOTP with Lu^{3+}. Experimental points are represented by the points and modeled protonation formation curves represented by the solid lines. The three titrations are depicted as follows: (○) 1 mmol.dm^{-3} Lu^{3+} and 1 mmol.cm^{-3} DOTP, (Δ) 1 mmol.dm^{-3} Lu^{3+} and 2 mmol.dm^{-3} DOTP, and (□) 1 mmol.dm^{-3} Lu^{3+} and 3 mmol.dm^{-3} DOTP. All titrated against 0.05 mmol.dm^{-3} NaOH in 0.10 mol.dm^{-3} NaCl, at 25.0 °C and 0.15 mol.dm^{-3} total ionic strength. The dashed line represents the $\bar{n}$ curve, which is the protonation state of the ligand in the absence of the metal ion.*

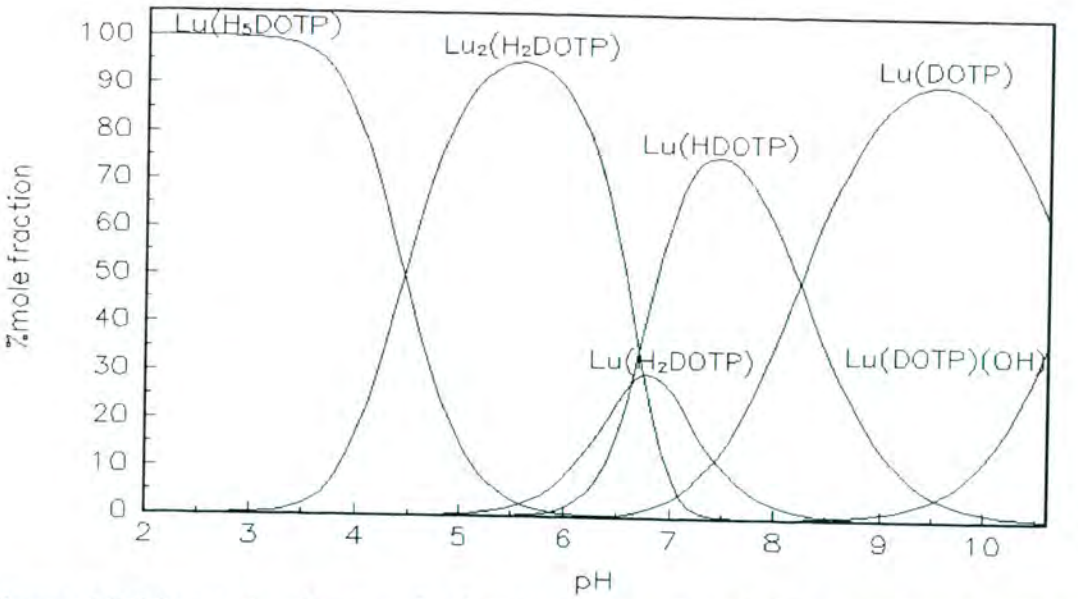

Figure 4.3.3 Speciation diagram for the distribution of Lu-DOTP complexes over the pH range 2 to 11, at 25.0 °C and 0.15 mol.dm^{-3} total ionic strength.

4.4 Speciation of DOTP with major metal-ions in blood plasma- Ca^{2+}, Mg^{2+}, Cu^{2+}

Formation constants of DOTP with selected transition metal ions, Ca^{2+}, Mg^{2+}, and Cu^{2+} are given in Table 4.1. DOTP form predominantly binuclear (M_2L-type) complexes with the metal ions when binding with the metal ions. The complexes are also known to be kinetically inert for several days *in vitro* as reported at ambient temperature and μ 0.1 mol.dm^{-3} [61]. The errors are mainly an indication of how well the modeled species compare with the observed experimental data as depicted by the $\bar{Z}$ and $\bar{Q}$ curves for all three models. The $\bar{Z}$ curve represents the complexation function, illustrating the number of ligands bound per metal ion; and the $\bar{Q}$ curve is the deprotonation function of the ligand resulting from the complexation of the metal ion. The goodness of fit is given by the statistical Hamilton R-factor – the lower the value the better the fit. Comparison of the complex formation constants with that of the protonations, it is evident that the metal ions are bound by the ring amines, with log K of approximately 7 and above.

4.4.1. Ca-DOTP model

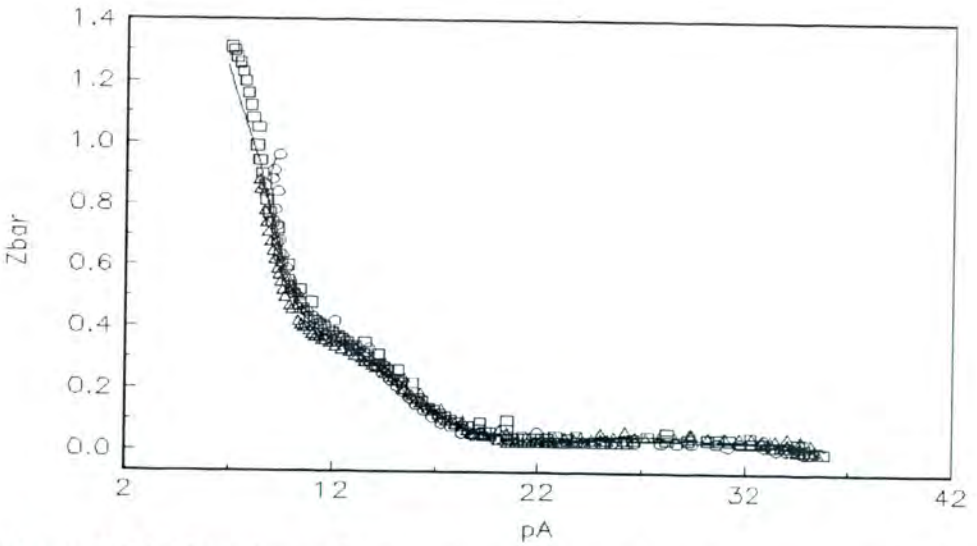

Figure 4.4.1. *Experimental (points) and modeled (lines) formation for Ca^{2+} complexation by DOTP. pA is the negative log of the free ligand concentration. The 3 titrations are represented by (○) 1 mmol.dm^{-3} Ca^{2+} and 1 mmol.cm^{-3} DOTP, (Δ) 1 mmol.dm^{-3} Ca^{2+} and 2 mmol.dm^{-3} DOTP, and (□) 1 mmol.dm^{-3} Ca^{2+} and 3 mmol.dm^{-3} DOTP. All titrated against 0.05 mmol.dm^{-3} NaOH in 0.10 mol.dm^{-3} NaCl, at 25.0 °C and 0.15 mol.dm^{-3} total ionic strength.*

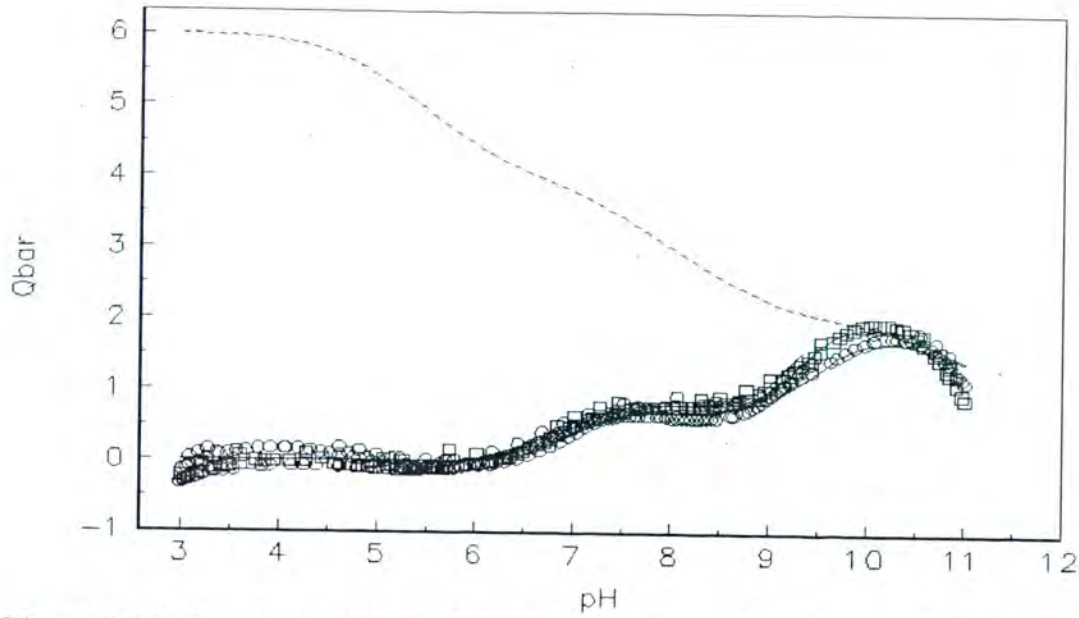

Figure 4.4.2 *Experimental (points) and modeled (lines) formation for Ca^{2+} complexation by DOTP. pA is the negative log of the free ligand concentration. The 3 titrations are represented by (○) 1 mmol.dm^{-3} Lu^{2+} and 1 mmol.cm^{-3} DOTP, (Δ) 1 mmol.dm^{-3} Ca^{2+} and 2 mmol.dm^{-3} DOTP, and (□) 1 mmol.dm^{-3} Ca^{2+} and 3 mmol.dm^{-3} DOTP. All titrated against 0.05 mmol.dm^{-3} NaOH in 0.10 mol.dm^{-3} NaCl, at 25.0 °C and 0.15 mol.dm^{-3} total ionic strength.*

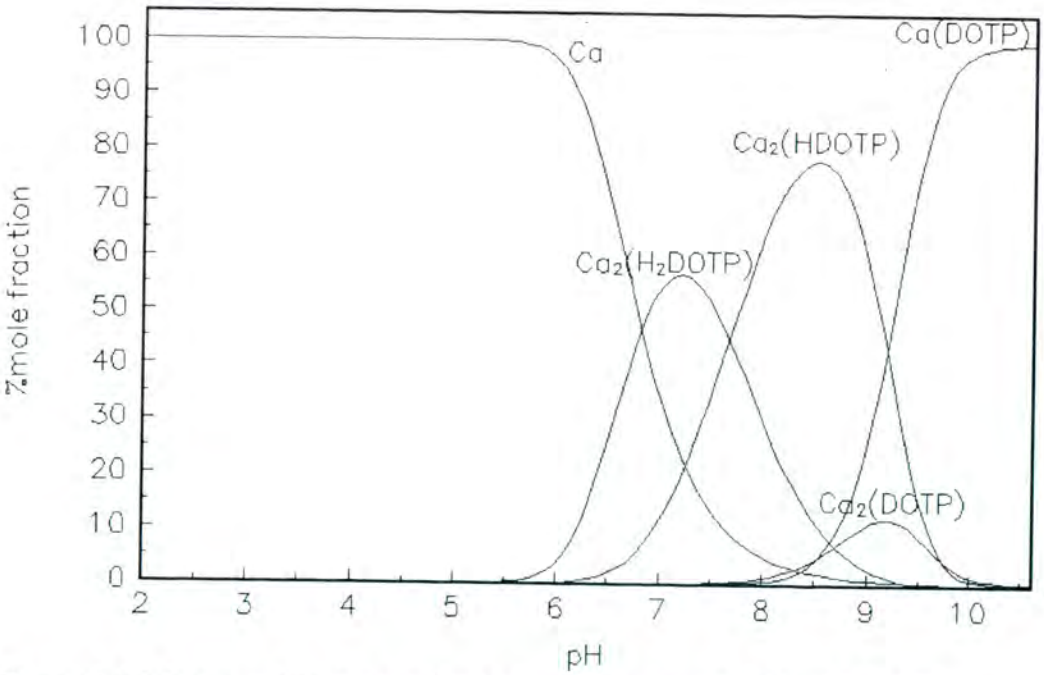

Figure 4.4.3 *Species distribution for the complexation of Ca^{2+} with DOTP.*

4.4.2 Cu-DOTP model

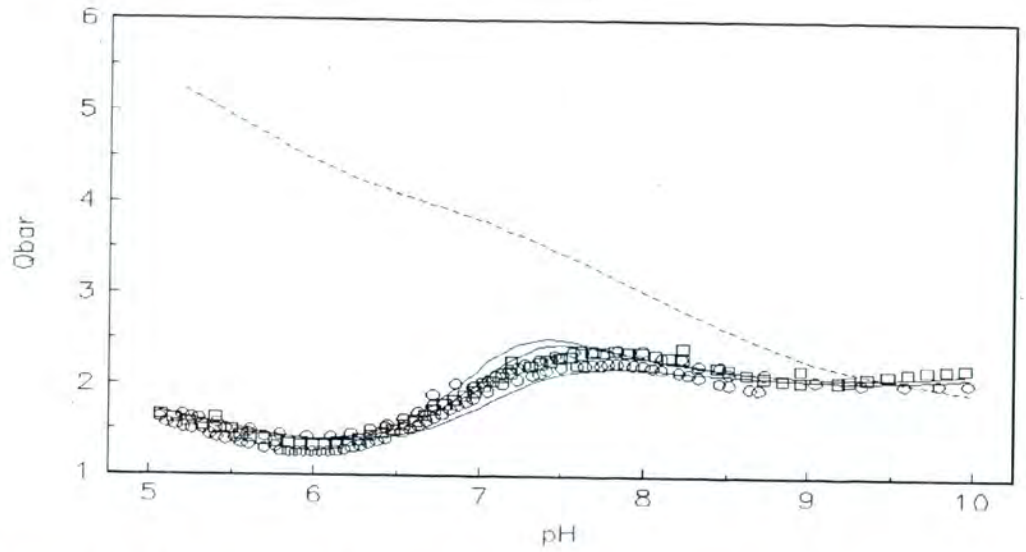

Figure 4.5.1 *Experimental (points) and modeled (lines) formation for Cu^{2+} complexation by DOTP. pA is the negative log of the free ligand concentration. The 3 titrations are represented by (○) 1 mmol.dm^{-3} Lu^{2+} and 1 mmol.dm^{-3} DOTP, (Δ) 1 mmol.dm^{-3} Cu^{2+} and 2 mmol.dm^{-3} DOTP, and (□) 1 mmol.dm^{-3} Cu^{2+} and 3 mmol.dm^{-3} DOTP. All titrated against 0.05 mmol.dm^{-3} NaOH in 0.10 mol.dm^{-3} NaCl, at 25.0 °C and 0.15 mol.dm^{-3} total ionic strength.*

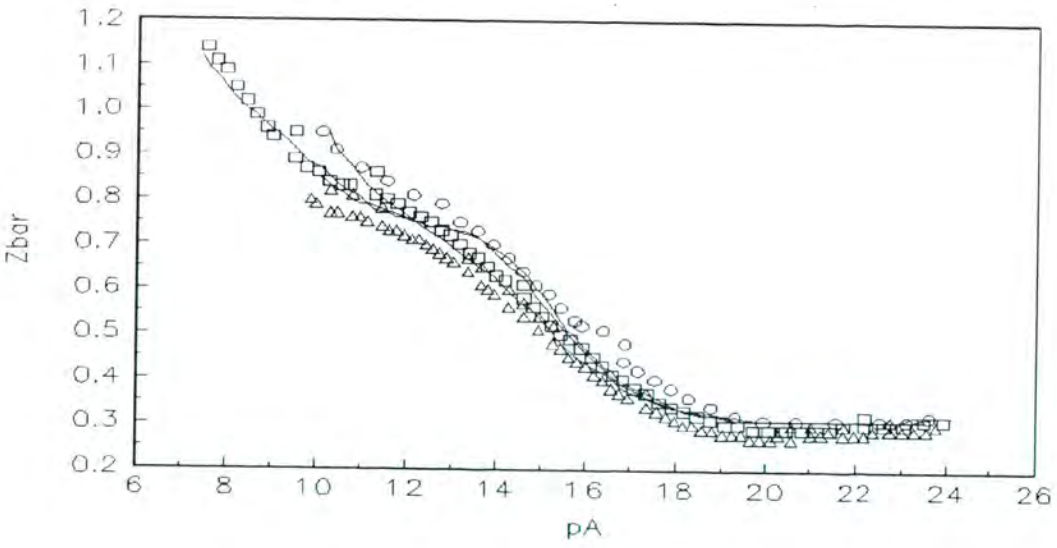

Figure 4.5.2 *Experimental (points) and modeled (lines) formation for Cu^{2+} complexation by DOTP. pA is the negative log of the free ligand concentration. The 3 titrations are represented by (○) 1 mmol.dm^{-3} Cu^{2+} and 1 mmol.dm^{-3} DOTP, (Δ) 1 mmol.dm^{-3} Cu^{2+} and 2 mmol.dm^{-3} DOTP, and (□) 1 mmol.dm^{-3} Cu^{2+} and 3 mmol.dm^{-3} DOTP. All titrated against 0.05 mmol.dm^{-3} NaOH in 0.10 mol.dm^{-3} NaCl, at 25.0 °C and 0.15 mol.dm^{-3} total ionic strength.*

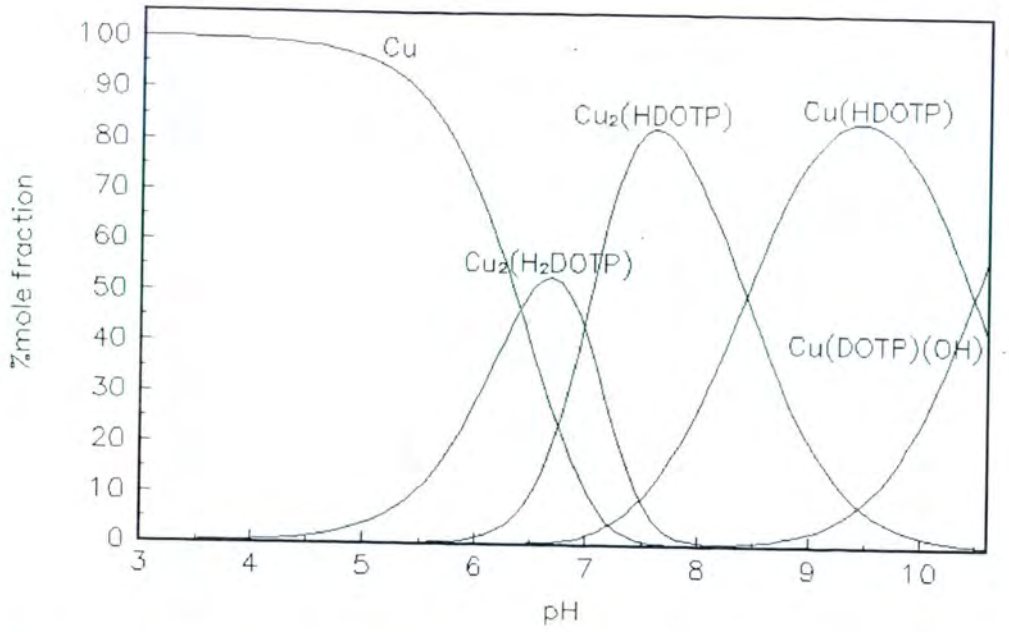

Figure 4.5.3 *Species distribution for the complexation of Cu^{2+} with DOTP.*

4.4.3 Mg-DOTP model

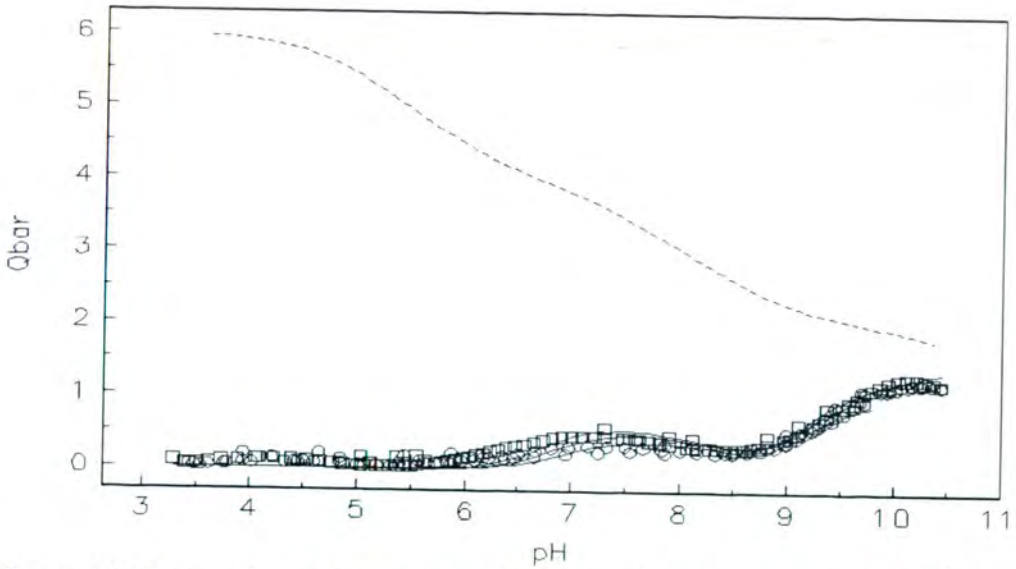

Figure 4.6.1. *Experimental (points) and modeled (lines) formation for Mg^{2+} complexation by DOTP. pA is the negative log of the free ligand concentration. The 3 titrations are represented by (○) 1 mmol.dm^{-3} Mg^{2+} and 1 mmol.cm^{-3} DOTP, (Δ) 1 mmol.dm^{-3} Mg^{2+} and 2 mmol.dm^{-3} DOTP, and (□) 1 mmol.dm^{-3} Mg^{2+} and 3 mmol.dm^{-3} DOTP. All titrated against 0.05 mmol.dm^{-3} NaOH in 0.10 mol.dm^{-3} NaCl, at 25.0 °C and 0.15 mol.dm^{-3} total ionic strength.*

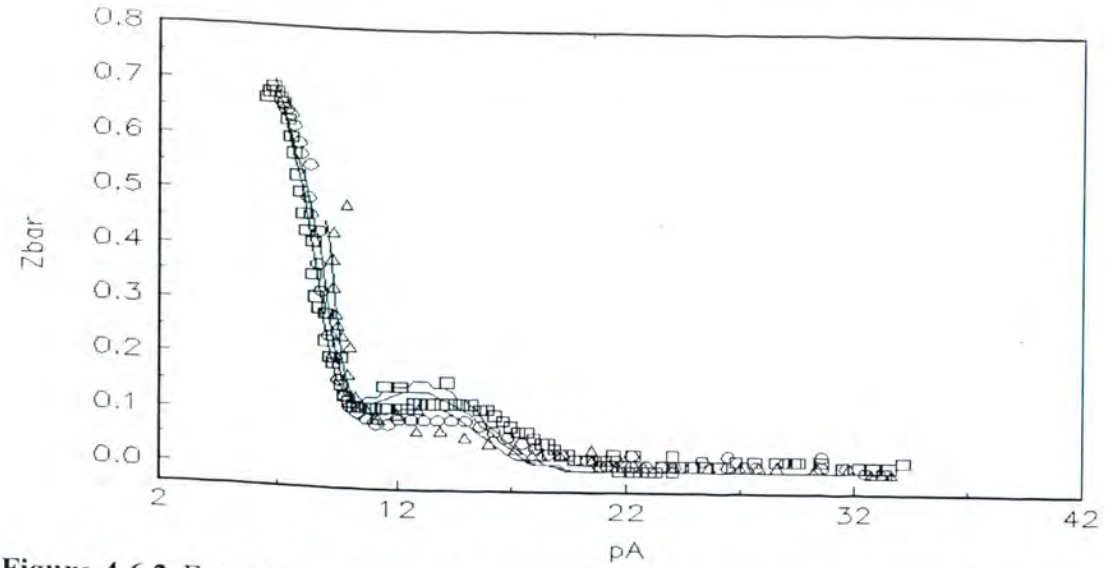

Figure 4.6.2 *Experimental (points) and modeled (lines) formation for Mg^{2+} complexation by DOTP. pA is the negative log of the free ligand concentration. The 3 titrations are represented by (○) 1 mmol.dm^{-3} Mg^{2+} and 1 mmol.cm^{-3} DOTP, (Δ) 1 mmol.dm^{-3} Mg^{2+} and 2 mmol.dm^{-3} DOTP, and (□) 1 mmol.dm^{-3} Mg^{2+} and 3 mmol.dm^{-3} DOTP. All titrated against 0.05 mmol.dm^{-3} NaOH in 0.10 mol.dm^{-3} NaCl, at 25.0 °C and 0.15 mol.dm^{-3} total ionic strength.*

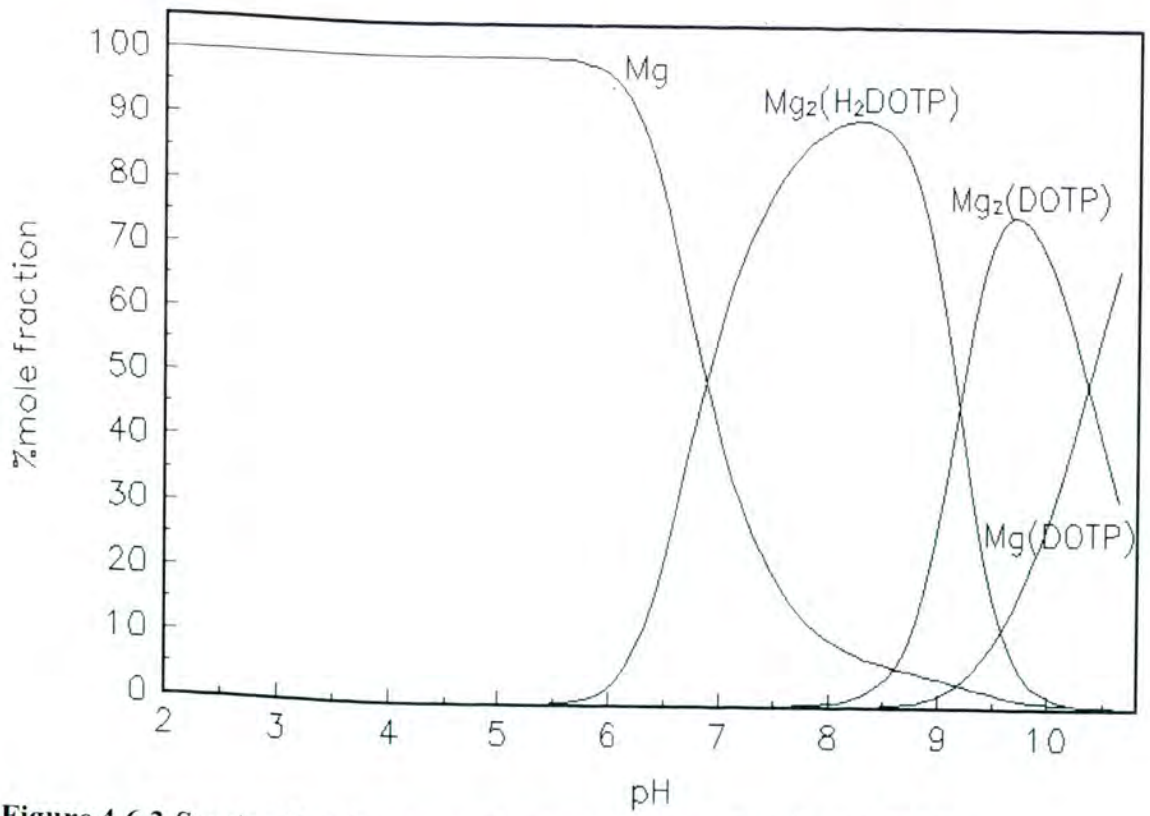

Figure 4.6.3 *Species distribution for the complexation of Mg^{2+} with DOTP.*

Good fit was possible for all the models as it is evident in the $\bar{Z}$ and $\bar{Q}$ curves. As observed in the $\bar{Q}$ curves for all three systems – DOTP with Ca^{2+}, Cu^{2+}, Mg^{2+} - the calculated models (lines) follow the experimental data points. In the pH region 3-6 for Mg-DOTP model (Figure 4.6.1), a $\bar{Q}$ value of 0 is recorded, meaning that there is no complexation taking place between DOTP and the metal-ion (Mg^{2+})in that region. The curve then rises to 0.5 indicating the presence of binuclear species (M_2L) at the physiological pH 7.4 which is of interest in this study due to in vivo conditions. The curve then rises to 1 at pH 8-9 which is interpreted as one proton being lost per metal ion. The model shows that the ligand does not hydrolyse the metal ion because the $\bar{Q}$ curve does not go above the $\bar{n}$ curve. This is also demonstrated by the $\bar{Z}$ curve (Figure 4.6.2) as there are no 'curl backs' or observed. It can be deduced from the above information that Mg^{2+} shows less complexation with DOTP.

The Cu-DOTP model was the most troublesome, and as a result a good fit could not be obtained with experimental and calculated as it is evident in the $\bar{Q}$ (Figure 4.5.1) and $\bar{Z}$ curves (Figure 4.5.2). And this is also seen by high standard deviations of the formation constants of the Ca-DOTP complexes in Table 4.1. The first formation constant CuL differs with the one in literature which could be because of the different ionic strength used. Between pH 7 and 8 the $\bar{n}$ drops to 3 and the $\bar{Q}$ is at 2.5 indicating that 2 protons are released by the ligand on every two metal ions on complexation verifying the presence of binuclear species, in this case M_2LH_2. At pH 6 the $\bar{Q}$ curve averages at 1.5 whereas the $\bar{n}$ is at 4 meaning that one proton is lost per two metal ions, i.e M_2LH species is formed. Hydrolysis of the metal ion takes place at the high pH region whereby the $\bar{Q}$ rises above the $\bar{n}$ curve. This is also supported by the $\bar{Z}$ where backfanning occurs in the low pA region in Figure 4.4.2 indicating the presence of OH species. The $\bar{Z}$ and $\bar{Q}$ curves both follows the experimental data points very closely. The $\bar{Q}$ does not rise above the $\bar{n}$ curve, indicating that the metal ion does not hydrolyse in the system. This is also substantiated in the $\bar{Z}$ whereby the graph exhibit no backfanning. At

pH 3-6 region, a $\overline{Q}$ of 0 is recorded, suggesting that no complexation is taking place in this region. The curve then rises to 0.5 at approximately pH 7 denoting that M_2LH_2 species is present in the system. The two binuclear species present have formation constants which follow literature values very closely.

The speciation for the Ca^{2+}, Cu^{2+}, Mg^{2+} complexes with DOTP can be seen in Figure 4.4.3, Figure 4.5.3 and Figure 4.6.3 respectively. At the start of the titrations the system comprise of 100% free metal ion and coordination of the ligand with the metal ion starts at pH 5.5 for both Ca^{2+} and Mg^{2+} and at pH 4 for Cu^{2+}. At pH 7.4 the complex Mg_2(HDOTP) shows to be predominant with a mole fraction of 90%. This is clearly substantiated by the absence of hydrolysis as seen in the $\overline{Z}$ curves and $\overline{Q}$ curves. 100% of the uncomplexed Mg is dominant at the low pH region (pH 2-6). At the physiological pH 7.4 the species present are $Cu_2(H_2DOTP)$, Cu_2(HDOTP) and Cu(HDOTP) with the molar fractions of 80%, 10% and 10% respectively. The hydroxyl species are present in the high pH region contributing 55% mole fraction of the ligand. Two binuclear species $Ca_2(H_2DOTP)$ and Ca_2(HDOTP) are the main species at pH 7 with mole fraction of 60% and 20% respectively whereby the remaining 20% exist as the free metal ion. This can be clearly shown in Table 4.2.

Table 4.2 *The dominant species of each system at the physiological pH 7.4 and their percentage mole fraction.*

System	**Species Dominating at pH 7.4**	**Mole fraction percentage**
Ca-DOTP	$Ca_2(H_2DOTP)$	55%
	Ca_2(HDOTP)	25%
	Free Ca^{2+} ions	20%
Cu-DOTP	$Cu_2(H_2DOTP)$	80%
	Cu_2(HDOTP)	10%
	Cu(HDOTP)	10%
Mg-DOTP	Mg_2(HDOTP)	80%
	Free Mg^{2+} ions	20%

4.4.4 Discussion

The speciation of Lu^{III} in the presence of DOTP in blood plasma is illustrated in Figure 4.7.1 and Figure 4.7.2. The blood plasma prediction is consistent with the Lu-DOTP speciation, where the most dominant complex of DOTP with Lu^{3+} is that with the highest occurrence at pH 7.4, viz. Lu(HDOTP) accounting for 7.5% of the ligand (Figure 4.7.2), with the remaining species being present in order of their abundance. Although the binuclear complex $Lu_2(H_2DOTP)$ is the second most prominent species at physiological pH, the model shows a preference for the mononuclear complexes. Calcium accounts a large component of the complexed DOTP, with a total of 69.7% of the ligand being consumed. Magnesium accounts for 11.5% and lutetium complexing about 9.9% with the balance remaining as the uncomplexed DOTP (protonated and deprotonated).

The blood plasma simulation revealed that the Lu complexed favourably with the DOTP ligand (Figure 4.7.1), accounting for 98.1% (Lu(HDOTP):73.7%, $Lu(H_2DOTP)$:12.6%, Lu(DOTP):10.95, $Lu_2(H_2DOTP)$:0.9%) of the plasma bound metal ion. Although a large component of the ligand was scavenged by calcium, due to the large excess of DOTP almost all of the Lu^{3+} remained securely complexed as initially prepared and administered. The remaining small percentage of Lu, 1.0 and 0.9 binds with two blood plasma ligands, Lu(Glycine) and Lu(Threonine) respectively. The Lu^{3+} blood plasma results as shown in Figure 4.7.1 compares well with that of the DOTP – Figure 4.7.2, where the largest fraction of the DOTP-bound lutetium (73.7%) corresponds with the most prevalent Lu^{3+}-species of DOTP (7.5%) at pH 7.4. Similarly, this correlation can be seen for the rest of the Lu-DOTP complexes. The physiological stability observed for the complexes demonstrates that Lu-DOTP may be ideal as a radiotherapeutic agent. This could explain the biodistribution of [^{177}Lu]Lu-DOTP in rats, with selective skeletal uptake and retention of approximately 37-% of the initial administered activity for up to 7 days post injection [34]. This further substantiates that the Lu-DOTP drug complex is a promising bone-seeking palliative for the treatment of bone pain.

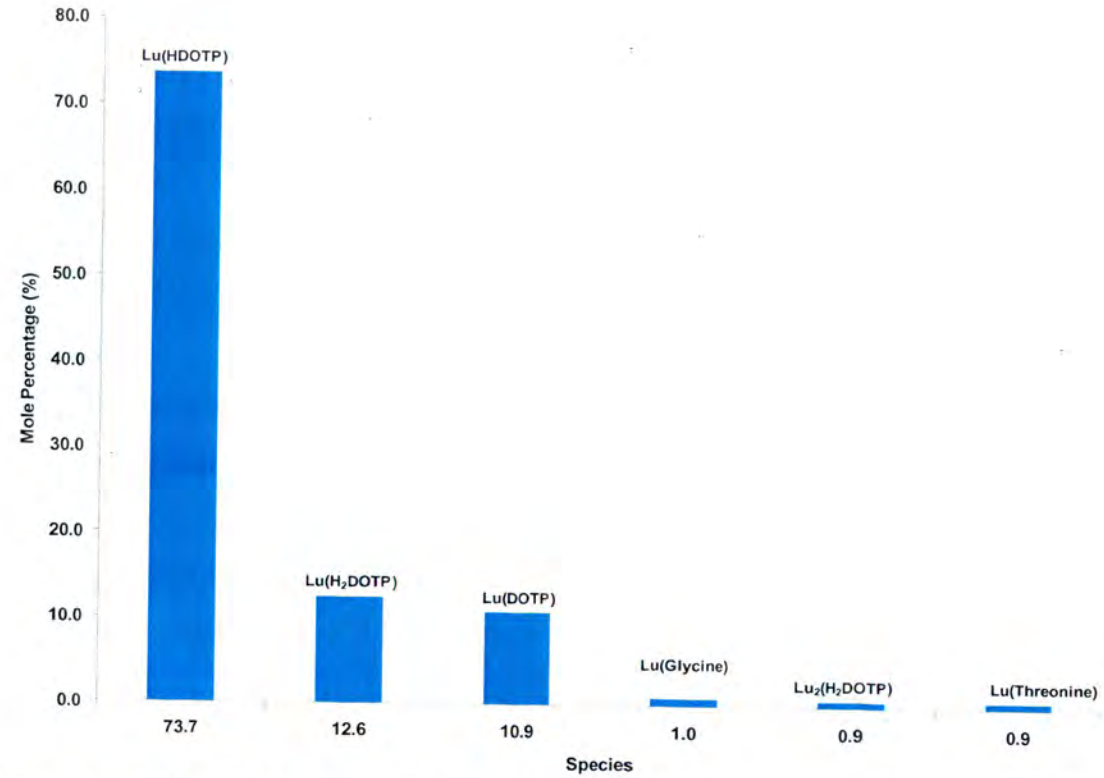

Figure 4.7.1. Blood plasma model for Lu^{3+} when administered as Lu-DOTP

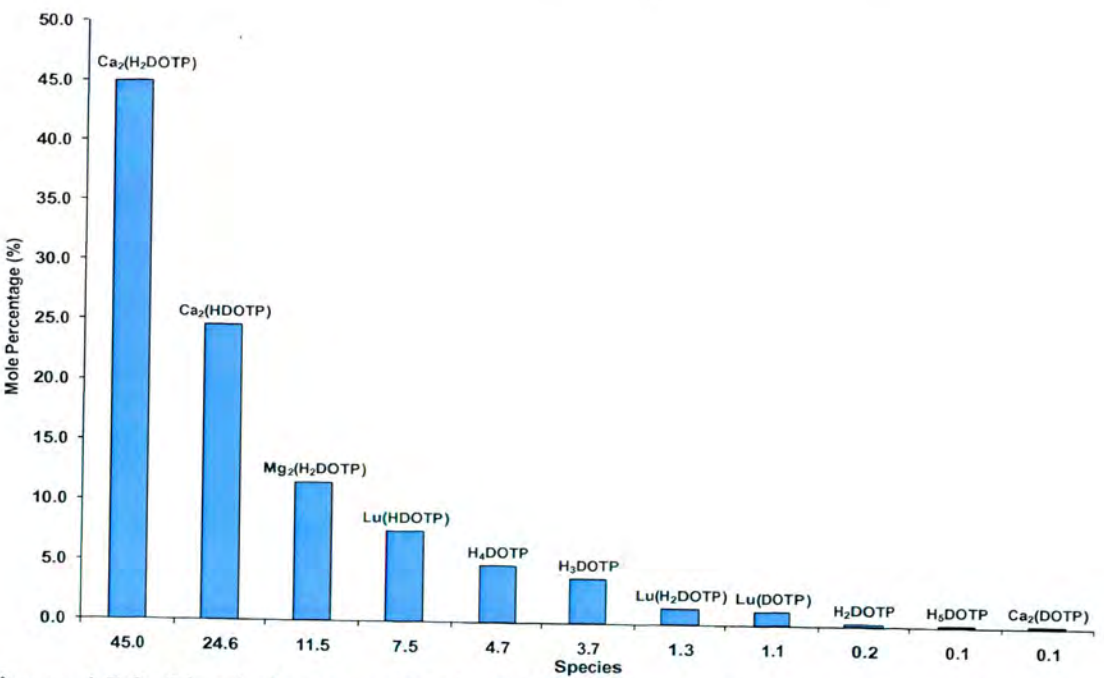

Figure 4.7.2. Blood plasma model for DOTP showing the complexation preferences of the ligand under physiological conditions for Lu: DOTP of 1:10.

The plasma mobilization indexes, as illustrated in Figure 4.8, indicate that the ligand has the propensity to flush the essential mineral ions from the blood at the typical administered DOTP concentration of 8.5×10^{-5} mol.dm^{-3} (with a metal ion to ligand ratio of 1:10), and may result in significant systemic deficiency thereof. The most significant being that of Cu^{2+}, mobilizes at approximately half of the administered concentration of the ligand. This is not surprising, as copper yields very high stability constants when complexed with DOTP [62]. Calcium and magnesium are present in larger quantities within blood plasma, therefore the effect of mobilization by the ligand is not as significant. During a treatment regime, which would normally comprise of a series of administrations over a period of time this could lead to severe chronic deficiencies, and would therefore require the co-administration of sufficient supplements. Especially Cu^{2+}, if not supplemented effectively the deficiency could present with conditions such as myelodysplasia, anemia, leukopenia, neutropenia, sensory ataxia, peripheral neuropathy and myelopathy [63, 64]. However, this would only apply should the treatment require several, and regular administrations of the DOTP-containing drug.

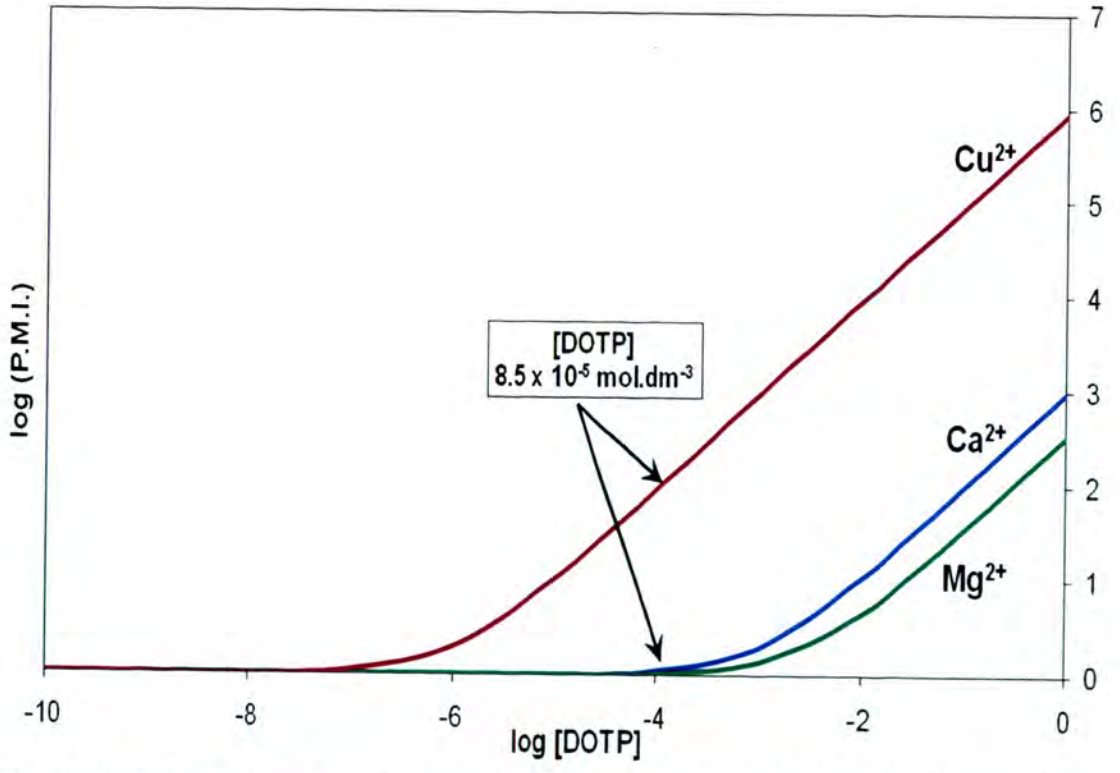

Figure 4.8. *Blood plasma mobilization indexes (PMI) of DOTP for Ca^{2+}, Mg^{2+} and Cu^{2+}.*

4.5 Speciation of Lu^{III} with EDTMP and selected blood plasma ligands– Citrate, Lactate, Glutamine, Threoninate, Glycinate

Blood plasma is a highly coordinating medium containing many potential ligands. It contains a number of low molar mass ligands like phosphate, carbonate, amino acids, carboxylic acids, and proteins which are potential coordinators of lutetium. An attempt was made to study the behaviour of ^{177}Lu when administered at as ^{177}Lu-EDTMP in vivo. This forms a part which aimed at establishing a blood plasma model for ^{177}Lu. The blood plasma ligands where selected by running the ECCLES program and from the results taking all the lutetium complexes. And also the JESS program was used to extract all the ligands complexing with ^{166}Gd and ^{153}Sm. All this values were added into ECCLES and then the program was run to give forth the ligands in Table 4.3. These ligands were then taken to be evaluated with Lu as they showed competition for EDTMP in blood plasma. One can notice that Glutamine is not included in Table 4.3 but it is evaluated with ^{177}Lu. This is because the formation constants of Glutamine with Gd and Sm could not be found in both ECCLES and JESS databases.

Corrections for temperature and ionic strength were made to obtain estimates for constants measured under biological conditions. In the absence of any value from the literature, an estimate was made based on the corresponding constants for Lu(III) complexation. These constants were then used in computer simulations to give percentage distributions of Lu^{3+} ion amongst the LMW complexes in blood plasma. From the results of these simulations, the species of major importance were identified and the formation constants of these complexes were experimentally determined by potentiometric titration. Then from the information acquired, a plot of Lu vs Gd was determined. Excellent linear correlations were found and are indicated in Figure 4.5.1(a). This curve clearly indicates the ligands that would be bound to ^{177}Lu when it is introduced as ^{177}Lu-EDTMP into the bloodstream.

Table 4.3. ECCLES results of potential ligands that will complex with Lu^{3+}

Composition	Log Stability constant	Species Concentration	% Concentration
GLY1(1) Lu^{3+}(1)	13.22	2.4300E-04	1.7
THR1(1) Lu^{3+}(1)	12.74	1.5000E-04	1.1
CTA3(1) Lu^{3+}(1)	8.12	1.1257E-04	0.8
LTA1(1) Lu^{3+}(1)	3.27	2.7309E-05	0.2

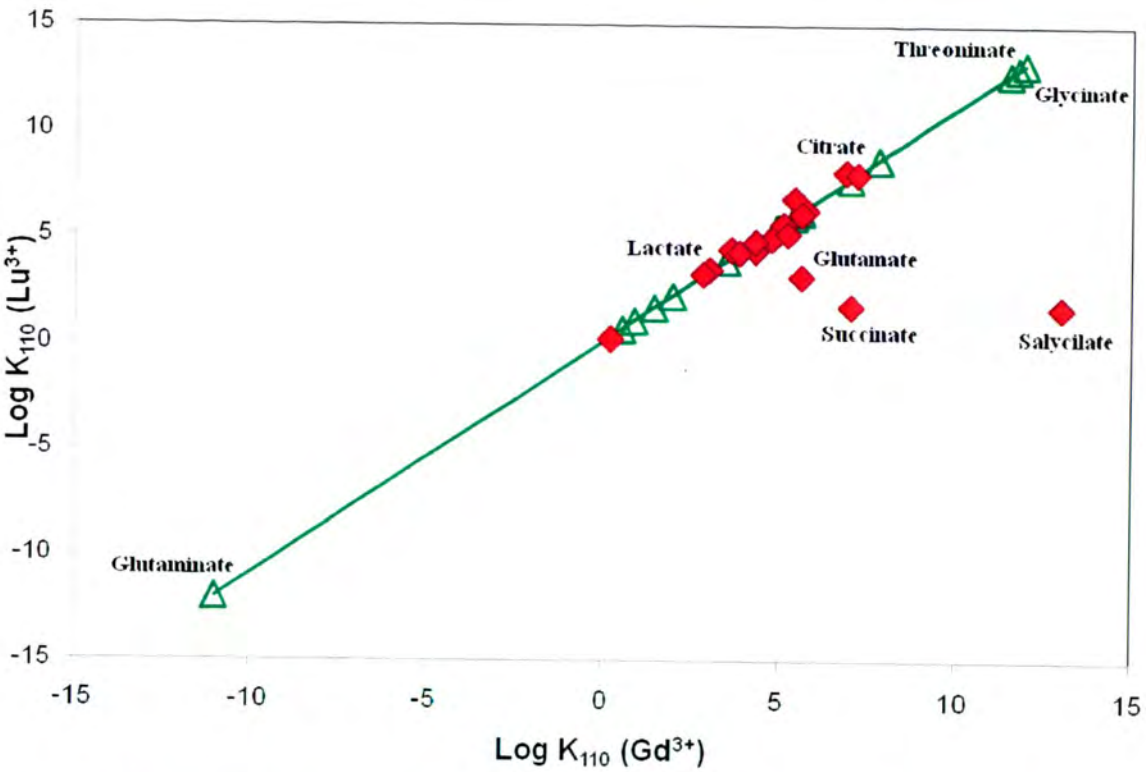

***Figure 4.9**. Linear free energy relationship of formation constants for blood plasma ligands (◆) represents literature constants: Lu^{3+} vs Gd^{3+} and (Δ) represents the calculated constants for Lu^{3+}*

Table 4.4. *Protonation constants of EDTMP, citrate, Lactate, Glycinate, Glutaminate, and Threoninate, determined at 25 °C and 0.15 M NaCl.*

Equilibrium Species[#]	Log K		Hamilton R-factor	Number of points
	This work	Literature[4]		
	25 °C, 0.15 M NaCl	*25 °C, 0.1 M NaCl*		
Citrate				
$H + L \rightleftharpoons HL$	5.55	5.74	0.00683	301
$2H + L \rightleftharpoons H_2L$	4.45	4.41		
$3H + L \rightleftharpoons H_3L$	3.14	3.01		
Lactate				
$H + L \rightleftharpoons HL$	3.51	3.66	0.00302	212
Glycinate				
$H + L \rightleftharpoons HL$	9.58	9.56	0.00891	227
$2H + L \rightleftharpoons H_2L$	2.43	2.36		
Glutaminate				
$H + L \rightleftharpoons HL$	9.11	9.00	0.00756	211
$2H + L \rightleftharpoons H_2L$	2.15	2.18		
Threoninate				
$H + L \rightleftharpoons HL$	8.96	8.96	0.00831	222
$2H + L \rightleftharpoons H_2L$	2.38	2.21		

The charges on the ligands and complexes have been omitted for simplicity

Experiments where performed under blood plasma conditions and the protonation results for the ligands citrate, lactate, glycinate, glutaminate and threonine are given Table 4.3. Good fit were found between experimental and calculated models as shown by the low Hamilton R-factor. These protonation constants closely resemble literature [59] values. $\overline{Z_H}$ curves and species distribution curves for all the ligands were drawn and the experimental points agrees well with the calculated data. Complexation of the ligands with Lu^{3+} was not possible due to the sensitivity of our electrode which can only measure the pH range of 2 -11. This was also observed in the Q and Z curves where nice fit could

not be attained. Protonation constants of EDTMP were not plausible as compared to literature values. The differences in the protonation constants of the EDTMP which was due to the impurities of the ligand made it impossible for one to conclude the blood plasma modeling of ^{177}Lu.

Chapter 5

CONCLUSION AND FUTUREWORK

Conclusion and Future Work

5.1 Conclusion

The Lu-DOTP complex has been shown to be thermodynamically stable; and in combination with previously reported kinetic data [36, 39-41] and *in vivo* biodistribution results [34] this study has demonstrated that [^{177}Lu]Lu-DOTP is robust and may be suitable as a radiotherapeutic for the treatment of bone pain. Blood plasma modeling using the complex stability constants provided an indication of the complexation preferences of the Lu^{3+} ions and DOTP *in vivo*. Formation constants for the complexation of Lu and selected blood plasma metal-ions (Ca^{2+}, Cu^{2+} and Mg^{2+}) with DOTP were calculated using potentiometry. Good fits indicated by low standard deviations and Hamilton R factors in log K values were obtained for the protonation of the ligand and for complexation with all the metal-ions studied. In each of the three metals, M_2L type species (binuclear complexes) were formed. The most dominant complexes formed at the physiological pH 7.4 were Cu_2HDOTP, Ca_2H_2DOTP, and Mg_2H_2DOTP for Cu^{2+}, Ca^{2+} and Mg^{2+} respectively.

According to the simulation the ligand complexes predominantly with Cu^{2+}, however when administered in large excess the Lu-DOTP complex can be maintained *in vivo*. Although only 9.9% of the DOTP is complexed as Lu-DOTP almost all of the Lu^{3+} ions (about 98.1%) remained bound to DOTP when administered at Lu:DOTP of 1:10 in blood plasma. This implies that a large fraction of an injected dose of [^{177}Lu]Lu-DOTP would accumulate selectively in bone, and possibly circumvent any unwanted distribution and radiotoxicity to other non-target and sensitive organs. The *in vivo* studies as performed by Chakraborty *et al.* [34] successfully demonstrated the bone-selective distribution of [^{177}Lu]Lu-DOTP. The PMI curves (Figure 4.8) showed that only Cu^{2+}-ions are mobilized by DOTP at a ligand concentration indicated by an arrow, which would be used clinically. Unfortunately the blood plasma model for Lu^{177} could not be established due to the impureness of the EDTMP sample used and failure in determining the formation constants of Lu^{3+} with the amino acids.

5.2 Future Work

- Protonation constants of EDTMP must be determined and these constants must be compared with the literature values. A new source of EDTMP of analytical grade must be used in all the experiments where it is evaluated with ^{177}Lu in order to finalize the complexation studies of Lu-EDTMP and in vivo behaviour of the radiodrug.
- An attempt was made to establish a blood plasma model for Lu(III). In order to establish the blood plasma model for Lu^{III}, another method e.g. polarography, should be used to determine the formation constants of the three amino acids (glutamine, glycine and threonine) which could not be measured by potentiometry due to the sensitivity of the pH-electrode that could measure only pH 2-11 region. After these stability constants have been measured successfully, blood plasma models using ECCLES can then be constructed. It will be possible also to construct PMI curves to be able to deduce which metal ions will be mobilized by EDTMP. ECCLES calculations could not be pursued.
- The Zn-DOTP was never reported in literature. The knowledge of this system could be beneficial as this metal ion has the tendency to be mobilized by ligands like MDP, HEDP and EDTMP in blood plasma. These formation constants should be studied and included in the ECCLES database and the PMI curve should then be constructed.
- Biodistribution studies should be done in animal models to test the radiopharmaceutical ^{177}Lu-DOTP. This will give a practical insight on the behaviour of the complex *in vivo*.

5.3 References

1. G.R. Mundy, Mechanism of bone metastasis, Cancer, 1997, 80: 1546-1556
2. O.S. Nielsen, A.J. Munro, I.F. Tannoock. Bone metastasis:pathology and management policy, Journal of Clinical Oncology. 1991, 2: 320-323
3. L.J. Petersen, L. Lund, M. Jonler, J.J. Abrahamsen. Samarium-153 treatment of bone pain in patients with metastatic prostate cancer, Danish medical Bulletin. 2010, 57: 1-5
4. S. Paget, The distribution of secondary growths in cancer of the breast, Lancet, 1889, 1:571-572
5. D.A. Casciato, H.A. Chansky, B.B. Lowitz, Bone and joint complications, Manual of Clinical Oncology, 2000, 4: 601-614
6. A.N. Serafini, Therapy of metastatic bone pain, Journal of Nuclear Medicine, 2001, 42: 895-906
7. R. Massey, Current use of therapeutic radiopharmaceuticals for patient care, Medscape Portals, 2000, 1-7
8. T. Das, S. Chakraborty, H.D. Sarma, S. Banerjee, ^{177}Lu-DOTMP: A viable agent for palliative radiotherapy of painful bone metastasis, Radiochimica Acta, 2008, 96: 55-61
9. J.E. Hamaoka, D.A. Madewell, G.N. Podoloff, N.T. Hortobagyi, Bone imaging in metastatic breast cancer, Journal of Clinical Oncology, 2004, 22: 2942-2953
10. G.M. Blake, S.J. Park-Holohan, G.J. Cook, I. Fogelman, Quantitative studies of bone with the use of ^{18}F-fluoride and ^{99m}Tc-methylene disphosphonate. Seminar of Nuclear Medicine, 2001, 31: 28-49
11. K. De, S. Chandra, B. Sarkar, S. Ganguly, M. Misra. Synthesis and biological evaluation of ^{99m}Tc-DHPM complex: a potential new radiopharmaceutical for lung imaging studies, Journal of Radioanalytical Nuclear Chemistry, 2010, 283: 621-628
12. G.Van der Pluijm, H. Vloedgraven, E. van Beek, L. van der Wee-pals, C. Lowik, S. Papapous. Bisphosphonates inhibit the adhesion of breast cancer cells to bone matrices in vitro, J Clin Invest, 1996, 98: 698-705

13. R.K. Doot, M. Muzi, L.M. Peterson, E.K. Schubert, J.M. Specht, D.A. Mankoff. Kinetic analysis of ^{18}F-Fluoride PET images of breast cancer bone metastases, Journal of Nuclear Medicine, 2010, 51: 521-527

14. F.D. Grant, F.H. Fahey, A.B. Packard, R.T. Davis, A. Alavi, S.T. Treves, Skeletal PET with ^{18}F-Fluoride: Applying new technology to an old tracer, Journal of Nuclear Medicine. 2008, 49: 68-78

15. M. Tripathi, T. Singhal, N. Chandrasekhar, P. Kumar, C. Bal, P.K. Jhulka, G. Bandopadhyaya, A. Malhotra. Samarium-153 ethylenediamine tetramethylene phosphonate therapy for bone palliation in skeletal metastases, Indian Journal of cancer, 2006, 43: 86-92

16. T. Das, S. Chakraborty, S. Barnerjee, K.V.V. Nair, V. Chirayil, M. Venkatesh, H.D. Sarma, C.S. Bal, G. Arora, ^{177}Lu-EDTMP: A new radiopharmaceutical for palliation of bone pain in cancer patients with skeletal metastases, Dr Homi Bhabha Centenary Year, 2009, 305: 2-11

17. E.B. Silberstein, A.H. Elgazzar, A. Kapilivsky. Phosphorus-32 radiopharmaceuticals for the treatment of painful osseous metastases. Seminars of Nuclear Medicine. 1992, 22: 17-27

18. H.L. Atkins, L.F. Mausner, S.C. Srivastava, G.E. Meinken, R.F. Straub, C.J. Cabahug, D.A. Weber, C.T.C. Wong, D.F. Sacker, S. Madajewicz, T.L. Park, A.G. Meek, Biodistribution of Sn-117m (4+)DTPA for palliative therapy of painful osseous metastases, Radiology, 1993, 186: 279-83

19. P.M. May, P.W. Linder, D.R. Williams. Journal of Chemical Society, Dalton Trans, 1977, 588

20. D. Ma, A.R. Ketring, G.J. Ehrhardt, W. Jia, Production of radiolanthanides and radiotherapy research at MURR. Journal of Radioanalytical and Nuclear Chemistry, 1996, 206:119-126

21. M.P. Capello, F. Marques, L. Gano, S. Lacerda, I. Santos. Radiochemical and biological behaviour of ^{153}Sm and ^{166}Ho complexes anchored by a novel bis(methylphosphonate) tetraazamacrocycle. Radiochimica acta, 2007, 95: 329-334

22. B. Mathew, S. Chakraborty, T. Das, H.D. Sarma, S. Barnejee, G. Samuel, M. Venkatesh, M.R.A. Pillai, ^{175}Yb labeled polyaminophosphonates as potential agents for bone pain palliation, Applied Radiation and Isotopes, 2004, 60: 635-642

23. N.V. Jarvis, J.M. Wagener. Complexation of trivalent lanthanides by ethylenediaminetetramethylenephosphonate (EDTMP), South African Journal of Chemistry, 1995, 48: 85-89

24. M.R.A. Pillai, S. Chakraborty, T. Das, M. Venkatesh, N. Ramamoorthy, Production logistic of ^{177}Lu for radionuclide therapy, Applied Radiation and Isopes, 2003, 59: 109-118

25. K. Wang, R.C. Li, Y. Cheng, B. Zhu, Lanthanides—the future drugs? Coordination Chemistry Reviews, 1999, 297- 308

26. R.B. Lauffer. Chemical Review, 1987, 87: 901

27. M.F. Tweedle, Relaxation agents in NMR imaging, Lanthanides Probes in Life, Chemical and Earth Science (Eds,: J.-C., Bunzli, G.R. Choppin, Elsevier, Amsterdam, 1989, 127-179

28. L.Burai, R. Kiraly, I. Lazar, E. Brucher. Formation and dissociation kinetics of the complexes Gd(DOTP)$^{-5}$ and Gd(DOTPMB)$^{-}$, EuropeanJournal of Inorganic Chemistry, 2001, 813-820

29. P. Caravan, J.J. Ellison, T.J. McMurry, Gadolinium(III) chelates as MRI contrast agents: structure, dynamics and applications, Chemical Reviews, 1999, 99: 2293

30. F. Albaaj, A.J. Hutchison, Expect Opin. Pharmacother, 2005, 6: 319

31. P. Tandon, S. Barnejee, M. Venkatesh, M.R.A. Pillai, ^{170}Tm-EDTMP: a potential cost effective alternative to $^{89}SrCl_2$ for bone palliation palliation, Nuclear Medicine and Biology, 2009, 36: 561-568

32. G.A. Rutty Sola, M.G. Arguelles, D.L. Bottazzini, J.C. Funari, I.G. Parada, A.M. Rojo, H.V. Ruiz, Lutetium-177-EDTMP for bone pain palliation, Preparations, biodistribution and pre-studies. Publicado en Radiochimica. 2000, 3: 157-161

33. T. Das, S. Chakraborty, P.R. Unni, S. Barnejee, G. Samuel, H.D. Sarma, M. Venkatesh, M.R.A. Pillai, ^{177}Lu-labeled cyclic polyaminophosphonates as

potential agents for bone pain palliation, Applied Radiation and isotope, 2002, 57: 177-184

34. S. Chakraborty. T. Das, H.D. Sarma, M. Venkatesh, S. Banerjee, Comparative studies of ^{177}Lu-EDTMP and ^{177}Lu-DOTMP as potential agents for palliative radiotherapy of bone metastasis, Applied Radiation and Isotopes, 66 (2008) 1196-1205
35. K. W. Logan, W.A. Volkart, R.A. Holmes, Radiation dose calculations in persons receiving injection of ^{153}Sm-EDTMP, Journal Nuclear Medicine, 1987, 28: 505
36. L. Smentek. Lanthanides caged by the organic chelates; structural properties. Journal of Physics: Condensed Matter, 2011, 23: 1-15
37. S. Lacerda, F. Marques, P. Capello, L. Gano, V. Kubicek, P. Hermann, I. Santos. Chemical, radiochemical and biological studies of Sm and Ho complexes of H DOTA analogues containing one methylphosphonic/phosphinic acid pendant arm. Journal of Labelled Compounds Radiopharmaceutiticals, 2010, 53:36-43
38. S. Banerjee, S. Chakraborty, T. Das, K. Kothari, G. Samuel, M. Venkatesh, M.R.A. Pillai, B. Mathew, H.D. Sarma, P.R. Chaudhari, ^{177}Lu-DOTMP, ^{153}Sm-DOTMP, ^{175}Yb-EDTMP and $^{186/188}$Re-CTMP: Novel agents for bone pain palliation and their comparison with ^{153}Sm-EDTMP, Founder's Day Special Issue, 2005, 22-37
39. A.D. Sherry, J. Ren, J. Huskens, E. Brucher, E. Toth, C.F.C.G. Geraldes, M.M.C.A. Castro, W.P. Cacheris. Characterization of lanthanide (III) DOTP complexes: Thermodynamic, protonation and coordination to alkali metal ions. Inorganic Chemistry, 1996, 35: 4604-4612
40. R. Delgado, J.J.R. Frausto Da Silva, Metal complexes of cyclic tetra-azatetra-acetic acids, Talanta, 1982, 29: 815-822
41. F. Marques, L. Gano, M.P. Capello, S. Lacerda, I. Santos, L.M.P. Lima, J. Costa, P. Antunes, R. Delgado, 13- and 14-membered macrocyclic ligands containing methylcarboxylate or methylphosphonate pendant arms: Chemical and biological evaluation of their ^{153}Sm and ^{166}Ho complexes as potential agents for therapy or bone pain palliation, Journal of Inorganic Biochemistry, 2006, 100: 270-280

42. S. Liu, D.S. Edwards, Bifunctional chelators for therapeutic lanthanide radiopharmaceuticals, Bioconjugate Chemistry, 2001, 12: 7-34

43. X. Sun, M. Wuest, Z. Kovacs, A.D. Sherry. R. Motekaitis, Z. Wang, A.E. Martell, M.J. Welch, C.J. Anderson, Journal of Biological Inorganic Chemistry, 2003, 8: 217-225

44. D.A. Skoog, D.M. West, F.J. Foller, Fundamentals of Analytical Chemistry, 7th Edition, Harcourt College Publishers, 1996, 423-427

45. D.R. Jansen, MSc thesis, The study of the complexation of Sn(II)-APDDMP and Sn(IV)-PEI-MP, considered as potential therapeutic agents for bone metastases. University of Cape Town, 2005

46. O. Yamauchi, A. Odani, Pure and Applied Chemistry, 1996, 68: 469-496

47. P.M. May, K. Murray, D.R. Williams, The use glass electrodes for the determination of formation constants-II: Simulation of titration data, Talanta, 1985, 32: 483-489

48. P.M. May, K. Murray, D.R. Williams, The use glass electrodes for the determination of formation constants-III: Optimization of titration data : The Esta library of computer programs, Talanta, 1988, 72: 1453-1470

49. D.M. Templeton, F. Ariese, R. Cornelis, L. Danielsson, H. Muntau, H.P. Van leewen, R. Lobinski, Pure and Applied Chemistry, 2000, 72: 1453-1470

50. J.R. Zeevaart. PhD thesis, Metal ion speciation in blood plasma as a tool in predicting the in vivo behaviour of potential bone-seeking radiopharmaceuticals, Delft University of Technology, Delft University Press, The Netherlands, 2001, 127-144

51. N. Ingri, W. Kakolowicz, L.G. Sillen, B. Warnqvist, Talanta, 1969, 14: 1261

52. R.D. Handcock, Approaches to predicting stability constants, Analyst, 1997, 122, 51R.

53. L.P Hammett, Journal of American Chemical Society, 1937, 59:96

54. D.R. Jansen. PhD thesis, An in vitro approach to evaluate and develop potential ^{117m}Sn-based bone-seeking radiopharmaceuticals, Delft University of Technology, Delft University Press, The Netherlands, 2010, 127-151

55. I. Cukrowski, D.M. Mogano, J.R. Zeevaart. Voltametry as a virtual potentiometric sensor in modeling of a metal-ligand system and refinement of stability constants. Part4. An electrochemical study of Ni complexes with methylene diphosphonic acid, Journal of Inorganic Biochemistry, 2005, 99:2308

56. J.H. Turner, A.A. Martindale, P. Sorby, E.L. Hetherington, R.F. Fleay, R.F. Hoffman, P.G. Claringbold, Samarium-153 EDTMP therapy of disseminated skeletal metastasis, European Journal of Nuclear Medicine, 1989, 15: 784-795

57. P. Gans and B. O'Sullivan, GLEE, a new computer program for glass electrode calibration, Talanta, 2000, 51: 33-37

58. A.E. Martell and R.M. Smith, Critical Stability constants, Plenum Press, New York, 1974-1989, Vols 1-6

59. NIST Standard Reference Database46, NIST Critically Selected Stability Constants of Metal Complexes Database, Version 3.0, Data collected and selected by A.E. Martell and R.M. Smith, U.S. Department of commerce, National Institute of Standards and Technology, 1997

60. R. Delgado, L.C. Siegfried, T. A. Kaden, Helvica Chimica Acta, 1990, 73:140-148

61. L. Burai, R. Kiraly, I. Lazar, E. Brucher, European Journal of Inorganic Chemistry, 2001, 813-820

62. F.K. Kálman, Z. Baranyai, I. Tóth, I. Bányai, R. Király, E. Brücher, S. Aime, X. Sun, A.D. Sherry, Z. Kovács, Inorg. Chem. 47 (2008) 3851–3862.

63. T. R. Halfdanarson, N. Kumar, C. Y. Li, R. L. Phyliky, W. J. Hogan, Haematological manifestations of copper deficiency: a retrospective review, European Journal of Haematology, 2008, 80: 523-531

64. S. R. Jaiser, G. P. Winston, Journal of Neurology, 2010, 257:869-881

APPENDIX A

The dominant species, Lu-DOTP-H was observed at pH 7.4. Lu^{3+} metal ion is postulated to be caged inside the ring, attached to the central four nitrogens and also coordinating with the phosphonate arms whereby the other phosphonate is protonated. The molecular geometry of the structure is therefore thought to be a square planar/distorted octahedral.

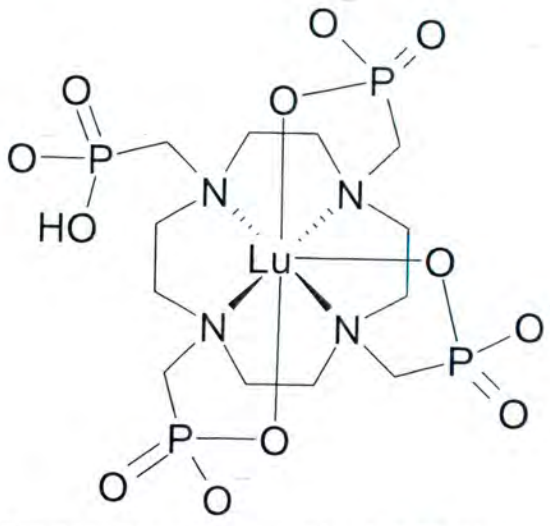

The possible structure of Lu-DOTP-H.

APPENDIX B

1. Typical E_0 and gradient titration data

0.000	283.728
0.101	283.388
0.200	282.841
0.301	282.223
0.401	281.603
0.500	281.607
0.601	281.608
0.701	279.662
0.800	279.665
0.901	278.263
1.001	278.262
1.100	276.819
1.201	276.080
1.301	275.331
1.400	274.554
1.501	273.780
1.601	273.784
1.700	272.089
1.801	271.174
1.901	270.283
2.000	270.287
2.101	268.442
2.201	267.471
2.300	266.468
2.401	265.393
2.501	265.388
2.601	263.115
2.701	263.119
2.800	263.120
2.901	259.516
3.001	258.186
3.100	258.183
3.201	255.316
3.301	253.725
3.400	252.003
3.501	250.227
3.601	248.368
3.700	248.368
3.801	244.348
3.901	244.351
4.000	239.455
4.101	236.593

4.201	233.403
4.300	229.829
4.401	225.712
4.501	220.935
4.600	215.153
4.701	207.405
4.801	196.752
4.900	196.747
5.001	137.737
5.023	126.987
5.068	60.633
5.077	24.044
5.086	-11.104
5.101	-52.466
5.120	-75.331
5.147	-93.709
5.185	-109.972
5.238	-125.183
5.312	-141.462
5.402	-157.165
5.503	-157.167
5.602	-186.617
5.635	-190.262
5.699	-196.955
5.800	-205.466
5.899	-212.065
5.999	-217.396
6.100	-221.925
6.199	-225.749
6.299	-229.162
6.400	-232.253
6.499	-234.985
6.599	-237.430
6.700	-239.645
6.799	-241.660
6.899	-241.664
7.000	-245.209
7.099	-246.829
7.199	-248.380
7.300	-249.844
7.399	-251.186
7.499	-252.413
7.600	-253.626
7.699	-254.733
7.799	-255.814
7.900	-255.815

7.999	-257.900
8.099	-258.853
8.200	-259.770
8.299	-260.629
8.400	-261.457
8.499	-262.254
8.599	-263.028
8.700	-263.785
8.799	-264.518
8.899	-265.216
9.000	-265.894
9.099	-266.558
9.199	-267.163
9.300	-267.806
9.399	-267.806
9.499	-269.005
9.600	-269.006
9.699	-270.140
9.799	-270.674
9.900	-271.204
9.999	-271.688
10.001	-271.689

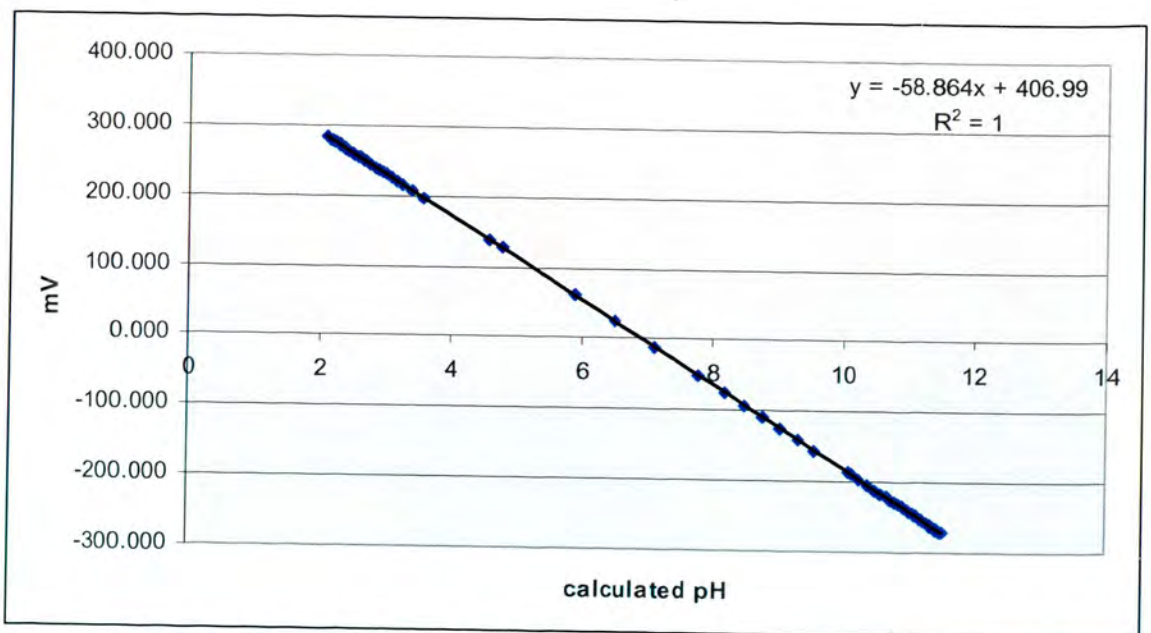

The graph of potential (mV) against the calculated pH values for the determination of E° and gradient values.

APPENDIX C

DOTP protonation titration data

```
TASK OBJE 1       DOT8
MODL     DOT8 H +1
CPLX 0  1 -13.79   DOT8( 0) H +1(-1)
CPLX 1  1 51.0679  DOT8( 1) H +1( 6)
CPLX 1  1 46.0452  DOT8( 1) H +1( 5)
CPLX 1  1 40.1865  DOT8( 1) H +1( 4)
CPLX 1  1 32.6892  DOT8( 1) H +1( 3)
CPLX 0  1 24.1090  DOT8( 1) H +1( 2)
CPLX 1  1 13.1864  DOT8( 1) H +1( 1)
CONC
VESL IVOL 39.9962200  0 0
VESL DOT8 0.00124940  8 0
VESL H +1 0.01261168  0 0
BUR1 H +1 -0.0499181  0 0
ELEC
ZERO H +1 406.048      0
GRAD H +1 58.438       0
WGHT 1
VESL DOT8 0.00000249
VESL H +1 0.00002483
BUR1 H +1 -0.0001009
ZERO H +1 0.25
GRAD H +1 0.02
TITR RNDE 0.001
EOBS RNDE 0.08
DATA
11.171    230.777
11.200    229.088
11.301    225.660
11.401    221.708
11.500    221.713
11.572    214.931
11.601    212.149
11.675    207.661
11.774    200.339
11.874    200.341
11.939    185.883
11.975    178.114
12.013    172.839
12.092    161.923
12.192    149.571
12.292    149.567
```

12.347	139.368
12.392	130.901
12.436	127.569
12.523	121.331
12.622	121.328
12.682	113.445
12.723	108.018
12.779	104.614
12.880	104.619
12.940	97.570
12.980	92.908
13.041	89.519
13.142	83.968
13.241	83.967
13.341	72.679
13.405	68.773
13.506	62.162
13.605	62.159
13.705	47.965
13.758	43.771
13.859	35.472
13.958	26.512
14.059	17.142
14.159	7.405
14.258	7.402
14.359	-10.998
14.403	-14.616
14.493	-21.771
14.592	-29.281
14.692	-36.375
14.793	-43.524
14.892	-50.551
14.992	-57.775
15.093	-65.180
15.192	-72.479
15.292	-79.644
15.393	-86.958
15.492	-92.683
15.592	-101.096
15.693	-101.099
15.792	-116.941
15.841	-121.190
15.939	-129.843
16.040	-129.844
16.140	-149.441
16.182	-153.711

16.267	-162.538
16.366	-172.029
16.467	-172.033
16.567	-188.153
16.616	-191.329
16.713	-196.980
16.812	-196.976
16.913	-206.205
16.988	-208.873
17.089	-212.167
17.188	-215.008
17.288	-217.681
17.389	-217.685
17.488	-222.479
17.588	-224.548
17.689	-226.469
17.788	-228.180
17.888	-229.767
17.989	-229.771
18.088	-232.695
18.188	-234.081
18.289	-234.085
18.388	-236.781
18.488	-237.893
18.589	-237.896
18.688	-240.015
18.789	-241.022
18.888	-241.970
18.988	-242.941
19.089	-243.868
19.188	-244.772
19.288	-245.598
19.389	-246.414
19.488	-246.413
19.588	-247.891
19.689	-248.603
19.788	-249.337
19.888	-250.043
19.989	-250.722
20.088	-251.366
20.188	-251.979
20.289	-251.980
20.388	-253.224
20.488	-253.823
20.589	-254.413
20.688	-254.952

20.788	-255.495
20.889	-256.026
20.988	-256.488
21.088	-257.021
21.189	-257.506
21.288	-257.510
21.389	-258.477
21.488	-258.481
21.588	-259.380
21.689	-259.827
21.788	-260.239
21.888	-260.653
21.989	-261.060
22.088	-261.465
22.188	-261.867
22.289	-262.281
22.388	-262.654
22.488	-263.031
22.589	-263.036
22.688	-263.754
22.788	-264.098
22.889	-264.450
22.988	-264.792
23.088	-265.146
23.189	-265.150
23.288	-265.822
23.388	-266.136
23.489	-266.428
23.588	-266.740
23.688	-267.045
23.789	-267.362
23.888	-267.364
23.989	-267.979
24.088	-268.255
24.188	-268.539
24.289	-268.823
24.388	-269.099
24.488	-269.369
24.589	-269.650
24.688	-269.912
24.788	-270.168
24.889	-270.423
24.988	-270.678
25.001	-270.674

CONC

VESL IVOL 39.9924400 0 0
VESL DOT8 0.00249904 8 0
VESL H +1 0.01261792 0 0
BUR1 H +1 -0.0499181 0 0
ELEC
ZERO H +1 404.109 0
GRAD H +1 58.516 0
WGHT 1
VESL DOT8 0.00000498
VESL H +1 0.00002483
BUR1 H +1 -0.0001009
ZERO H +1 0.25
GRAD H +1 0.02
TITR RNDE 0.001
EOBS RNDE 0.08
DATA

5.501	286.852
5.601	286.852
5.700	286.095
5.801	286.090
5.901	285.325
6.000	284.966
6.101	284.586
6.201	284.585
6.300	283.826
6.401	283.830
6.501	283.019
6.600	282.616
6.701	282.171
6.801	282.174
6.900	281.386
7.001	280.962
7.101	280.966
7.200	280.129
7.301	279.667
7.401	279.208
7.500	278.772
7.601	278.319
7.700	278.323
7.801	277.419
7.901	276.966
8.000	276.963
8.101	275.963
8.201	275.471
8.300	275.053
8.401	274.444

8.501	273.938
8.600	273.936
8.701	272.893
8.801	272.354
8.900	271.791
9.001	271.786
9.101	270.650
9.200	270.095
9.301	269.503
9.401	268.910
9.500	268.906
9.601	267.657
9.701	267.657
9.800	266.343
9.901	266.344
10.001	265.011
10.100	264.350
10.201	263.627
10.300	262.900
10.401	262.898
10.501	262.898
10.600	260.563
10.701	259.780
10.801	258.965
10.900	258.161
11.001	257.288
11.101	256.402
11.200	255.426
11.301	254.439
11.401	253.400
11.500	252.420
11.601	251.369
11.701	250.263
11.800	250.259
11.869	248.634
11.901	247.872
12.001	246.620
12.100	246.625
12.169	244.776
12.201	243.900
12.301	242.482
12.400	242.481
12.470	240.373
12.501	239.448
12.601	237.768
12.701	237.769

12.770	235.091
12.801	233.888
12.900	231.738
13.001	229.502
13.101	227.077
13.200	227.082
13.272	223.137
13.301	221.511
13.401	218.277
13.500	214.478
13.601	210.095
13.701	205.061
13.712	204.434
13.800	199.327
13.901	199.324
14.001	199.324
14.054	186.751
14.100	175.806
14.138	172.217
14.212	165.613
14.313	156.928
14.412	156.931
14.469	149.056
14.512	143.026
14.567	139.921
14.667	134.758
14.767	134.759
14.866	125.826
14.944	122.620
15.044	118.664
15.145	114.991
15.244	114.987
15.344	108.249
15.442	105.164
15.541	102.184
15.642	99.240
15.742	96.265
15.841	93.252
15.942	90.347
16.042	87.465
16.141	84.659
16.242	81.829
16.342	79.114
16.441	76.359
16.542	73.455
16.642	70.491

16.741	70.488
16.842	64.280
16.942	61.294
17.041	58.158
17.142	54.934
17.242	51.589
17.341	51.585
17.442	44.147
17.532	40.545
17.633	36.412
17.732	32.113
17.832	27.799
17.933	24.110
18.032	18.684
18.133	13.741
18.233	8.704
18.332	3.410
18.433	-1.348
18.533	-6.068
18.632	-10.460
18.733	-14.748
18.833	-14.749
18.932	-23.065
19.014	-26.397
19.115	-30.536
19.214	-34.353
19.314	-38.071
19.415	-41.718
19.514	-45.188
19.614	-48.765
19.715	-52.431
19.814	-52.437
19.914	-59.910
20.004	-63.202
20.103	-66.740
20.204	-66.746
20.304	-73.841
20.398	-77.535
20.497	-81.304
20.597	-85.043
20.698	-88.723
20.797	-92.386
20.897	-96.057
20.998	-99.763
21.097	-103.455
21.197	-107.265

21.298 -107.267
21.397 -115.366
21.480 -118.932
21.581 -123.304
21.681 -127.889
21.780 -132.579
21.881 -137.649
21.981 -142.815
22.082 -142.819
22.181 -155.205
22.240 -158.979
22.341 -166.128
22.440 -172.954
22.540 -179.778
22.641 -185.934
22.740 -191.637
22.840 -191.636
22.941 -201.536
23.011 -204.485
23.112 -204.482
23.212 -211.686
23.305 -214.410
23.404 -217.040
23.504 -219.412
23.604 -221.656
23.704 -223.757
23.804 -223.753
23.904 -227.685
24.004 -229.345
24.105 -230.889
24.204 -232.361
24.304 -232.358
24.405 -235.110
24.504 -236.362
24.604 -237.574
24.705 -238.730
24.804 -239.825
24.904 -240.831
25.001 -241.756

CONC
VESL IVOL 39.9886600 0 0
VESL DOT8 0.00374891 8 0
VESL H +1 0.01261911 0 0
BUR1 H +1 -0.0499181 0 0
ELEC

ZERO H +1 404.109 0
GRAD H +1 58.516 0
WGHT 1
VESL DOT8 0.00000750
VESL H +1 0.00002520
BUR1 H +1 -0.0000998
ZERO H +1 0.25
GRAD H +1 0.02
TITR RNDE 0.001
EOBS RNDE 0.08
DATA

6.701	286.866
6.801	286.862
6.900	286.218
7.001	285.894
7.101	285.558
7.200	285.554
7.301	284.846
7.401	284.493
7.500	284.138
7.601	283.784
7.700	283.787
7.801	283.076
7.901	282.721
8.000	282.720
8.101	281.946
8.201	281.951
8.300	281.175
8.401	280.799
8.501	280.412
8.600	280.015
8.701	279.609
8.801	279.206
8.900	278.795
9.001	278.361
9.101	277.938
9.200	277.520
9.301	277.088
9.401	277.090
9.500	276.219
9.601	275.783
9.701	275.301
9.800	274.831
9.901	274.362
10.001	273.896
10.100	273.437

10.201	273.439
10.300	272.449
10.401	272.446
10.501	271.416
10.600	271.415
10.701	270.374
10.801	269.858
10.900	269.347
11.001	268.804
11.101	268.238
11.200	268.243
11.301	267.056
11.401	267.059
11.500	265.848
11.601	265.851
11.701	264.621
11.800	263.988
11.901	263.323
12.001	263.327
12.100	261.938
12.201	261.230
12.301	261.234
12.400	259.815
12.501	259.083
12.601	258.327
12.701	257.507
12.801	256.676
12.900	256.682
13.001	254.949
13.101	254.952
13.200	253.213
13.301	252.276
13.401	251.320
13.500	250.289
13.601	249.214
13.701	248.121
13.800	246.994
13.901	245.848
14.001	244.655
14.100	243.424
14.201	243.424
14.301	240.668
14.400	240.664
14.501	237.564
14.601	237.569
14.700	234.268

14.801	234.272
14.870	231.642
14.901	230.497
15.000	228.351
15.101	228.347
15.201	223.408
15.301	223.412
15.370	219.364
15.401	217.572
15.500	214.296
15.601	210.585
15.701	210.590
15.770	204.168
15.800	201.359
15.875	197.069
15.976	190.760
16.076	190.760
16.175	190.759
16.226	180.089
16.276	169.509
16.316	166.967
16.396	161.924
16.497	156.181
16.597	150.829
16.696	145.981
16.797	145.984
16.858	140.886
16.897	137.635
16.978	134.730
17.078	134.736
17.128	131.601
17.179	128.466
17.278	128.472
17.378	122.763
17.479	122.761
17.578	117.375
17.678	114.938
17.779	112.572
17.878	110.387
17.978	108.232
18.079	106.173
18.178	104.001
18.278	101.917
18.379	99.766
18.478	97.787
18.578	95.821

18.679	95.825
18.778	92.059
18.878	92.059
18.945	89.479
18.978	88.224
19.078	86.280
19.179	84.305
19.278	82.420
19.378	80.541
19.479	78.689
19.578	78.691
19.678	74.976
19.779	74.974
19.844	72.323
19.878	70.919
19.978	68.995
20.079	66.946
20.178	64.974
20.278	63.035
20.379	60.804
20.478	58.536
20.578	56.335
20.679	54.024
20.778	54.020
20.878	49.417
20.979	47.024
21.078	44.533
21.178	42.072
21.279	39.361
21.378	36.617
21.478	33.714
21.578	30.781
21.678	27.744
21.779	27.739
21.878	21.549
21.978	21.547
22.079	15.210
22.178	11.790
22.278	8.366
22.379	4.918
22.478	1.653
22.578	-1.561
22.679	-4.673
22.778	-7.745
22.878	-10.764
22.979	-10.765

23.078 -16.861
23.178 -19.724
23.279 -22.536
23.378 -25.210
23.478 -27.766
23.579 -30.351
23.678 -32.932
23.778 -35.501
23.879 -38.125
23.978 -40.670
24.079 -43.157
24.178 -45.568
24.278 -45.566
24.379 -50.474
24.478 -52.940
24.578 -52.935
24.679 -57.974
24.778 -60.368
24.878 -62.824
24.979 -65.191
25.001 -65.190

2. Lu-DOTP titration data

TASK OBJT 1 DOT8-LU+3
MODL LU+3 DOT8 H +1
CPLX 0 1 -13.79 LU+3(0) DOT8(0) H +1(-1)
CPLX 0 1 12.9922 DOT8(1) H +1(1)
CPLX 0 1 21.6639 DOT8(1) H +1(2)
CPLX 0 1 29.2456 DOT8(1) H +1(3)
CPLX 0 1 35.1661 DOT8(1) H +1(4)
CPLX 0 1 40.2780 DOT8(1) H +1(5)
CPLX 0 1 42.1176 DOT8(1) H +1(6)
CPLX 0 1 -7.9900 LU+3(1) H +1(-1)
CPLX 0 1 41.3355 LU+3(1) DOT8(1) H +1(4)
CPLX 1 1 39.1605 LU+3(2) DOT8(1) H +1(2)
CPLX 1 1 34.5102 LU+3(2) DOT8(1) H +1(1)
CPLX 1 1 28.4110 LU+3(2) DOT8(1) H +1(0)
CPLX 1 1 21.7494 LU+3(2) DOT8(1) H +1(-1)
CPLX 1 1 07.7318 LU+3(2) DOT8(1) H +1(-3)
CPLX 1 1 -2.2450 LU+3(2) DOT8(1) H +1(-4)
CONC
VESL IVOL 39.982990 0 0
VESL DOT8 0.0009963 7 0
VESL H +1 0.0126906 0 0
VESL LU+3 0.0010006 0 0

```
BUR1 H +1 -0.049918   0 0
ELEC
ZERO H +1 400.889      0
GRAD H +1 58.174       0
WGHT 1
VESL DOT8 0.0000020
VESL H +1 0.0000254
VESL LU+3 0.0000017
BUR1 H +1 -0.000100
ZERO H +1 0.82
GRAD H +1 0.12
TITR RNDE 0.001
EOBS RNDE 0.08
DATA
 9.001    259.326
 9.101    258.567
 9.200    258.570
 9.301    257.021
 9.401    256.211
 9.500    255.376
 9.601    255.373
 9.701    253.605
 9.800    252.656
 9.901    251.701
10.001    250.743
10.201    248.708
10.300    247.664
10.401    246.480
10.501    246.481
10.568    244.854
10.600    244.068
10.701    242.810
10.801    241.501
11.001    238.764
11.101    238.760
11.170    236.575
11.200    235.602
11.301    233.834
11.401    231.963
11.500    230.062
11.601    230.057
11.669    227.128
11.701    225.788
11.800    223.455
11.901    220.766
12.001    217.850
```

12.100	214.563
12.201	210.943
12.301	206.966
12.470	200.289
12.501	197.342
12.573	193.074
12.674	193.079
12.738	182.753
12.774	176.945
12.823	172.305
12.920	161.957
13.019	161.960
13.075	149.453
13.119	139.737
13.158	135.698
13.235	127.666
13.391	116.491
13.435	107.823
13.477	104.021
13.560	96.446
13.660	87.702
13.761	79.065
13.860	70.891
13.960	62.717
14.119	52.910
14.160	45.986
14.208	42.124
14.302	34.182
14.402	25.641
14.502	17.258
14.602	9.118
14.702	6.622
14.802	3.625
14.902	-4.009
15.001	-4.012
15.102	-11.363
15.194	-11.436
15.293	-13.066
15.394	-21.260
15.488	-20.656
15.588	-29.449
15.670	-26.647
15.769	-27.803
15.869	-37.716
15.945	-36.597
16.044	-41.158

```
16.144    -54.543
16.212    -59.992
16.313    -81.484
16.362    -93.215
16.434    -110.097
16.520    -123.837
16.620    -142.279
16.706    -155.810
16.807    -169.026
16.906    -169.021
17.006    -188.251
17.049    -191.373
17.134    -197.015
17.235    -202.844
17.334    -207.758
17.434    -212.111
17.535    -215.968
17.634    -215.973
17.734    -222.143
17.835    -222.148
17.934    -226.915
18.034    -228.921

CONC
VESL IVOL 39.965980   0 0
VESL DOT8 0.0019936   7 0
VESL H +1 0.0127122   0 0
VESL LU+3 0.0010030   0 0
BUR1 H +1 -0.049918   0 0
ELEC
ZERO H +1 399.573      0
GRAD H +1 57.992       0
WGHT 1
VESL DOT8 0.0000034
VESL H +1 0.0000254
VESL LU+3 0.0000017
BUR1 H +1 -0.000100
ZERO H +1 0.82
GRAD H +1 0.12
TITR RNDE 0.001
EOBS RNDE 0.08
DATA
10.100    258.438
10.201    257.767
10.300    257.074
10.401    256.322
```

10.501	256.327
10.600	254.821
10.701	254.064
10.801	253.283
11.001	251.690
11.200	249.931
11.301	249.016
11.401	248.051
11.500	247.097
11.601	247.101
11.800	244.055
11.901	242.939
12.001	241.761
12.100	240.542
12.201	239.278
12.301	237.983
12.400	236.673
12.501	235.283
12.601	233.835
12.701	232.172
12.801	230.453
12.900	228.642
13.001	226.737
13.101	224.752
13.200	224.747
13.272	221.693
13.301	220.413
13.401	217.929
13.500	215.173
13.601	215.176
13.758	209.308
13.800	205.004
13.870	202.324
13.969	197.979
14.070	197.976
14.136	191.112
14.170	187.569
14.237	183.575
14.337	176.621
14.498	167.682
14.538	161.824
14.590	158.020
14.689	158.025
14.747	149.918
14.789	144.108
14.843	140.711

14.943	134.531
15.044	134.527
15.103	127.656
15.143	123.007
15.206	119.723
15.306	114.876
15.405	110.277
15.506	110.272
15.659	103.583
15.705	97.858
15.765	95.507
15.864	91.461
15.964	87.689
16.065	83.871
16.164	80.233
16.264	76.567
16.365	76.563
16.430	71.879
16.464	69.440
16.557	66.117
16.657	66.111
16.758	58.540
16.846	55.168
16.946	51.326
17.045	47.603
17.146	43.773
17.246	39.912
17.345	35.871
17.446	31.691
17.546	27.427
17.646	27.422
17.746	18.889
17.825	15.775
17.926	14.091
18.025	10.293
18.125	10.297
18.226	1.771
18.306	-1.614
18.406	-0.675
18.505	-4.490
18.606	-4.494
18.706	-7.542
18.805	-7.654
18.906	-11.755
19.006	-16.137
19.105	-20.493

19.306 -29.807
19.379 -29.085
19.480 -33.571
19.580 -38.206
19.679 -43.204
19.780 -48.510
19.880 -54.061
19.979 -54.065
20.080 -65.879
20.141 -69.390
20.242 -75.528
20.342 -81.714
20.441 -88.743
20.542 -95.634
20.642 -102.419
20.741 -109.030
20.842 -115.857
20.942 -122.561
21.041 -129.351
21.142 -129.355
21.242 -143.088
21.296 -146.889
21.396 -153.854
21.497 -161.153
21.596 -168.183
21.696 -168.186
21.797 -182.007
21.851 -185.463
21.951 -191.452
22.050 -197.050
22.151 -202.447
22.352 -211.533
22.428 -214.332
22.527 -217.730
22.627 -220.675
22.728 -223.436

CONC
VESL IVOL 39.948970 0 0
VESL DOT8 0.0029916 7 0
VESL H +1 0.0126857 0 0
VESL LU+3 0.0010021 0 0
BUR1 H +1 -0.049918 0 0
ELEC
ZERO H +1 400.020 0
GRAD H +1 58.363 0

WGHT 1
VESL DOT8 0.0000034
VESL H +1 0.0000254
VESL LU+3 0.0000017
BUR1 H +1 -0.000100
ZERO H +1 0.82
GRAD H +1 0.12
TITR RNDE 0.001
EOBS RNDE 0.08
DATA

11.301	259.463
11.401	258.791
11.500	258.146
11.601	257.477
11.701	256.799
11.800	256.111
11.901	255.357
12.001	255.359
12.100	253.852
12.201	253.057
12.301	252.282
12.400	251.485
12.501	250.677
12.701	248.909
12.801	247.963
12.900	247.959
13.001	246.017
13.101	245.055
13.200	244.059
13.301	244.055
13.401	241.904
13.500	240.711
13.601	239.476
13.701	238.197
13.800	236.894
13.901	235.566
14.001	234.165
14.100	234.168
14.170	232.048
14.201	231.101
14.301	229.424
14.400	227.606
14.501	225.694
14.601	223.700
14.700	221.625
14.801	219.336

14.901	216.922
15.000	214.156
15.101	211.130
15.201	207.820
15.301	204.207
15.401	200.202
15.500	195.951
15.601	191.184
15.701	185.959
15.800	180.070
15.901	173.878
15.939	171.485
16.001	167.620
16.100	161.601
16.260	154.951
16.301	150.390
16.365	147.209
16.464	142.492
16.565	137.868
16.665	133.401
16.764	133.397
16.827	128.435
16.865	125.421
16.950	122.492
17.051	119.128
17.216	115.037
17.250	112.912
17.351	109.903
17.516	106.089
17.550	104.097
17.651	101.305
17.750	98.664
17.850	96.169
17.950	93.662
18.050	93.660
18.150	88.834
18.300	86.298
18.350	83.764
18.451	83.758
18.550	79.025
18.650	76.781
18.751	74.457
18.850	74.459
18.918	71.284
18.950	69.780
19.051	67.296

19.150	67.300
19.250	62.575
19.351	59.975
19.450	57.633
19.550	55.315
19.651	52.783
19.750	50.196
19.850	47.570
19.951	47.565
20.050	42.085
20.150	42.090
20.251	36.785
20.350	33.971
20.450	31.018
20.550	28.079
20.650	25.099
20.751	22.361
20.850	19.516
20.950	16.667
21.051	14.065
21.150	14.062
21.250	8.209
21.351	8.208
21.450	4.656
21.550	3.891
21.651	1.621
21.750	-0.896
21.850	-3.957
21.951	-5.370
22.050	-8.174
22.150	-11.052
22.251	-14.384
22.350	-14.387
22.450	-20.401
22.551	-23.505
22.650	-23.501
22.750	-29.866
22.851	-29.869
22.950	-36.513
23.048	-39.871
23.149	-43.427
23.249	-43.422
23.348	-50.313
23.445	-53.603
23.544	-57.083
23.644	-57.082

```
23.745    -64.472
23.835    -67.864
23.936    -71.828
24.035    -75.635
24.136    -79.444
24.236    -83.294
24.335    -87.174
24.436    -91.207
24.536    -91.211
24.635    -99.473
24.717    -102.782
24.818    -106.998
24.917    -111.129
25.001    -111.134
```

3. Cu-DOTP titration data

```
TASK OBJT 1        DOT8-CU+2
MODL     CU+2 DOT8 H +1
CPLX 0  1 -13.79   CU+2( 0) DOT8( 0) H +1(-1)
CPLX 0  1 12.9922  DOT8( 1) H +1( 1)
CPLX 0  1 21.6639  DOT8( 1) H +1( 2)
CPLX 0  1 29.2456  DOT8( 1) H +1( 3)
CPLX 0  1 35.1661  DOT8( 1) H +1( 4)
CPLX 0  1 40.2780  DOT8( 1) H +1( 5)
CPLX 0  1 42.1176  DOT8( 1) H +1( 6)
CPLX 0  1 40.6299  CU+2( 2) DOT8( 1) H +1( 2)
CPLX 1  1 36.5374  CU+2( 2) DOT8( 1) H +1( 1)
CPLX 1  1 23.4907  CU+2( 2) DOT8( 1) H +1(-1)
CPLX 1  1 08.6305  CU+2( 2) DOT8( 1) H +1(-3)
CONC
VESL IVOL 39.982990   0 0
VESL DOT8 0.0009962   7 0
VESL H +1 0.0127951   0 0
VESL CU+2 0.0010079   0 0
BUR1 H +1 -0.049918   0 0
ELEC
ZERO H +1 400.068      0
GRAD H +1 57.717       0
WGHT 1
VESL DOT8 0.0000020
VESL H +1 0.0000254
VESL CU+2 0.0000020
BUR1 H +1 -0.000100
ZERO H +1 0.82
```

GRAD H +1 0.12
TITR RNDE 0.001
EOBS RNDE 0.08
DATA

4.000	283.828
4.101	283.456
4.201	283.454
4.300	282.729
4.401	282.353
4.501	281.989
4.600	281.631
4.701	281.632
4.801	280.885
4.900	280.887
5.001	280.109
5.101	279.718
5.201	279.318
5.301	279.323
5.400	278.536
5.501	278.164
5.601	277.755
5.700	277.751
5.801	276.899
5.901	276.900
6.000	276.050
6.101	275.628
6.201	275.201
6.300	274.774
6.401	274.773
6.501	273.843
6.600	273.386
6.701	273.382
6.801	272.447
6.900	272.442
7.001	271.511
7.101	271.036
7.200	270.548
7.301	270.023
7.401	270.024
7.500	268.993
7.601	268.995
7.700	267.946
7.801	267.412
7.901	267.417
8.000	266.305
8.101	265.711

8.201	265.111
8.300	264.519
8.401	264.516
8.501	263.314
8.600	263.319
8.701	262.053
8.801	261.409
8.900	260.730
9.001	260.040
9.101	259.327
9.200	258.630
9.301	258.629
9.401	257.175
9.500	256.407
9.601	255.591
9.701	254.787
9.800	253.929
9.901	253.924
10.001	252.190
10.100	252.189
10.201	250.388
10.300	250.391
10.401	248.395
10.501	247.356
10.600	246.269
10.701	246.273
10.801	244.037
10.900	244.040
11.001	241.655
11.101	241.650
11.169	239.791
11.200	238.947
11.301	237.458
11.401	235.899
11.500	234.297
11.601	234.292
11.669	231.894
11.701	230.783
11.800	228.887
11.901	226.766
12.001	226.771
12.070	223.402
12.100	221.922
12.201	219.178
12.301	216.193
12.400	212.962

12.501	212.957
12.572	207.251
12.601	205.011
12.685	200.694
12.785	194.692
12.885	187.255
12.985	178.539
13.085	168.451
13.185	168.451
13.243	155.777
13.285	146.630
13.324	142.302
13.402	133.767
13.502	133.762
13.561	120.630
13.603	111.542
13.641	107.171
13.719	98.015
13.765	92.382
13.819	85.837
13.919	74.199
14.018	63.410
14.119	53.999
14.219	45.533
14.318	38.226
14.419	31.444
14.519	25.463
14.618	20.093
14.719	14.772
14.819	9.759
14.918	9.761
15.019	9.762
15.072	1.882
15.119	-5.025
15.171	-7.629
15.270	-12.689
15.371	-17.608
15.470	-22.992
15.570	-28.296
15.671	-34.062
15.770	-40.495
15.870	-47.860
15.971	-55.983
16.070	-64.672
16.170	-78.405
16.254	-92.030

16.350 -107.758
16.449 -126.165

CONC
VESL IVOL 39.965980 0 0
VESL DOT8 0.0019933 7 0
VESL H +1 0.0127336 0 0
VESL CU+2 0.0010039 0 0
BUR1 H +1 -0.049918 0 0
ELEC
ZERO H +1 399.896 0
GRAD H +1 57.696 0
WGHT 1
VESL DOT8 0.0000040
VESL H +1 0.0000254
VESL CU+2 0.0000020
BUR1 H +1 -0.000100
ZERO H +1 0.82
GRAD H +1 0.12
TITR RNDE 0.001
EOBS RNDE 0.08
DATA
4.900 283.751
5.001 283.413
5.101 283.088
5.201 282.731
5.301 282.730
5.400 282.070
5.501 281.746
5.601 281.392
5.700 281.025
5.801 280.651
5.901 280.646
6.000 279.944
6.101 279.613
6.201 279.613
6.300 278.873
6.401 278.490
6.501 278.487
6.600 277.724
6.701 277.728
6.801 276.983
6.900 276.581
7.001 276.209
7.101 275.799
7.200 275.390

7.301	274.959
7.401	274.551
7.500	274.128
7.601	274.129
7.700	273.299
7.801	272.874
7.901	272.467
8.000	272.464
8.101	271.542
8.201	271.546
8.300	270.622
8.401	270.164
8.501	269.688
8.600	269.220
8.701	268.714
8.801	268.714
8.900	267.757
9.001	267.249
9.101	267.245
9.200	266.213
9.301	265.708
9.401	265.705
9.500	264.638
9.601	264.039
9.701	264.036
9.800	262.896
9.901	262.316
10.001	261.698
10.100	261.119
10.201	260.492
10.300	259.878
10.401	259.877
10.501	258.532
10.600	257.846
10.701	257.843
10.801	256.476
10.900	255.812
11.001	255.115
11.101	255.113
11.200	253.591
11.301	252.697
11.401	251.838
11.500	251.840
11.601	250.192
11.701	249.327
11.800	249.326

11.901	247.465
12.001	247.463
12.100	245.416
12.201	244.349
12.301	244.346
12.400	242.162
12.501	241.043
12.601	241.042
12.669	239.292
12.701	238.467
12.801	237.125
12.900	235.660
13.001	234.129
13.101	232.606
13.200	231.010
13.301	229.284
13.401	227.443
13.500	225.372
13.601	223.070
13.701	223.067
13.770	219.685
13.800	218.169
13.901	215.443
14.001	215.446
14.072	210.800
14.100	208.995
14.201	205.012
14.301	200.528
14.400	200.531
14.467	192.768
14.501	188.878
14.564	184.597
14.725	175.025
14.763	169.055
14.813	164.881
14.911	156.781
15.012	148.553
15.112	141.064
15.211	134.181
15.312	127.840
15.412	121.940
15.513	116.483
15.612	111.390
15.712	106.277
15.722	105.747
15.813	101.074

15.912	96.107
16.012	91.253
16.113	86.432
16.212	86.429
16.275	80.676
16.312	77.333
16.388	73.936
16.488	69.666
16.587	65.150
16.606	64.280
16.688	60.532
16.788	56.147
16.887	51.683
16.988	47.512
17.087	43.393
17.187	39.458
17.288	35.370
17.387	31.407
17.487	27.389
17.588	23.440
17.687	19.727
17.788	16.027
17.888	12.532
17.987	9.140
18.088	5.707
18.188	2.228
18.287	-1.369
18.388	-5.027
18.488	-8.321
18.587	-11.767
18.688	-15.095
18.788	-18.368
18.887	-18.370
18.988	-25.251
19.083	-28.670
19.184	-32.411
19.284	-35.987
19.383	-39.597
19.484	-43.206
19.584	-46.849
19.683	-50.842
19.784	-55.088
19.884	-59.562
19.983	-64.162
20.084	-69.068
20.184	-73.970

20.285 -79.142
20.484 -91.250
20.544 -95.032
20.645 -101.447
20.744 -107.751
20.844 -114.319
20.944 -120.952

CONC
VESL IVOL 39.948970 0 0
VESL DOT8 0.0029912 7 0
VESL H +1 0.0128448 0 0
VESL CU+2 0.0010058 0 0
BUR1 H +1 -0.049918 0 0
ELEC
ZERO H +1 400.990 0
GRAD H +1 58.589 0
WGHT 1
VESL DOT8 0.0000060
VESL H +1 0.0000255
VESL CU+2 0.0000020
BUR1 H +1 -0.000100
ZERO H +1 0.82
GRAD H +1 0.12
TITR RNDE 0.001
EOBS RNDE 0.08
DATA
5.001 286.521
5.101 286.517
5.201 285.934
5.301 285.649
5.400 285.351
5.501 285.061
5.601 284.757
5.801 284.116
5.901 283.836
6.000 283.536
6.101 283.219
6.201 282.913
6.401 282.272
6.600 281.620
6.701 281.615
6.801 280.971
6.900 280.661
7.001 280.656
7.101 279.999

7.200	280.001
7.301	279.280
7.401	278.921
7.500	278.918
7.801	277.548
8.000	276.827
8.201	276.096
8.300	275.681
8.501	274.951
8.600	274.586
8.701	274.166
8.801	273.747
8.900	273.353
9.001	272.933
9.101	272.521
9.200	272.092
9.301	271.690
9.401	271.264
9.500	270.845
9.601	270.403
9.800	269.521
9.901	269.039
10.001	268.587
10.100	268.593
10.201	267.645
10.401	266.663
10.501	266.196
10.600	265.672
10.701	265.147
10.801	264.641
10.900	264.156
11.001	263.625
11.200	262.500
11.301	262.496
11.401	261.342
11.500	260.789
11.601	260.786
11.701	259.632
11.800	259.010
11.901	258.358
12.001	258.354
12.100	257.049
12.201	256.354
12.301	256.349
12.400	255.039
12.501	255.037

12.601	253.708
12.701	252.910
12.801	252.041
12.900	251.252
13.001	251.253
13.101	249.648
13.200	248.771
13.301	247.900
13.401	247.018
13.500	246.032
13.601	245.023
13.701	244.016
13.800	242.980
13.901	241.917
14.001	241.917
14.100	239.731
14.201	238.469
14.301	237.214
14.400	235.853
14.501	234.445
14.601	234.445
14.671	232.450
14.700	231.626
14.801	229.958
14.901	228.270
15.000	228.265
15.101	224.383
15.201	224.384
15.301	219.907
15.401	219.909
15.471	216.378
15.500	214.910
15.601	211.964
15.701	208.741
15.800	204.958
15.901	200.564
16.001	200.560
16.068	193.670
16.100	190.376
16.170	186.150
16.269	179.689
16.369	172.902
16.470	172.898
16.528	164.787
16.569	159.082
16.624	155.603

16.723	149.173
16.824	143.392
16.924	138.121
17.023	133.423
17.124	129.111
17.224	125.032
17.323	121.082
17.424	117.217
17.524	113.534
17.623	110.034
17.724	110.037
17.789	105.802
17.824	103.554
17.923	100.487
18.024	97.551
18.124	94.628
18.223	94.627
18.289	90.604
18.324	88.484
18.424	85.618
18.523	82.772
18.624	82.774
18.690	79.142
18.724	77.302
18.824	74.564
18.924	74.559
19.023	68.959
19.124	68.957
19.190	65.181
19.224	63.244
19.323	60.441
19.424	57.733
19.524	55.048
19.623	52.297
19.724	49.456
19.824	46.537
19.923	43.639
20.024	40.757
20.124	37.964
20.223	35.159
20.324	32.430
20.424	29.372
20.523	26.424
20.624	26.423
20.724	20.701
20.823	17.897

20.924	15.076
21.024	12.387
21.124	9.609
21.224	6.907
21.324	4.144
21.424	1.359
21.524	-1.370
21.623	-4.011
21.724	-4.016
21.824	-9.352
21.923	-9.354
22.024	-14.495
22.124	-14.496
22.223	-19.830
22.324	-19.828
22.424	-25.206
22.523	-27.794
22.624	-30.323
22.724	-30.328
22.823	-35.515
22.924	-35.517
23.024	-40.951
23.123	-43.699
23.224	-46.462
23.324	-49.253
23.423	-51.999
23.524	-54.807
23.624	-57.627
23.724	-60.686
23.824	-63.819
23.924	-67.044
24.024	-70.274
24.223	-76.743
24.324	-80.124
24.424	-83.662
24.624	-90.926
24.716	-94.246
24.916	-101.590
25.001	-104.637

4. Ca-DOTP titration data

```
TASK OBJT 1        DOT8-CA+2
MODL     CA+2 DOT8 H +1
CPLX 0  1 -13.79   CA+2( 0) DOT8( 0) H +1(-1)
CPLX 0  1 13.1864  DOT8( 1) H +1( 1)
```

```
CPLX 0  1 24.1090   DOT8( 1) H +1( 2)
CPLX 0  1 32.6892   DOT8( 1) H +1( 3)
CPLX 0  1 40.1865   DOT8( 1) H +1( 4)
CPLX 0  1 46.0452   DOT8( 1) H +1( 5)
CPLX 0  1 51.0679   DOT8( 1) H +1( 6)
CPLX 1  1 32.2755   CA+2( 2) DOT8( 1) H +1( 2)
CPLX 1  1 24.6116   CA+2( 2) DOT8( 1) H +1( 1)
CPLX 1  1 14.8732   CA+2( 2) DOT8( 1) H +1( 0)
CPLX 1  1 10.4178   CA+2( 1) DOT8( 1) H +1( 0)
CONC
VESL IVOL 39.982990   0 0
VESL DOT8 0.0009983   8 0
VESL H +1 0.0125696   0 0
VESL CA+2 0.0009962   0 0
BUR1 H +1 -0.049918   0 0
ELEC
ZERO H +1 401.066      0
GRAD H +1 58.279       0
WGHT 1
VESL DOT8 0.0000020
VESL H +1 0.0000254
VESL CA+2 0.0000020
BUR1 H +1 -0.000100
ZERO H +1 0.82
GRAD H +1 0.12
TITR RNDE 0.001
EOBS RNDE 0.08
DATA
10.401    226.236
10.501    224.017
10.600    221.580
10.701    218.940
10.801    216.059
10.900    212.960
11.001    212.960
11.073    207.297
11.101    205.083
11.185    200.794
11.285    194.741
11.386    194.747
11.453    183.018
11.485    177.395
11.530    172.262
11.622    159.927
11.671    152.651
11.721    145.305
```

11.822	131.753
11.922	120.413
12.021	110.688
12.122	102.220
12.222	94.585
12.321	87.545
12.422	80.807
12.521	80.811
12.585	72.329
12.622	67.302
12.677	63.356
12.776	56.092
12.877	48.389
12.963	41.815
12.977	40.741
13.076	33.101
13.177	25.689
13.277	18.805
13.378	12.188
13.477	6.212
13.577	0.543
13.678	-4.825
13.777	-10.026
13.877	-15.069
13.978	-20.360
14.077	-25.619
14.177	-31.377
14.278	-37.404
14.377	-37.407
14.439	-45.663
14.477	-50.625
14.532	-54.566
14.633	-61.909
14.733	-69.342
14.832	-69.342
14.933	-85.231
14.982	-89.226
15.079	-96.991
15.180	-104.761
15.280	-112.025
15.379	-118.983
15.480	-125.588
15.580	-131.656
15.679	-137.582
15.780	-143.586
15.879	-149.511

15.980 -149.508
16.080 -160.919
16.143 -164.385
16.242 -169.919
16.342 -175.228
16.443 -180.627
16.542 -185.905
16.642 -185.901
16.743 -196.754
16.808 -200.028
16.907 -204.973
17.008 -209.326
17.108 -213.328
17.207 -213.328
17.308 -220.536
17.400 -223.415
17.501 -223.410
17.600 -229.155
17.700 -231.579
17.801 -231.577
17.900 -235.812
18.000 -237.630
18.100 -239.385
18.200 -241.078

CONC
VESL IVOL 39.965980 0 0
VESL DOT8 0.0019933 8 0
VESL H +1 0.0125709 0 0
VESL CA+2 0.0010099 0 0
BUR1 H +1 -0.049918 0 0
ELEC
ZERO H +1 401.066 0
GRAD H +1 58.279 0
WGHT 1
VESL DOT8 0.0000040
VESL H +1 0.0000254
VESL CA+2 0.0000020
BUR1 H +1 -0.000100
ZERO H +1 0.82
GRAD H +1 0.12
TITR RNDE 0.001
EOBS RNDE 0.08
DATA
12.062 225.805
12.100 223.517

12.201	221.239
12.301	218.808
12.400	216.193
12.501	213.293
12.601	213.291
12.673	208.130
12.701	206.084
12.793	202.040
12.892	196.909
12.993	190.864
13.093	190.862
13.157	180.930
13.192	175.580
13.243	170.977
13.342	160.990
13.443	151.077
13.543	151.072
13.598	141.683
13.642	134.107
13.689	130.877
13.781	125.033
13.881	119.603
13.982	114.562
14.081	110.036
14.181	105.640
14.282	105.639
14.344	100.496
14.381	97.437
14.463	94.323
14.562	94.321
14.628	89.659
14.663	87.111
14.755	84.006
14.856	80.560
14.955	77.084
15.055	73.533
15.156	70.008
15.255	66.449
15.355	66.445
15.455	66.445
15.555	55.866
15.622	53.424
15.721	49.701
15.821	49.699
15.922	41.614
16.005	38.144

16.104	33.989
16.205	29.763
16.305	25.661
16.404	21.637
16.505	17.621
16.605	13.559
16.704	9.499
16.805	5.579
16.905	1.667
17.004	1.669
17.105	-5.643
17.195	-8.897
17.296	-8.902
17.396	-16.428
17.483	-19.869
17.584	-23.811
17.683	-23.810
17.784	-31.572
17.870	-34.802
17.970	-34.803
18.070	-42.440
18.158	-45.950
18.257	-50.071
18.358	-54.451
18.458	-58.573
18.557	-62.722
18.658	-66.848
18.758	-70.916
18.857	-75.018
18.958	-79.352
19.058	-83.695
19.157	-83.695
19.258	-92.270
19.337	-95.433
19.437	-95.432
19.537	-103.181
19.623	-106.498
19.724	-110.422
19.824	-110.421
19.923	-118.260
20.008	-121.529
20.109	-125.290
20.208	-125.294
20.309	-132.544
20.400	-136.191
20.500	-140.013

```
20.600    -143.769
20.700    -147.518
20.800    -151.182
20.900    -154.940
21.000    -154.942
21.100    -162.705
21.186    -166.133
21.285    -170.420
21.385    -174.891
21.486    -179.708
21.585    -184.506
21.686    -189.583
21.786    -194.472
21.885    -199.249
21.986    -203.771
22.086    -208.110
22.185    -212.253
22.286    -216.058
22.386    -216.053
22.485    -222.437
22.586    -225.192
22.686    -225.188
22.785    -229.892
22.886    -232.001
22.985    -232.003
23.085    -235.939
23.186    -235.940
23.285    -239.303
23.385    -240.781

CONC
VESL IVOL 39.948970   0 0
VESL DOT8 0.0029912   8 0
VESL H +1 0.0122690   0 0
VESL CA+2 0.0010014   0 0
BUR1 H +1 -0.049918   0 0
ELEC
ZERO H +1 399.100      0
GRAD H +1 57.929       0
WGHT 1
VESL DOT8 0.0000060
VESL H +1 0.0000255
VESL CA+2 0.0000020
BUR1 H +1 -0.000100
ZERO H +1 0.82
GRAD H +1 0.12
```

TITR RNDE 0.001
EOBS RNDE 0.08
DATA
13.500 224.076
13.601 221.949
13.701 219.756
13.800 219.758
13.901 214.838
14.001 214.843
14.100 209.044
14.201 209.041
14.271 203.720
14.301 201.491
14.388 197.455
14.489 192.215
14.588 186.197
14.688 179.571
14.789 171.885
14.888 163.950
14.903 162.719
14.988 155.883
15.089 148.454
15.188 141.871
15.288 136.228
15.389 131.072
15.488 131.077
15.550 125.838
15.588 122.586
15.668 119.572
15.768 119.576
15.831 115.009
15.867 112.368
15.959 109.419
16.058 109.416
16.123 105.460
16.159 103.242
16.259 100.565
16.358 100.569
16.459 95.379
16.558 95.378
16.624 91.961
16.658 90.221
16.759 87.674
16.858 85.197
16.958 82.756
17.059 80.374

17.158	78.091
17.259	75.837
17.338	73.859
17.359	73.323
17.458	70.887
17.559	68.400
17.659	68.399
17.758	63.579
17.859	63.576
17.959	58.787
18.058	56.483
18.159	53.891
18.259	51.203
18.358	48.491
18.459	45.782
18.559	43.065
18.658	40.408
18.759	40.404
18.859	34.835
18.958	31.810
19.059	28.722
19.158	25.637
19.258	25.635
19.359	19.544
19.458	16.672
19.558	13.741
19.659	10.715
19.758	10.717
19.859	4.541
19.959	1.590
20.058	-1.418
20.159	-1.420
20.259	-7.112
20.358	-10.145
20.459	-13.324
20.559	-16.336
20.658	-16.336
20.759	-22.211
20.859	-25.100
20.958	-27.953
21.059	-30.887
21.159	-33.716
21.258	-36.628
21.359	-39.582
21.458	-42.515
21.558	-45.358

21.659	-45.363
21.758	-51.136
21.858	-51.132
21.959	-56.771
22.058	-59.613
22.158	-62.574
22.259	-65.591
22.358	-68.661
22.459	-71.597
22.559	-74.496
22.658	-77.328
22.759	-80.264
22.859	-83.115
22.958	-86.050
23.059	-88.957
23.159	-91.961
23.258	-91.961
23.359	-91.962
23.459	-100.277
23.539	-102.461
23.640	-102.460
23.739	-108.006
23.839	-110.832
23.940	-113.494
24.039	-116.350
24.139	-118.945
24.240	-121.702
24.339	-124.364
24.439	-127.140
24.540	-129.933
24.639	-132.748
24.739	-135.525
24.840	-135.529
24.939	-141.154
25.001	-142.802

5. Mg-DOTP titration data

```
TASK OBJT 1       DOT8-MG+2
MODL     MG+2 DOT8 H +1
CPLX 0  1 -13.79   MG+2( 0) DOT8( 0) H +1(-1)
CPLX 0  1 13.1864  DOT8( 1) H +1( 1)
CPLX 0  1 24.1090  DOT8( 1) H +1( 2)
CPLX 0  1 32.6892  DOT8( 1) H +1( 3)
CPLX 0  1 40.1865  DOT8( 1) H +1( 4)
CPLX 0  1 46.0452  DOT8( 1) H +1( 5)
```

```
CPLX 0  1 51.0679  DOT8( 1) H +1( 6)
CPLX 0  1 32.3472  MG+2( 2) DOT8( 1) H +1( 2)
CPLX 1  1 13.9892  MG+2( 2) DOT8( 1) H +1( 0)
CPLX 1  1 08.7165  MG+2( 1) DOT8( 1) H +1( 0)
CONC
VESL IVOL 39.982990  0 0
VESL DOT8 0.0009922  8 0
VESL H +1 0.0123530  0 0
VESL MG+2 0.0009981  0 0
BUR1 H +1 -0.049918  0 0
ELEC
ZERO H +1 402.331     0
GRAD H +1 58.018      0
WGHT 1
VESL DOT8 0.0000020
VESL H +1 0.0000253
VESL MG+2 0.0000020
BUR1 H +1 -0.000100
ZERO H +1 0.82
GRAD H +1 0.12
TITR RNDE 0.001
EOBS RNDE 0.08
DATA
11.281    192.547
11.382    184.117
11.481    173.576
11.581    173.576
11.638    157.629
11.682    145.266
11.714    140.830
11.781    132.352
11.881    132.353
11.935    120.945
11.980    111.462
12.021    107.912
12.100    101.357
12.200    93.924
12.301    86.838
12.400    86.838
12.462    78.881
12.501    73.846
12.557    70.212
12.658    63.266
12.757    56.113
12.857    48.760
12.958    40.942
```

13.057 32.965
13.157 24.539
13.258 15.767
13.357 6.626
13.457 -2.967
13.558 -13.057
13.657 -22.928
13.757 -32.934
13.858 -42.751
13.957 -52.583
14.058 -62.380
14.158 -72.158
14.257 -81.608
14.358 -90.836
14.457 -99.138
14.557 -106.634
14.658 -113.593
14.757 -119.818
14.857 -125.393
14.958 -130.896
15.057 -136.237
15.157 -141.268
15.258 -146.462
15.357 -146.463
15.457 -156.744
15.525 -160.243
15.626 -160.243
15.725 -171.479
15.788 -175.238
15.889 -181.584
15.989 -187.529
16.088 -193.349
16.189 -198.814

CONC
VESL IVOL 39.965980 0 0
VESL DOT8 0.0019133 8 0
VESL H +1 0.0123184 0 0
VESL MG+2 0.0010117 0 0
BUR1 H +1 -0.049918 0 0
ELEC
ZERO H +1 400.024 0
GRAD H +1 57.679 0
WGHT 1
VESL DOT8 0.0000040
VESL H +1 0.0000254

VESL MG+2 0.0000020
BUR1 H +1 -0.000100
ZERO H +1 0.82
GRAD H +1 0.12
TITR RNDE 0.001
EOBS RNDE 0.08
DATA

12.501	209.850
12.573	204.086
12.601	201.883
12.685	197.491
12.785	191.409
12.884	184.100
12.985	175.300
13.085	165.601
13.101	164.014
13.184	155.797
13.285	146.414
13.384	138.176
13.484	130.904
13.585	124.377
13.684	118.781
13.784	113.710
13.885	109.159
13.984	109.164
14.048	103.951
14.084	100.983
14.166	97.744
14.267	93.979
14.366	90.161
14.466	90.156
14.531	85.528
14.567	82.991
14.659	79.892
14.759	79.887
14.826	75.416
14.858	73.241
14.956	69.852
15.056	66.307
15.157	62.714
15.256	59.119
15.356	55.466
15.457	51.706
15.556	47.995
15.656	44.153
15.757	39.986

15.856	35.482
15.956	31.006
16.057	26.241
16.156	21.378
16.256	16.337
16.357	11.283
16.456	6.131
16.556	0.823
16.657	-4.875
16.756	-10.351
16.856	-15.939
16.957	-21.436
17.056	-21.431
17.156	-31.693
17.224	-35.102
17.325	-40.330
17.424	-45.512
17.524	-50.715
17.625	-55.801
17.724	-55.804
17.824	-65.604
17.895	-68.985
17.994	-68.983
18.095	-78.403
18.169	-81.911
18.268	-86.732
18.369	-91.725
18.469	-96.200
18.568	-100.687
18.669	-105.045
18.769	-109.268
18.868	-109.266
18.969	-117.680
19.049	-121.496
19.149	-125.889
19.250	-125.891
19.349	-134.223
19.430	-137.423
19.529	-141.274
19.630	-141.274
19.730	-149.265
19.813	-152.737
19.914	-156.925
20.013	-161.259
20.113	-165.428
20.214	-169.761

20.313 -174.065
20.413 -179.044
20.514 -183.956
20.613 -188.761
20.713 -193.285
20.814 -197.723
20.913 -201.893

CONC
VESL IVOL 39.990790 0 0
VESL DOT8 0.0004978 8 0
VESL H +1 0.0123304 0 0
VESL MG+2 0.0010137 0 0
BUR1 H +1 -0.049918 0 0
ELEC
ZERO H +1 402.795 0
GRAD H +1 57.371 0
WGHT 1
VESL DOT8 0.0000034
VESL H +1 0.0000254
VESL MG+2 0.0000017
BUR1 H +1 -0.000100
ZERO H +1 0.82
GRAD H +1 0.12
TITR RNDE 0.001
EOBS RNDE 0.08
DATA
10.372 203.229
10.401 199.860
10.464 195.165
10.564 185.500
10.665 171.797
10.757 154.384
10.792 146.905
10.829 138.754
10.904 124.612
11.004 108.111
11.105 93.309
11.204 79.643
11.304 65.879
11.405 65.875
11.464 48.602
11.504 36.754
11.537 31.512
11.601 21.032
11.702 3.836

11.802	-13.102
11.901	-30.535
12.002	-48.465
12.102	-48.468
12.154	-65.785
12.201	-81.045
12.232	-85.363
12.292	-93.251
12.392	-104.210
12.493	-113.381
12.592	-113.382
12.650	-121.916
12.693	-128.295
12.744	-131.544
12.845	-137.887
12.944	-143.930
13.044	-149.827
13.145	-155.787
13.244	-155.784
13.344	-167.918
13.404	-171.645
13.504	-178.182
13.604	-184.521
13.704	-190.523
13.804	-196.094

APPENDIX D

The ESTA output results of the DOTP protonation, LU-DOTP, Ca-DOTP, Cu-DOTP and Mg-DOTP titrations.

DOTP protonation titrations

```
*******  ******  *******  *****
*        *          *     *     *
*        *          *     *     *
******   *****      *     *******
*              *    *     *     *
*              *    *     *     *
*******  ******     *     *     *

 PROGRAM ESTA2A          VERSION 3.0
 TASK OBJE  1      OT8
 MODL     DOT8 H +1
 CPLX 0  1 -13.7900  DOT8( 0) H +1(-1)
 CPLX 1  1  51.0679  DOT8( 1) H +1( 6)
 CPLX 1  1  46.0452  DOT8( 1) H +1( 5)
 CPLX 1  1  40.1865  DOT8( 1) H +1( 4)
 CPLX 1  1  32.6892  DOT8( 1) H +1( 3)
 CPLX 0  1  24.1090  DOT8( 1) H +1( 2)
 CPLX 1  1  13.1864  DOT8( 1) H +1( 1)
 CONC
 VESL IVOL    39.996  0 0
 VESL DOT8   .0012494  8 0
 VESL H +1   .0126117  0 0
 BUR1 H +1  -.0499181  0 0
 ELEC
 ZERO H +1    406.048    0
 GRAD H +1     58.438    0
 WGHT 1
 VESL DOT8   .0000025
 VESL H +1   .0000248
 BUR1 H +1  -.0001009
 ZERO H +1      .250
 GRAD H +1      .020
 TITR RNDE      .0010
 EOBS RNDE      .0800
 DATA

 CONC
 VESL IVOL    39.992  0 0
 VESL DOT8   .0024990  8 0
 VESL H +1   .0126179  0 0
 BUR1 H +1  -.0499181  0 0
 ELEC
 ZERO H +1    404.109    0
 GRAD H +1     58.516    0
 WGHT 1
 VESL DOT8   .0000050
 VESL H +1   .0000248
```

```
BUR1 H +1  -.0001009
ZERO H +1      .250
GRAD H +1      .020
TITR RNDE      .0010
EOBS RNDE      .0800
DATA

CONC
VESL IVOL    39.989  0 0
VESL DOT8   .0037489  8 0
VESL H +1   .0126191  0 0
BUR1 H +1  -.0499181  0 0
ELEC
ZERO H +1    404.109    0
GRAD H +1     58.516    0
WGHT 1
VESL DOT8   .0000075
VESL H +1   .0000252
BUR1 H +1  -.0000998
ZERO H +1      .250
GRAD H +1      .020
TITR RNDE      .0010
EOBS RNDE      .0800
DATA


OPTIMIZATION CYCLE  0
*********************
OVERALL OBJE OBJECTIVE FUNCTION:    8.5489E+01      (N-R ITERATIONS:  1379)
FORMATION CONSTANTS:
--------------------
COMPLEX NUMBER:       2        3        4        5        7
 LOG BETA:      51.0679  46.0452  40.1865  32.6892  13.1864

GAUSS-NEWTON:           INITIAL SLOPE =  -1.0223E-05

                SLOPE AT PREDICTED SOLUTION  =  -2.9438E-07


OPTIMIZATION CYCLE  1
*********************
OVERALL OBJE OBJECTIVE FUNCTION:    8.5489E+01      (N-R ITERATIONS:  3086)
FORMATION CONSTANTS:
--------------------
COMPLEX NUMBER:       2        3        4        5        7
 LOG BETA:      51.0679  46.0452  40.1865  32.6892  13.1864
 STD DEVN:        .0088    .0088    .0072    .0075    .0136

GAUSS-NEWTON:           INITIAL SLOPE =  -9.2454E-08


OPTIMIZATION CYCLE  2   (CONVERGENCE)
*********************
OVERALL OBJE OBJECTIVE FUNCTION:    8.5489E+01      (N-R ITERATIONS:  4804)
FORMATION CONSTANTS:
--------------------
```

```
COMPLEX NUMBER:      2        3        4        5        7
 LOG BETA:      51.0679  46.0452  40.1865  32.6892  13.1864
 STD DEVN:        .0088    .0088    .0072    .0075    .0136
NO SIGNIFICANTLY CORRELATED PARAMETERS FOUND
HAMILTON R-FACTOR:  .01213
HAMILTON  R-LIMIT:  .00132
NO. OF TITRATIONS:  3        NO. OF POINTS:  553
Stop - Program terminated.
```

Lu^{III}-DOTP complexiometric titrations

```
*******  ******  *******  *****
*        *          *     *     *
*        *          *     *     *
******   *****      *     *******
*              *    *     *     *
*              *    *     *     *
*******  ******     *     *     *

 PROGRAM ESTA2A          VERSION 3.0
 TASK OBJT  1       DOT8-LU+3
 MODL     LU+3 DOT8 H +1
 CPLX 0  1 -13.7900  LU+3( 0) DOT8( 0) H +1(-1)
 CPLX 0  1  13.1864  DOT8( 1) H +1( 1)
 CPLX 0  1  24.1090  DOT8( 1) H +1( 2)
 CPLX 0  1  32.6892  DOT8( 1) H +1( 3)
 CPLX 0  1  40.1865  DOT8( 1) H +1( 4)
 CPLX 0  1  46.0452  DOT8( 1) H +1( 5)
 CPLX 0  1  51.0679  DOT8( 1) H +1( 6)
 CPLX 0  1  -7.9900  LU+3( 1) H +1(-1)
 CPLX 0  1  56.3685  LU+3( 1) DOT8( 1) H +1( 5)
 CPLX 1  1  53.0222  LU+3( 2) DOT8( 1) H +1( 2)
 CPLX 1  1  39.6412  LU+3( 1) DOT8( 1) H +1( 2)
 CPLX 1  1  33.0058  LU+3( 1) DOT8( 1) H +1( 1)
 CPLX 1  1  24.7778  LU+3( 1) DOT8( 1) H +1( 0)
 CPLX 1  1  13.9398  LU+3( 1) DOT8( 1) H +1(-1)
 CONC
 VESL IVOL    39.983  0 0
 VESL DOT8   .0009910  8 0
 VESL H +1   .0127800  0 0
 VESL LU+3   .0010006  0 0
 BUR1 H +1  -.0499180  0 0
 ELEC
 ZERO H +1   400.509    0
 GRAD H +1    58.113    0
 WGHT 1
 VESL DOT8   .0000020
 VESL H +1   .0000254
 VESL LU+3   .0000017
 BUR1 H +1  -.0001000
 ZERO H +1      .820
 GRAD H +1      .120
 TITR RNDE      .0010
```

```
EOBS RNDE     .0800
DATA

CONC
VESL IVOL    39.966  0 0
VESL DOT8    .0020010  8 0
VESL H +1    .0127098  0 0
VESL LU+3    .0010030  0 0
BUR1 H +1   -.0499180  0 0
ELEC
ZERO H +1    399.793    0
GRAD H +1     58.138    0
WGHT 1
VESL DOT8    .0000034
VESL H +1    .0000254
VESL LU+3    .0000017
BUR1 H +1   -.0001000
ZERO H +1       .820
GRAD H +1       .120
TITR RNDE      .0010
EOBS RNDE      .0800
DATA

CONC
VESL IVOL    39.949  0 0
VESL DOT8    .0029814  8 0
VESL H +1    .0126653  0 0
VESL LU+3    .0010021  0 0
BUR1 H +1   -.0499180  0 0
ELEC
ZERO H +1    400.262    0
GRAD H +1     58.454    0
WGHT 1
VESL DOT8    .0000034
VESL H +1    .0000254
VESL LU+3    .0000017
BUR1 H +1   -.0001000
ZERO H +1       .820
GRAD H +1       .120
TITR RNDE      .0010
EOBS RNDE      .0800
DATA


OPTIMIZATION CYCLE  0
**********
OVERALL OBJT OBJECTIVE FUNCTION:    3.7729E+00      (N-R ITERATIONS:  594)
FORMATION CONSTANTS:
--------------------
COMPLEX NUMBER:      10        11        12        13        14
 LOG BETA:       53.0222   39.6412   33.0058   24.7778   13.9398

GAUSS-NEWTON:              INITIAL SLOPE =  -1.0889E-08

                  SLOPE AT PREDICTED SOLUTION =   5.4253E-10
```

```
OPTIMIZATION CYCLE  1
*********************
OVERALL OBJT OBJECTIVE FUNCTION:    3.7728E+00      (N-R ITERATIONS:  1382)
FORMATION CONSTANTS:
--------------------
COMPLEX NUMBER:      10        11        12        13        14
 LOG BETA:       53.0222   39.6412   33.0058   24.7778   13.9398
 STD DEVN:        .0373     .0507     .0259     .0362     .0665

GAUSS-NEWTON:            INITIAL SLOPE =  -5.4254E-10


OPTIMIZATION CYCLE  2   (CONVERGENCE)
*********************
OVERALL OBJT OBJECTIVE FUNCTION:    3.7728E+00      (N-R ITERATIONS:  2172)
FORMATION CONSTANTS:
--------------------
COMPLEX NUMBER:      10        11        12        13        14
 LOG BETA:       53.0222   39.6412   33.0058   24.7778   13.9398
 STD DEVN:        .0373     .0507     .0259     .0362     .0665
NO SIGNIFICANTLY CORRELATED PARAMETERS FOUND
HAMILTON R-FACTOR:  .01339
HAMILTON  R-LIMIT:  .00696
NO. OF TITRATIONS:  3       NO. OF POINTS:  255
Stop - Program terminated.
```

Ca^{III}-DOTP complexiometric titrations

```
*******  ******  *******  *****
*        *          *     *     *
*        *          *     *     *
******   *****      *     *******
*              *    *     *     *
*              *    *     *     *
*******  ******     *     *     *

 PROGRAM ESTA2A          VERSION 3.0
 TASK OBJT  1      DOT8-CA+2
 MODL     CA+2 DOT8 H +1
 CPLX 0  1 -13.7900  CA+2( 0) DOT8( 0) H +1(-1)
 CPLX 0  1  13.1864  DOT8( 1) H +1( 1)
 CPLX 0  1  24.1090  DOT8( 1) H +1( 2)
 CPLX 0  1  32.6892  DOT8( 1) H +1( 3)
 CPLX 0  1  40.1865  DOT8( 1) H +1( 4)
 CPLX 0  1  46.0452  DOT8( 1) H +1( 5)
 CPLX 0  1  51.0679  DOT8( 1) H +1( 6)
 CPLX 1  1  32.2755  CA+2( 2) DOT8( 1) H +1( 2)
 CPLX 1  1  24.6116  CA+2( 2) DOT8( 1) H +1( 1)
 CPLX 1  1  14.8732  CA+2( 2) DOT8( 1) H +1( 0)
 CPLX 1  1  10.4178  CA+2( 1) DOT8( 1) H +1( 0)
 CONC
 VESL IVOL    39.983  0 0
 VESL DOT8   .0009983  8 0
 VESL H +1   .0125696  0 0
```

```
VESL CA+2   .0009962  0 0
BUR1 H +1  -.0499180  0 0
ELEC
ZERO H +1    401.066    0
GRAD H +1     58.279    0
WGHT 1
VESL DOT8   .0000020
VESL H +1   .0000254
VESL CA+2   .0000020
BUR1 H +1  -.0001000
ZERO H +1       .820
GRAD H +1       .120
TITR RNDE       .0010
EOBS RNDE       .0800
DATA

CONC
VESL IVOL     39.966  0 0
VESL DOT8   .0019933  8 0
VESL H +1   .0125709  0 0
VESL CA+2   .0010099  0 0
BUR1 H +1  -.0499180  0 0
ELEC
ZERO H +1    401.066    0
GRAD H +1     58.279    0
WGHT 1
VESL DOT8   .0000040
VESL H +1   .0000254
VESL CA+2   .0000020
BUR1 H +1  -.0001000
ZERO H +1       .820
GRAD H +1       .120
TITR RNDE       .0010
EOBS RNDE       .0800
DATA

CONC
VESL IVOL     39.949  0 0
VESL DOT8   .0029912  8 0
VESL H +1   .0122690  0 0
VESL CA+2   .0010014  0 0
BUR1 H +1  -.0499180  0 0
ELEC
ZERO H +1    399.100    0
GRAD H +1     57.929    0
WGHT 1
VESL DOT8   .0000060
VESL H +1   .0000255
VESL CA+2   .0000020
BUR1 H +1  -.0001000
ZERO H +1       .820
GRAD H +1       .120
TITR RNDE       .0010
EOBS RNDE       .0800
DATA
```

```
OPTIMIZATION CYCLE  0
*********************
OVERALL OBJT OBJECTIVE FUNCTION:    3.0841E+00      (N-R ITERATIONS:  758)
FORMATION CONSTANTS:
--------------------
COMPLEX NUMBER:      8        9       10       11
 LOG BETA:      32.2755   24.6116   14.8732   10.4178

GAUSS-NEWTON:            INITIAL SLOPE =  -1.4040E-07

                SLOPE AT PREDICTED SOLUTION =   6.4999E-10


OPTIMIZATION CYCLE  1
*********************
OVERALL OBJT OBJECTIVE FUNCTION:    3.0840E+00      (N-R ITERATIONS: 1760)
FORMATION CONSTANTS:
--------------------
COMPLEX NUMBER:      8        9       10       11
 LOG BETA:      32.2755   24.6116   14.8732   10.4178
 STD DEVN:       .0449     .0399     .1433     .0252

GAUSS-NEWTON:            INITIAL SLOPE =  -1.0859E-10


OPTIMIZATION CYCLE  2   (CONVERGENCE)
*********************
OVERALL OBJT OBJECTIVE FUNCTION:    3.0841E+00      (N-R ITERATIONS: 2762)
FORMATION CONSTANTS:
--------------------
COMPLEX NUMBER:      8        9       10       11
 LOG BETA:      32.2755   24.6116   14.8732   10.4178
 STD DEVN:       .0449     .0399     .1433     .0252
NO SIGNIFICANTLY CORRELATED PARAMETERS FOUND
HAMILTON R-FACTOR:  .01197
HAMILTON  R-LIMIT:  .00686
NO. OF TITRATIONS:  3        NO. OF POINTS:  335
Stop - Program terminated.
```

Cu^{III}-DOTP complexiometric titrations

```
*******  ******  *******  *****
*        *          *     *     *
*        *          *     *     *
******   *****      *     *******
*              *    *     *     *
*              *    *     *     *
*******  ******     *     *     *

  PROGRAM ESTA2A          VERSION 3.0
  TASK OBJT  1      DOT8-CU+2
  MODL     CU+2 DOT8 H +1
  CPLX 0  1 -13.7900  CU+2( 0) DOT8( 0) H +1(-1)
```

```
CPLX 0  1  13.1864  DOT8( 1) H +1( 1)
CPLX 0  1  24.1090  DOT8( 1) H +1( 2)
CPLX 0  1  32.6892  DOT8( 1) H +1( 3)
CPLX 0  1  40.1865  DOT8( 1) H +1( 4)
CPLX 0  1  46.0452  DOT8( 1) H +1( 5)
CPLX 0  1  51.0679  DOT8( 1) H +1( 6)
CPLX 0  1  52.4342  CU+2( 2) DOT8( 1) H +1( 2)
CPLX 1  1  46.0328  CU+2( 2) DOT8( 1) H +1( 1)
CPLX 1  1  32.6327  CU+2( 1) DOT8( 1) H +1( 1)
CPLX 1  1  24.2045  CU+2( 1) DOT8( 1) H +1( 0)
CPLX 0  1  13.7318  CU+2( 1) DOT8( 1) H +1(-1)
CONC
VESL IVOL    39.983  0 0
VESL DOT8   .0009962  8 0
VESL H +1   .0127142  0 0
VESL CU+2   .0010079  0 0
BUR1 H +1  -.0499180  0 0
ELEC
ZERO H +1    401.066    0
GRAD H +1     58.279    0
WGHT 1
VESL DOT8   .0000020
VESL H +1   .0000254
VESL CU+2   .0000020
BUR1 H +1  -.0001000
ZERO H +1       .820
GRAD H +1       .120
TITR RNDE       .0010
EOBS RNDE       .0800
DATA

CONC
VESL IVOL    39.966  0 0
VESL DOT8   .0019933  8 0
VESL H +1   .0127196  0 0
VESL CU+2   .0010039  0 0
BUR1 H +1  -.0499180  0 0
ELEC
ZERO H +1    401.066    0
GRAD H +1     58.279    0
WGHT 1
VESL DOT8   .0000040
VESL H +1   .0000254
VESL CU+2   .0000020
BUR1 H +1  -.0001000
ZERO H +1       .820
GRAD H +1       .120
TITR RNDE       .0010
EOBS RNDE       .0800
DATA

CONC
VESL IVOL    39.949  0 0
VESL DOT8   .0029912  8 0
VESL H +1   .0127152  0 0
VESL CU+2   .0010029  0 0
```

```
BUR1 H +1  -.0499180  0 0
ELEC
ZERO H +1    399.100    0
GRAD H +1     57.929    0
WGHT 1
VESL DOT8   .0000060
VESL H +1   .0000255
VESL CU+2   .0000020
BUR1 H +1  -.0001000
ZERO H +1      .820
GRAD H +1      .120
TITR RNDE      .0010
EOBS RNDE      .0800
DATA


OPTIMIZATION CYCLE  0
**********
OVERALL OBJT OBJECTIVE FUNCTION:    4.7845E+00      (N-R ITERATIONS:  419)
FORMATION CONSTANTS:
--------------------
COMPLEX NUMBER:       9        10        11
 LOG BETA:      46.0328   32.6327   24.2045

GAUSS-NEWTON:            INITIAL SLOPE =  -8.6100E-08

                SLOPE AT PREDICTED SOLUTION  =   8.7421E-10


OPTIMIZATION CYCLE  1
**********
OVERALL OBJT OBJECTIVE FUNCTION:    4.7845E+00      (N-R ITERATIONS:  963)
FORMATION CONSTANTS:
--------------------
COMPLEX NUMBER:       9        10        11
 LOG BETA:      46.0328   32.6327   24.2045
 STD DEVN:       .0543     .0225     .0367

GAUSS-NEWTON:            INITIAL SLOPE =  -5.0522E-09


OPTIMIZATION CYCLE  2   (CONVERGENCE)
**********
OVERALL OBJT OBJECTIVE FUNCTION:    4.7845E+00      (N-R ITERATIONS: 1508)
FORMATION CONSTANTS:
--------------------
COMPLEX NUMBER:       9        10        11
 LOG BETA:      46.0328   32.6327   24.2045
 STD DEVN:       .0543     .0225     .0367
NO SIGNIFICANTLY CORRELATED PARAMETERS FOUND
HAMILTON R-FACTOR:  .02073
HAMILTON  R-LIMIT:  .00956
NO. OF TITRATIONS:   3        NO. OF POINTS:  176
Stop - Program terminated.
```

Mg^{III}-DOTP complexiometric titrations

```
*******  ******  *******  *****
*        *          *     *     *
*        *          *     *     *
******   *****      *     *******
*              *    *     *     *
*              *    *     *     *
*******  ******     *     *     *

 PROGRAM ESTA2A          VERSION 3.0
 TASK OBJT  1       DOT8-MG+2
 MODL     MG+2 DOT8 H +1
 CPLX 0  1 -13.7900  MG+2( 0) DOT8( 0) H +1(-1)
 CPLX 0  1  13.1864  DOT8( 1) H +1( 1)
 CPLX 0  1  24.1090  DOT8( 1) H +1( 2)
 CPLX 0  1  32.6892  DOT8( 1) H +1( 3)
 CPLX 0  1  40.1865  DOT8( 1) H +1( 4)
 CPLX 0  1  46.0452  DOT8( 1) H +1( 5)
 CPLX 0  1  51.0679  DOT8( 1) H +1( 6)
 CPLX 0  1  32.3472  MG+2( 2) DOT8( 1) H +1( 2)
 CPLX 1  1  13.9892  MG+2( 2) DOT8( 1) H +1( 0)
 CPLX 1  1   8.7165  MG+2( 1) DOT8( 1) H +1( 0)
 CONC
 VESL IVOL    39.983  0 0
 VESL DOT8   .0009922  8 0
 VESL H +1   .0123530  0 0
 VESL MG+2   .0009981  0 0
 BUR1 H +1  -.0499180  0 0
 ELEC
 ZERO H +1    402.331    0
 GRAD H +1     58.018    0
 WGHT 1
 VESL DOT8   .0000020
 VESL H +1   .0000253
 VESL MG+2   .0000020
 BUR1 H +1  -.0001000
 ZERO H +1       .820
 GRAD H +1       .120
 TITR RNDE      .0010
 EOBS RNDE      .0800
 DATA

 CONC
 VESL IVOL    39.966  0 0
 VESL DOT8   .0019133  8 0
 VESL H +1   .0123184  0 0
 VESL MG+2   .0010117  0 0
 BUR1 H +1  -.0499180  0 0
 ELEC
 ZERO H +1    400.024    0
```

```
GRAD H +1    57.679    0
WGHT 1
VESL DOT8   .0000040
VESL H +1   .0000254
VESL MG+2   .0000020
BUR1 H +1  -.0001000
ZERO H +1      .820
GRAD H +1      .120
TITR RNDE      .0010
EOBS RNDE      .0800
DATA

CONC
VESL IVOL    39.991  0 0
VESL DOT8   .0004978  8 0
VESL H +1   .0123304  0 0
VESL MG+2   .0010137  0 0
BUR1 H +1  -.0499180  0 0
ELEC
ZERO H +1   402.795    0
GRAD H +1    57.371    0
WGHT 1
VESL DOT8   .0000034
VESL H +1   .0000254
VESL MG+2   .0000017
BUR1 H +1  -.0001000
ZERO H +1      .820
GRAD H +1      .120
TITR RNDE      .0010
EOBS RNDE      .0800
DATA


OPTIMIZATION CYCLE  0
*********************
OVERALL OBJT OBJECTIVE FUNCTION:    4.0721E+00      (N-R ITERATIONS:  468)
FORMATION CONSTANTS:
--------------------
COMPLEX NUMBER:      9        10
 LOG BETA:       13.9892    8.7165

GAUSS-NEWTON:            INITIAL SLOPE =  -1.5861E-08

                SLOPE AT PREDICTED SOLUTION  =   3.1021E-10


OPTIMIZATION CYCLE  1
*********************
OVERALL OBJT OBJECTIVE FUNCTION:    4.0720E+00      (N-R ITERATIONS: 1106)
FORMATION CONSTANTS:
--------------------
COMPLEX NUMBER:      9        10
 LOG BETA:       13.9892    8.7165
 STD DEVN:        .0345     .0465

GAUSS-NEWTON:            INITIAL SLOPE =  -1.7110E-10
```

OPTIMIZATION CYCLE 2 (CONVERGENCE)
****
OVERALL OBJT OBJECTIVE FUNCTION: 4.0720E+00 (N-R ITERATIONS: 1744)
FORMATION CONSTANTS:

COMPLEX NUMBER: 9 10
LOG BETA: 13.9892 8.7165
STD DEVN: .0345 .0465
NO SIGNIFICANTLY CORRELATED PARAMETERS FOUND
HAMILTON R-FACTOR: .01883
HAMILTON R-LIMIT: .00938
NO. OF TITRATIONS: 3 NO. OF POINTS: 192
Stop - Program terminated.